NASA/TM-20220012395 CD–2021–187

40 kW Fission Surface Power System (FSPS) Deployability

Steven Oleson and Elizabeth Turnbull
Glenn Research Center, Cleveland, Ohio

Anthony Colozza
HX5, LLC, Brook Park, Ohio

Paul Schmitz
Power Computing Solutions Inc., Avon, Ohio

Brandon Klefman, Lucia Tian, Christopher Barth, and Scott Wilson
Glenn Research Center, Cleveland, Ohio

Thomas Packard
HX5, LLC, Brook Park, Ohio

James Fittje
SAIC, Brook Park, Ohio

John Gyekenyesi
HX5, LLC, Brook Park, Ohio

Nicholas Lantz, Bushara Dosa, Natalie Weckesser, Cassandra Chang, Marissa Conway, and Jonathan Drexler
Glenn Research Center, Cleveland, Ohio

November 2022

NASA STI Program . . . in Profile

Since its founding, NASA has been dedicated to the advancement of aeronautics and space science. The NASA Scientific and Technical Information (STI) Program plays a key part in helping NASA maintain this important role.

The NASA STI Program operates under the auspices of the Agency Chief Information Officer. It collects, organizes, provides for archiving, and disseminates NASA's STI. The NASA STI Program provides access to the NASA Technical Report Server—Registered (NTRS Reg) and NASA Technical Report Server—Public (NTRS) thus providing one of the largest collections of aeronautical and space science STI in the world. Results are published in both non-NASA channels and by NASA in the NASA STI Report Series, which includes the following report types:

- TECHNICAL PUBLICATION. Reports of completed research or a major significant phase of research that present the results of NASA programs and include extensive data or theoretical analysis. Includes compilations of significant scientific and technical data and information deemed to be of continuing reference value. NASA counter-part of peer-reviewed formal professional papers, but has less stringent limitations on manuscript length and extent of graphic presentations.

- TECHNICAL MEMORANDUM. Scientific and technical findings that are preliminary or of specialized interest, e.g., "quick-release" reports, working papers, and bibliographies that contain minimal annotation. Does not contain extensive analysis.

- CONTRACTOR REPORT. Scientific and technical findings by NASA-sponsored contractors and grantees.

- CONFERENCE PUBLICATION. Collected papers from scientific and technical conferences, symposia, seminars, or other meetings sponsored or co-sponsored by NASA.

- SPECIAL PUBLICATION. Scientific, technical, or historical information from NASA programs, projects, and missions, often concerned with subjects having substantial public interest.

- TECHNICAL TRANSLATION. English-language translations of foreign scientific and technical material pertinent to NASA's mission.

For more information about the NASA STI program, see the following:

- Access the NASA STI program home page at http://www.sti.nasa.gov

- E-mail your question to help@sti.nasa.gov

- Fax your question to the NASA STI Information Desk at 757-864-6500

- Telephone the NASA STI Information Desk at 757-864-9658

- Write to:
  NASA STI Program
  Mail Stop 148
  NASA Langley Research Center
  Hampton, VA 23681-2199

NASA/TM-20220012395 CD–2021–187

40 kW Fission Surface Power System (FSPS) Deployability

Steven Oleson and Elizabeth Turnbull
Glenn Research Center, Cleveland, Ohio

Anthony Colozza
HX5, LLC, Brook Park, Ohio

Paul Schmitz
Power Computing Solutions Inc., Avon, Ohio

Brandon Klefman, Lucia Tian, Christopher Barth, and Scott Wilson
Glenn Research Center, Cleveland, Ohio

Thomas Packard
HX5, LLC, Brook Park, Ohio

James Fittje
SAIC, Brook Park, Ohio

John Gyekenyesi
HX5, LLC, Brook Park, Ohio

Nicholas Lantz, Bushara Dosa, Natalie Weckesser, Cassandra Chang, Marissa Conway, and Jonathan Drexler
Glenn Research Center, Cleveland, Ohio

National Aeronautics and
Space Administration

Glenn Research Center
Cleveland, Ohio 44135

November 2022

Acknowledgments

This design concept study was performed for the NASA Fission Surface Power Project. The authors would also like to thank the following for their assistance with the design: Omar Bekdash and Christine Schmid.

This report contains preliminary findings, subject to revision as analysis proceeds.

Level of Review: This material has been technically reviewed by technical management.

This report is available in electronic form at http://www.sti.nasa.gov/ and http://ntrs.nasa.gov/

Contents

40 kW Fission Surface Power System (FSPS) Deployability

Steven Oleson and Elizabeth Turnbull
National Aeronautics and Space Administration
Glenn Research Center
Cleveland, Ohio 44135

Anthony Colozza
HX5, LLC
Brook Park, Ohio 44142

Paul Schmitz
Power Computing Solutions Inc.
Avon, Ohio 44011

Brandon Klefman, Lucia Tian, Christopher Barth, and Scott Wilson
National Aeronautics and Space Administration
Glenn Research Center
Cleveland, Ohio 44135

Thomas Packard
HX5, LLC
Brook Park, Ohio 44142

James Fittje
SAIC
Brook Park, Ohio 44142

John Gyekenyesi
HX5, LLC
Brook Park, Ohio 44142

Nicholas Lantz, Bushara Dosa, Natalie Weckesser, Cassandra Chang,
Marissa Conway, and Jonathan Drexler
National Aeronautics and Space Administration
Glenn Research Center
Cleveland, Ohio 44135

1.0 Introduction

Continuous power at the kilowatt level will be imperative for future lunar users including crew infrastructure, future science, and in-situ resource utilization (ISRU). The Compass Team explored both 10 and 40 kWe concepts, assuming planned lander and rover capabilities. Both concepts found that a crew pressurized rover chassis, repurposed for deploying reactor power components, could place a fission surface power system (FSPS, shown in Figure 1.1) at least 1 km from users. While the 10 kWe fission power system (FPS) could be deployed as a single unit, the 40 kWe system was too large and had to be deployed in multiple trips with the same rover. Key technologies and design approaches included a high-assay low-enriched uranium (HALEU), YH moderated heat pipe reactor, Stirling convertors, deployable radiators based on International Space Station (ISS) designs, and power conversion/transmission at ±2800 Vdc.

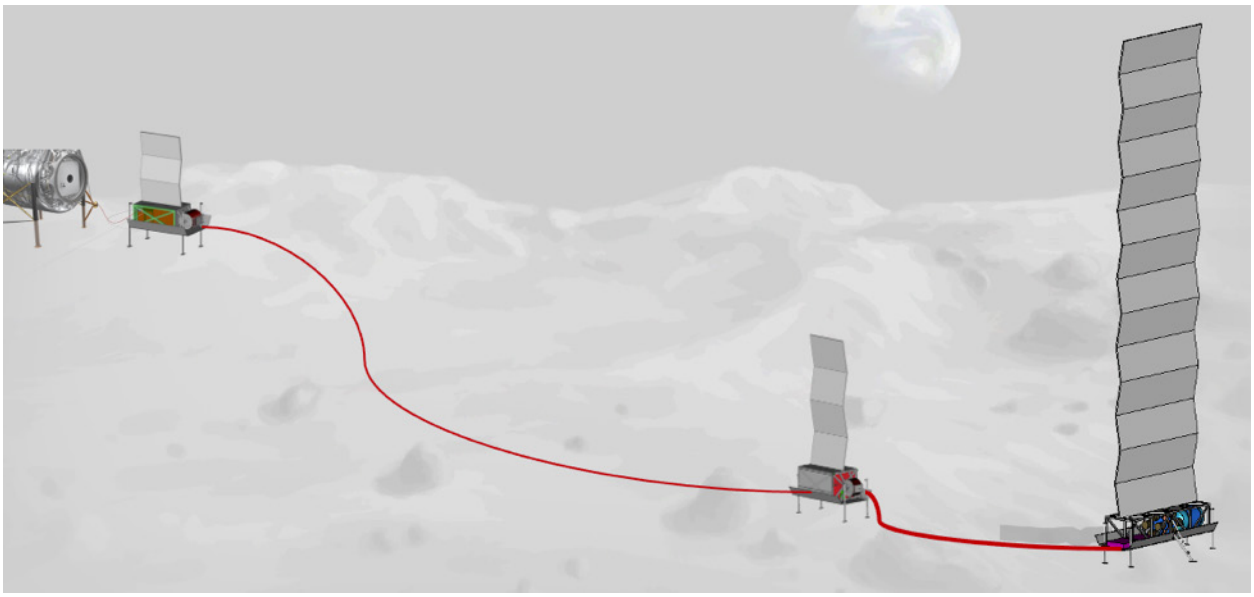

Figure 1.1.—Fission surface power system (FSPS).

2.0 Study Background and Approach

While propulsion is the key element in getting to places in space, power is certainly the limiting factor once one gets there. This is especially true for the Moon. While solar power is available without atmospheric attenuation, the Sun is only available roughly 2 weeks out of every month—necessitating either a large energy storage system (plus the additional solar arrays to gather this energy) or a nuclear reactor. A reactor can provide continuous power for long-duration missions. Such a nuclear power system is a compelling cornerstone to any sort of lunar base or ISRU systems. Past studies have shown that required power levels for such missions, on the Moon or Mars, are on the order of 10 to 40 kWe (at least in the near term) (Refs. 1 and 2). As little as a decade ago, a 40 kWe reactor design was explored and key technologies developed (Refs. 3 and 4).

The past studies showed that a major challenge was how to deliver both the reactor power system as well as the power to the users. While providing ample amounts of power, a reactor system must also be shielded from the crew. One option explored in a previous design looked at burying the reactor close to the base. This eliminated long cable systems, with their associated deployment systems and voltage convertors, but required preparing a sufficient hole for the reactor, transporting it there, placing it in the hole, and covering it.

An alternative approach, explored here, utilizes a transportation system to deploy the reactor to a remote location where the distance can minimize the required shielding. Such an approach eliminates the need for specialized construction equipment but does require a power delivery system with its own challenges. A separation distance on the order of kilometers is required and a 1 km distance was chosen as representative for this study. As such, a power transmission system will require high voltages to minimize the conductor mass (similar to terrestrial systems).

The conceptual point design described herein was commissioned to explore both what a 40 kWe fission surface power system (FSPS) might look like as well as how one might deploy it on the south pole of the Moon using large crew-class cargo landers. The requirements for this design come loosely from the FSPS request for proposal (RFP) (Ref. 5).

2.1 Requirements, Assumptions, and Trades

The top-level design requirements (DR) for the deployable FSPS are shown in Table 2.1.

For the conceptual design described herein, design goals (DG), as seen in Table 2.2, were sought, but the mass goal of 6000 kg was significantly exceeded. However, the final mass still fits on a planned cargo lander that has similar volume dimensions to those in DG-1 (Ref. 6). The conceptual design also focused on transporting and deploying the reactor instead of operating it on the lander.

A few more drivers included the use of low enriched uranium, the placement of the reactor near the lunar south pole, and a self-contained power system that requires no crew or robotic support for startup, operation, and maintenance. The design scalability of this approach to higher powers was considered outside of this effort.

The 40 kWe FSPS is designed to have the ability to be deployed on the lunar surface to a desired location away from the lander that delivers it to the surface. A 6-wheel, pre-deployed rover chassis concept, designed by NASA Johnson Space Center (JSC) to provide mobility to a pressurized crewed cabin (pressurized rover), is used for transporting the FSPS (Ref. 7). In addition to the rover chassis, a modified version of a NASA JSC sled concept is used to deploy the FSPS payloads to the lunar surface from the chassis (Ref. 8).

TABLE 2.1.—DEPLOYABLE FSPS TOP-LEVEL REQUIREMENTS (REF. 5)

DR-no.	Title	Requirements Details
DR-1	Power	The fission surface power system (FSPS) shall be designed to operate at a minimum end-of-life 40 kWe continuous power output for at least 10 years in the lunar environment. Higher power ratings are desirable provided remaining DRs are satisfied.
DR-2	Launch and Landing Loads	The FSPS shall be designed to withstand structural loads.
DR-3	Radiation Protection	The FSPS shall be designed to limit radiation exposure at a user interface location 1 km away to a baseline value of 5 rem/year above lunar background.

TABLE 2.2.—FSPS DESIGN GOALS (REF. 5)

DG-no.	Title	Goal Details
DG-1	Volume	The FSPS should fit within a 4 m diameter cylinder, 6 m in length in the stowed launch configuration.
DG-2	Mass	The total mass of the FSPS should not exceed 6,000 kg, which includes mass growth allowance and margin.
DG-3	Power Cycles	As a safety feature, the FSPS should be capable of multiple commanded and autonomous on/off power cycling.
DG-4	User Load	The FSPS should be capable of supporting user loads from zero to 100 percent power at the user interface.
DG-5	Fault Detection and Tolerance	The FSPS should minimize single-point failure modes, should be capable of detecting and responding to system faults, and have the capability to continue providing no less than 5 kWe under faulted conditions.
DG-6	System Transportability	The FSPS should be capable of operating from the deck of a lunar lander or be removed from the lander and placed on a separately provided mobile system and transported to another lunar site for operation.

The concept of deploying the sled from the chassis is to deploy the two sled legs on one end of the chassis down to the surface using a screw-drive mechanism, then slowly drive the rover out from underneath the sled until the second pair of legs on the other end can be deployed down to the surface, allowing the rover chassis to drive completely out from under the sled. The four legs on the sled can also be used for leveling the sled as needed while on the surface.

2.2 Concept of Operations and Layout

Launch and delivery of the 40 kWe FSPS is assumed to be achieved by a human class cargo lunar lander. No final lander design(s) have been chosen, and only a delivery mass (~12 t) and volume are defined. Cargo placement can be on top, inside, or underneath the lander. Given the long times that may be needed to refuel the cargo lander on its way to the Moon, it is assumed that the FSPS may spend five months getting to the lunar surface, but that the cargo lander will provide up to 2 kWe of power to the FSPS during this time and for up to 2 days after landing. An off-loading system for the cargo lander is required but undefined. A top-level Concept of Operations (CONOPS) of the mission is shown in Figure 2.1.

Given the high, 40 kW power requirement, the FSPS was divided into three separate main elements; the reactor system, the reactor control systems, and the 1 km cable and spool systems which also includes a power conversion system to convert the reactor power to the parameters required by the end user. This split is necessary not only due to the large size of the components, but also the mass of all three elements combined exceeds the limit that the rover chassis can transport. The components contained on each of the three elements were divided up not only by their functionality, but also by the need for each element to be in three different locations during operation. For this reason, each element is integrated with its own sled design to allow them to be individually deployed to the lunar surface from the rover chassis once transported to their desired locations.

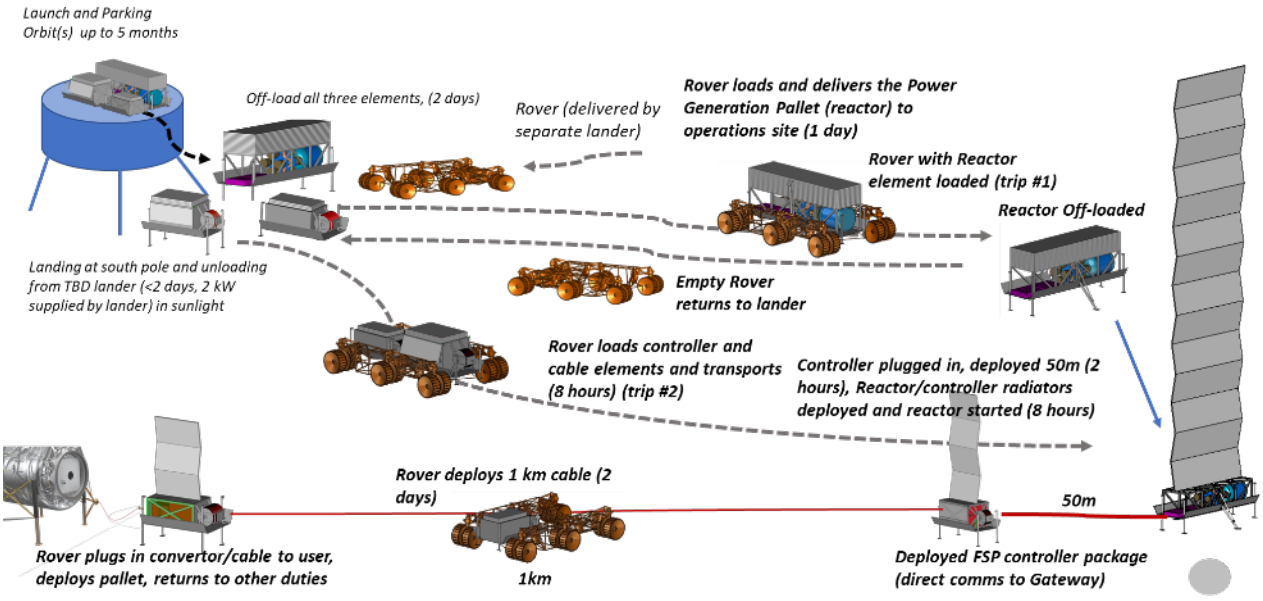

Figure 2.1.—FSPS Mission CONOPS.

While the same pre-deployed rover chassis will deliver all three elements to their respective locations, this is done through two separate trips. First, the rover chassis will deliver the reactor system element from the landing site to a location 1 km away from the end user location. Next, the rover will return to the landing site to retrieve and simultaneously transport both the control systems element and the cable and spool systems element to the reactor element to allow the proper cable connections to be made with the reactor. Finally, the rover will transport both systems 50 m away from the reactor system, deploy the control systems element, then transport and deploy the cable and spool systems element at the end user site 1 km away. The 50 m distance from the reactor system eliminates the need for radiation shielding on the control systems electronics, while the 1 km distance ensures radiation exposure to the crew is below allowable limits.

All three elements fit within the payload volume and mass capability for a single lunar cargo lander volume as described by the requirements document. Inclusion of the rover chassis on the lander would not allow the entire payload to fit within the payload envelope and would exceed the mass capability for a single lander, thus, as stated earlier, the rover chassis used to deliver the elements to their respective locations must be pre-deployed on a separate lander. Figure 2.2 shows the three elements contained within the payload envelope for the lander.

Figure 2.3 shows the reactor system element in its stowed configuration mated to the rover chassis while Figure 2.4 shows both the control systems and cable and spool systems elements in their stowed configuration mated to the same rover chassis. The method for deploying the payloads from the lander payload deck to the lunar surface, or directly onto the rover chassis, has yet to be defined and is considered beyond the scope of the FSPS design presented in this paper. All three elements will remain in their stowed configurations until deployed onto the lunar surface.

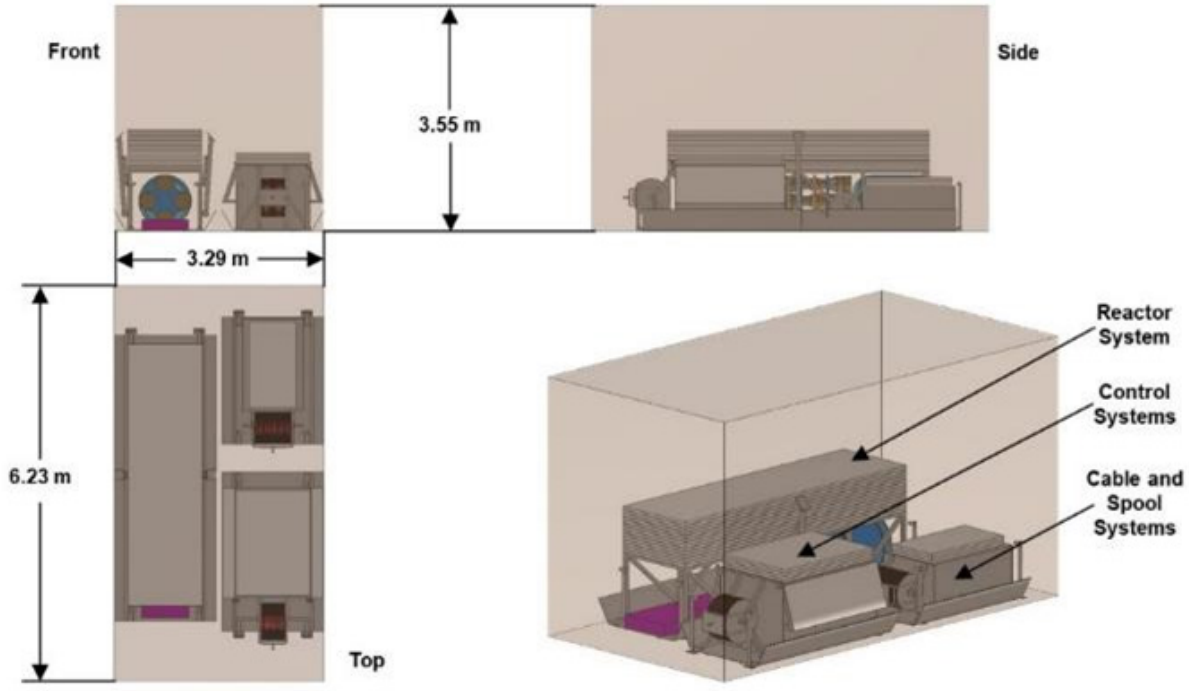

Figure 2.2.—Three elements of the FPS system within the lander payload envelope.

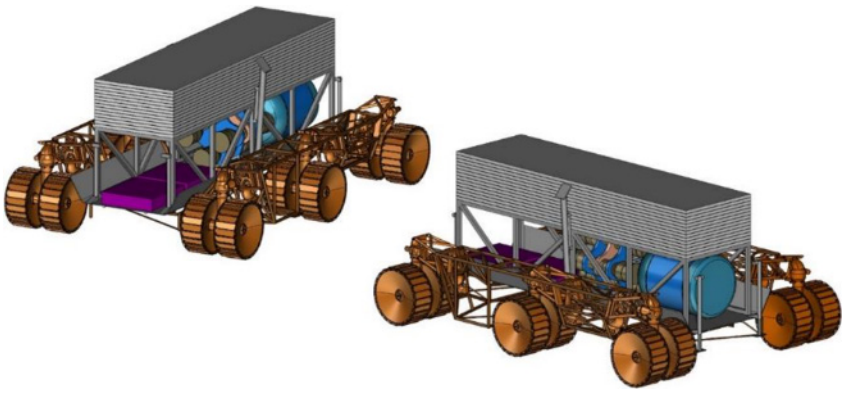

Figure 2.3.—Reactor system element mated to the rover chassis.

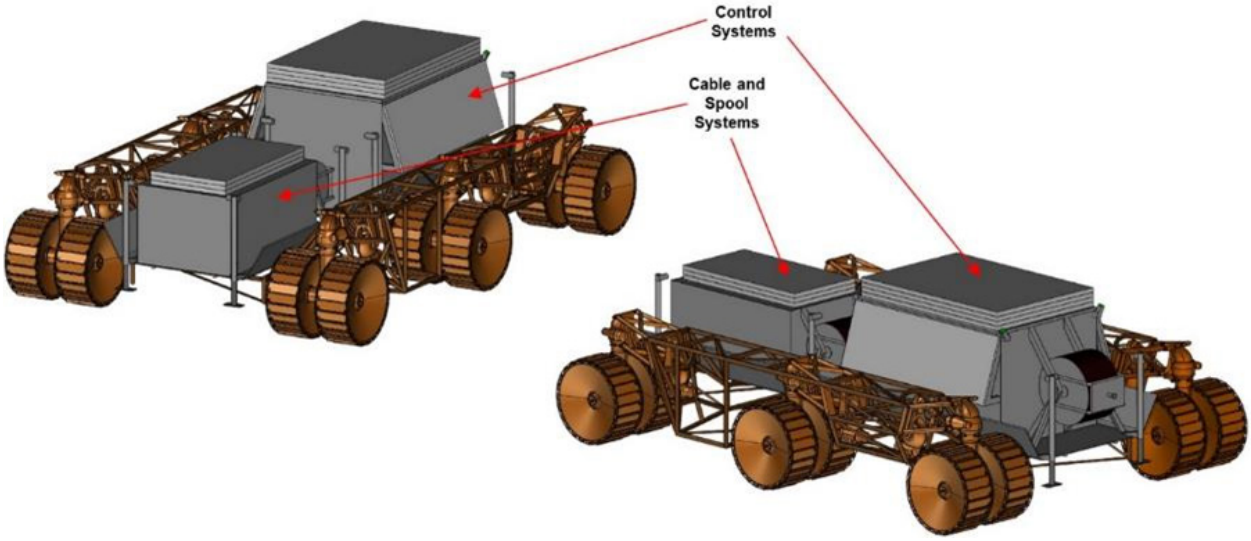

Figure 2.4.—The control systems and cable and spool systems elements both mated to the rover chassis.

Figure 2.5 shows the dimensions of the stowed reactor system element. Those components on the reactor system element that must be deployed after the chassis delivers and deploys it at its desired location are the two outriggers and the double sided reactor radiator. Located near the middle and on the long sides of the sled base are the outriggers, which will pivot downwards to the surface upon deployment. These outriggers are included to help widen the base of the reactor system element when on the lunar surface in the event the deployed radiator, standing 16 m above the reactor system structure, tilts to one side or the other due to any potential slack within the radiator's scissor jack deployment mechanism. The 14 individual, double-sided radiator panels that make up the full 133.4 m^2 reactor radiator are stacked on top of a box truss structure that is integrated to the sled base. The length of the box truss is maximized, running the full length between the pairs of sled legs located at each end of the sled base structure, while the width of the base of the box truss is maximized by running the full width of the horizontal portion of the sled base. An increase to the width of the top of the box truss by drafting the sides outward would reduce the number of panels needed to get the full 133.4 m^2 area, however the height of the fully deployed radiator is driven by the length of the box truss (width of the deployed panels). Further work could be done to examine how the width of the radiator panels could be increased, avoiding the sled legs, to reduce the overall deployed height, or to determine different radiator configurations that would provide the required area. The deployment concept for the reactor system element is shown in Figure 2.6.

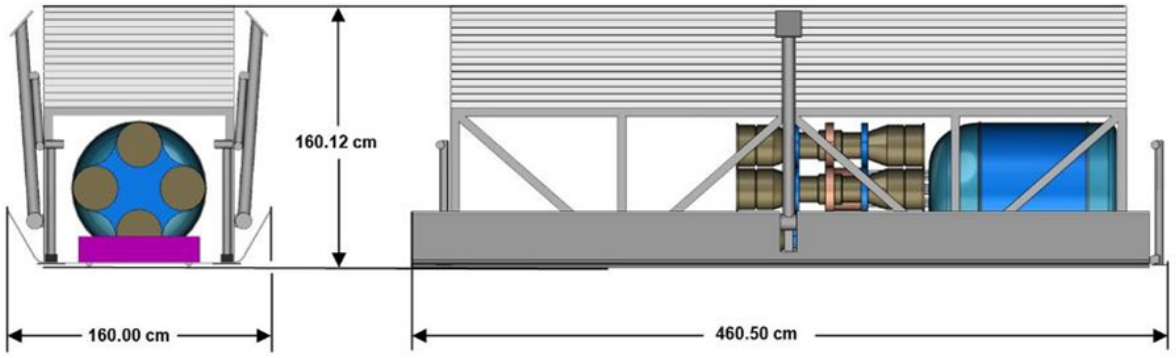

Figure 2.5.—Dimensions of the stowed reactor system element.

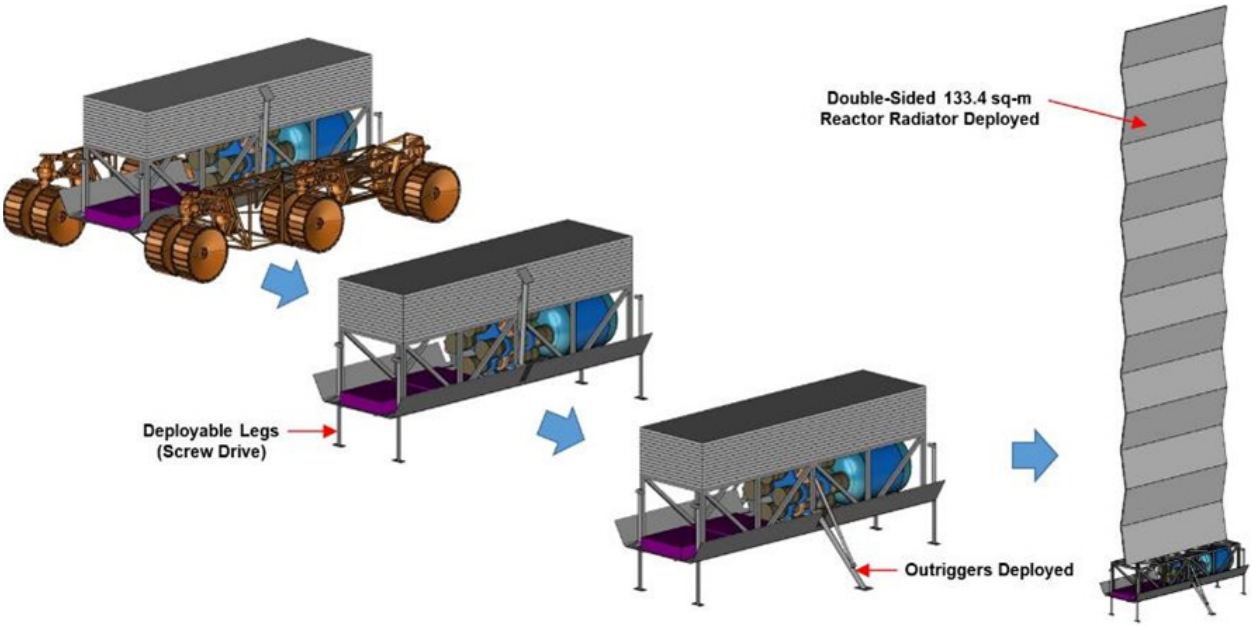

Figure 2.6.—Deployment concept for the reactor system element.

Dimensions for the fully deployed reactor system element are shown in Figure 2.7. The fully deployed outriggers create a footprint width of 320.20 cm, almost tripling the base width provided by the sled legs alone, creating a significant increase in stability. As stated earlier, the radiator panels run the length of the box truss to which they are mounted when stowed providing a panel width of 412.0 cm, thus requiring a deployed height of 1603.02 cm to achieve the required 133.4 m^2 radiator area. Note that the deployed radiator wing is not a flat plate as there is an assumed 20° angle between the individual panels. The radiator design and deployment concepts are derived from the radiators that are currently on the ISS.

In addition to the reactor radiator, outriggers, box truss structure, and sled structures and mechanisms, those components located on the reactor system element include the reactor itself, shield, heat exchangers, Stirling convertors and the coolant pump system for the radiators. All these components are shown in Figure 2.8.

The reactor system is located inside the box truss structure with the reactor side at one end of the truss and is mated directly to the base of the sled in a horizontal position. In addition to the actual reactor, the system includes radiation shielding, two cold heat exchangers, a hot heat exchanger, four opposing pairs of

Stirling converters, and the heat pipes used to transfer the heat from the reactor to the heat exchangers. Also mounted directly to the sled structure at the opposite end from the reactor are the two boxes that make up the coolant pump system for the reactor radiator. These locations can be modified in the event the Stirling converters need to be located at a further distance from the reactor as the reactor system design develops.

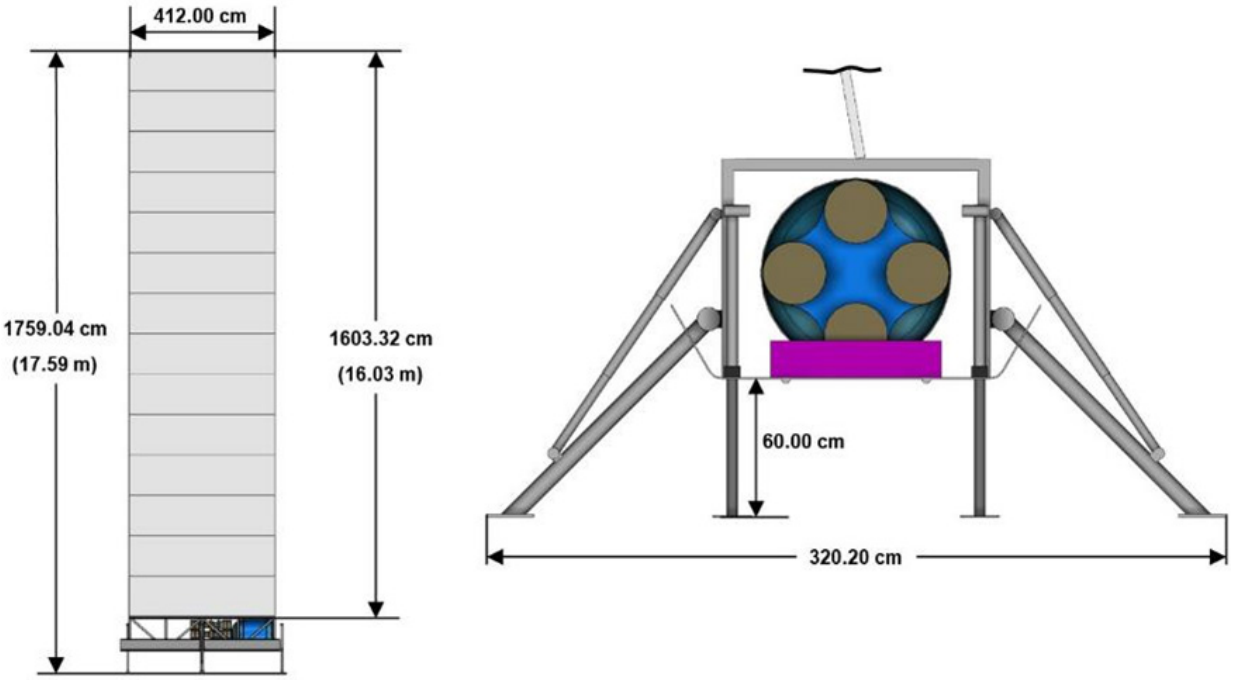

Figure 2.7.—Dimensions of the fully deployed reactor system element.

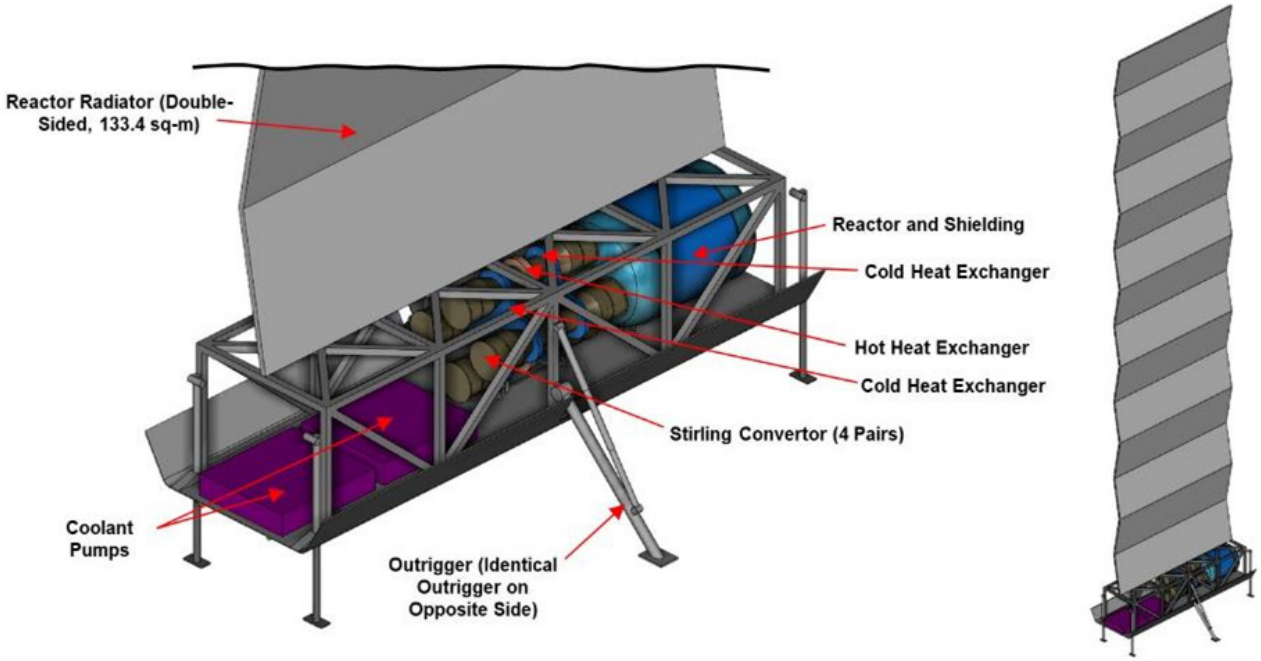

Figure 2.8.—Components located on the reactor system element.

The stowed control systems element, complete with dimensions, is shown in Figure 2.9. As with the reactor system element design, a box truss is used to provide space for the stacked electronics radiator panels stowed on top, however closeout panels are added to the box truss to assist in mounting the insulation required to provide an acceptable thermal environment for all the electronics contained inside the truss. The top closeout panel also provides the interface for mounting the heavier electronics boxes that are not mounted directly to the base of the sled. Those components that require deployment once deployed to the lunar surface include the double-sided electronics radiator and the 50 m of cabling that will be deployed as the rover transports the control systems element to a location 50 m away from the reactor system element. Again, the radiator design and deployment concept are based on the radiator wings currently flying on the ISS. The deployment concept for the control systems element is shown in Figure 2.10. Note that the control systems element is deployed from the rover chassis prior to deploying the cable and spool systems element.

Figure 2.11 shows the fully deployed dimensions for the control systems element. As with the reactor systems element, each radiator panel has the same dimensions as the box truss to which they stack when stowed. There are a total of four double-sided panels that when deployed create a wing that has a height 458.29 cm above the top of the closeout panel located on top of the box truss. This provides the 15.3 m^2 effective radiator area required to reject the waste heat from the electronics located inside the box truss. Once again, a 20° angle between adjacent radiator panels is assumed due to limitations on a scissor jack mechanism to place all four panels in the same plane.

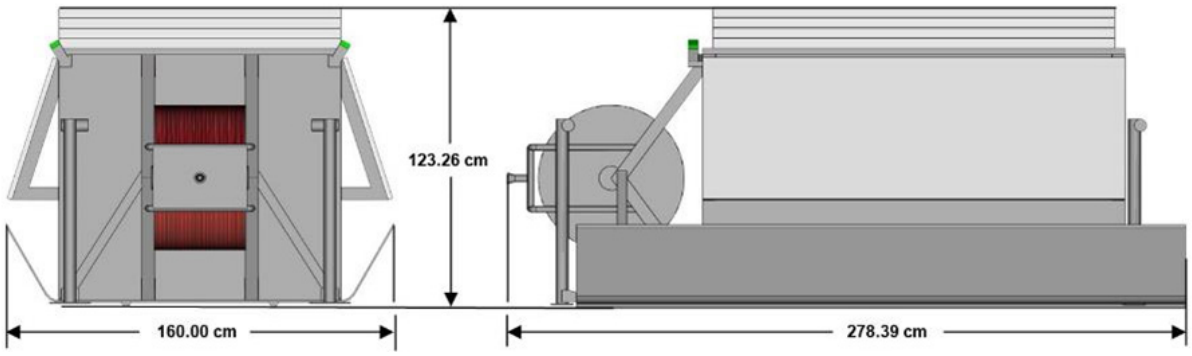

Figure 2.9.—Stowed dimensions of the control systems element.

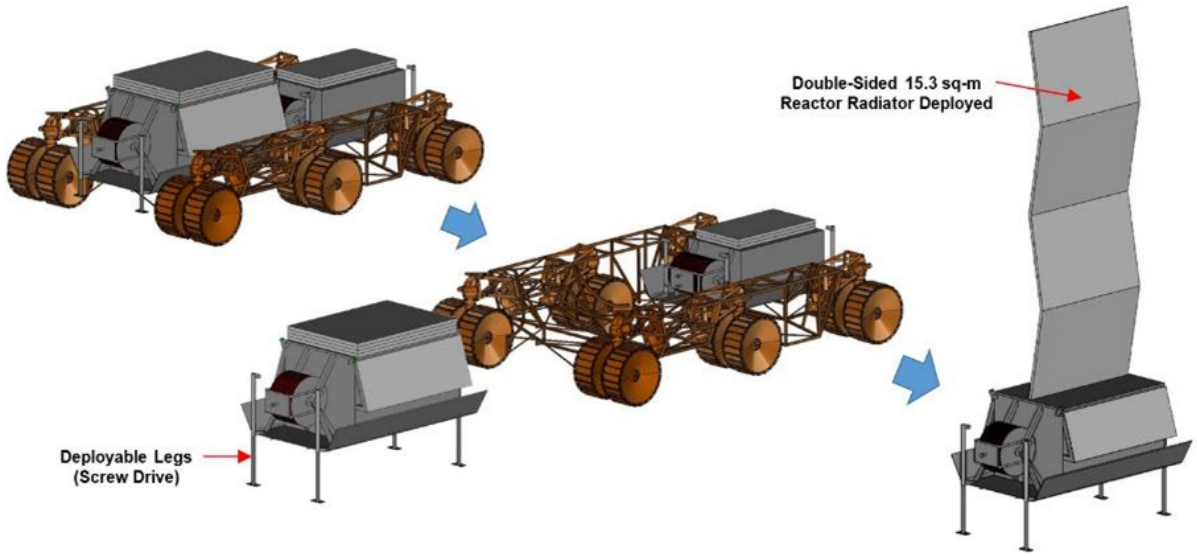

Figure 2.10.—Deployment concept for the control systems element.

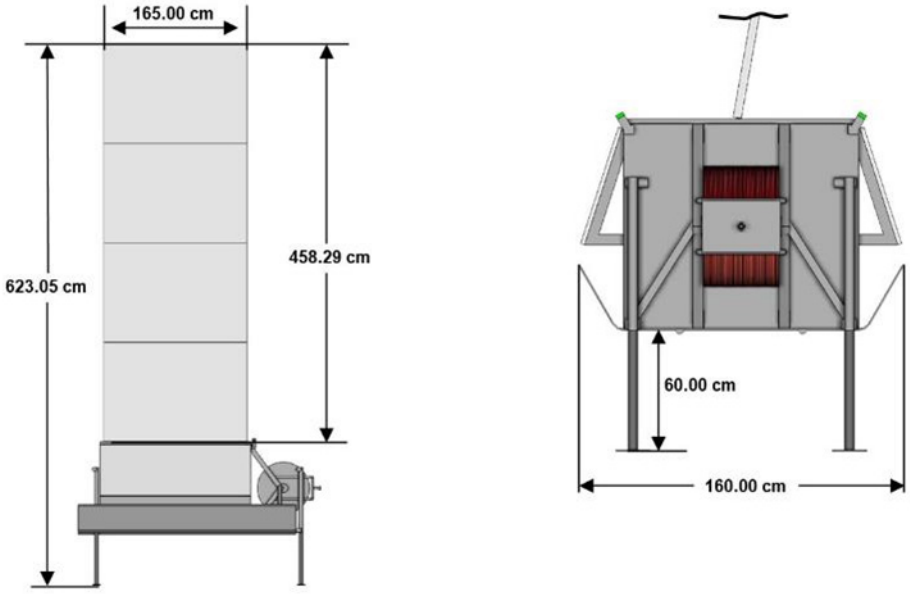

Figure 2.11.—Deployed dimensions for the control systems element.

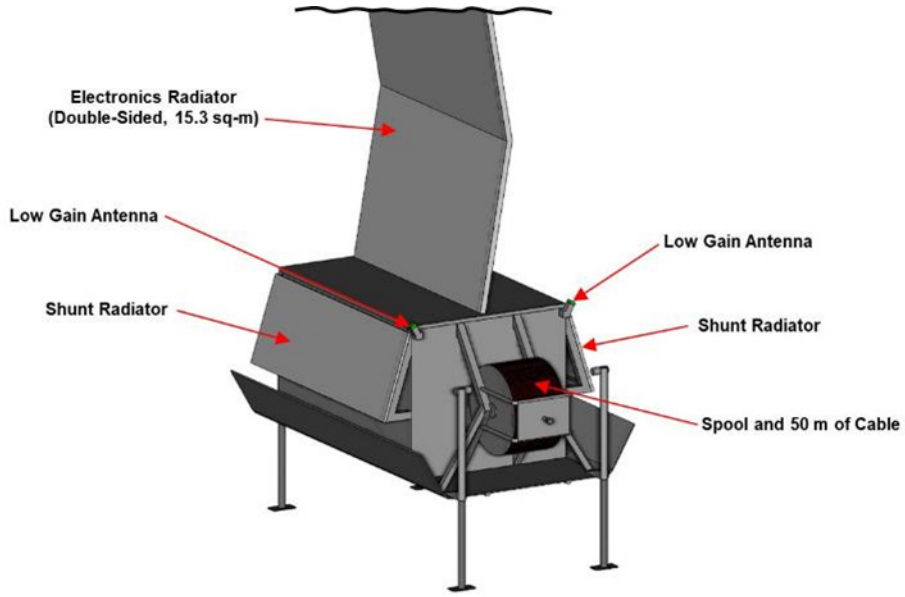

Figure 2.12.—External components on the control systems element.

In addition to the electronics radiator, those components located on the outside of the box truss structure include: two fixed, single-sided shunt radiators; the spool containing 50 m of cabling; and two low-gain Ka band antennas. All the external components can be seen in Figure 2.12.

The shunt radiator is split into two identical fixed, one-sided panels with a combined area of 2.1 m^2. Additional structure is incorporated to the two long sides of the box truss structure to mount the shunt radiator panels at an upward angle along those sides. This angle minimizes the amount of heat that would be radiated into the sled structure, preventing a hot spot and the need for a larger radiator area.

The spool is sized to carry the 50 m of cable that runs between the reactor system and control systems elements. To keep the overall length of the control systems element at a minimum, the diameter of the

spool design was minimized, thus increasing the spool width. However, the larger width still fits well within the distance between the two sled legs located on the same end of the sled. Additional structure is incorporated to the end of the box truss structure to support the spool and to tie it into the base of the sled structure for reinforcement.

Located at the top two corners on the spool end of the box truss structure are the two low-gain Ka band antennas. The structure for mounting the antennas was incorporated to the box truss structure as small extensions from the top two corners. Each antenna provides a hemispherical coverage area, thus eliminating the obstruction from the deployed electronics radiator. Each antenna is angled outwards from their respective sides 30° from vertical to also help reduce the obstruction caused by the electronics radiator. Coverage can be passed from one antenna to the other as the Gateway becomes obstructed by the electronics radiator ensuring continual coverage while the Gateway is in view.

Those components on the control systems element that are located inside the box truss structure include: all the electronics of the Electrical Power System (EPS); all the electronics for the Communications System; and the enclosure for the cards that comprise the Command and Data Handling system (C&DH). Figure 2.13 shows all these components located inside the box truss structure.

Those components that make up the EPS include two Stirling controllers, two DC to DC converter units (DDCU), two auxiliary DDCUs, and a Li-ion battery. Overall length of the box truss structure is driven by the length of the Stirling controllers as they are the largest of the electronics boxes. Both Stirling controllers are mounted directly to the base of the sled structure. The remaining EPS electronics and battery are mounted directly to the top closeout panel for the box truss. This top panel is a 1 in. thick honeycomb panel rather than the thin face sheets used for the other four side closeout panels. Use of the honeycomb structure for the top panel was driven by the fact that cross members could not be used on the top side of the truss for reinforcement to allow the full area of the panel to be used to mount the EPS electronics and battery. In addition to the needed area for mounting, this panel must carry the loads of those boxes that are mounted to it, as well as the stowed stack of radiator panels located on top.

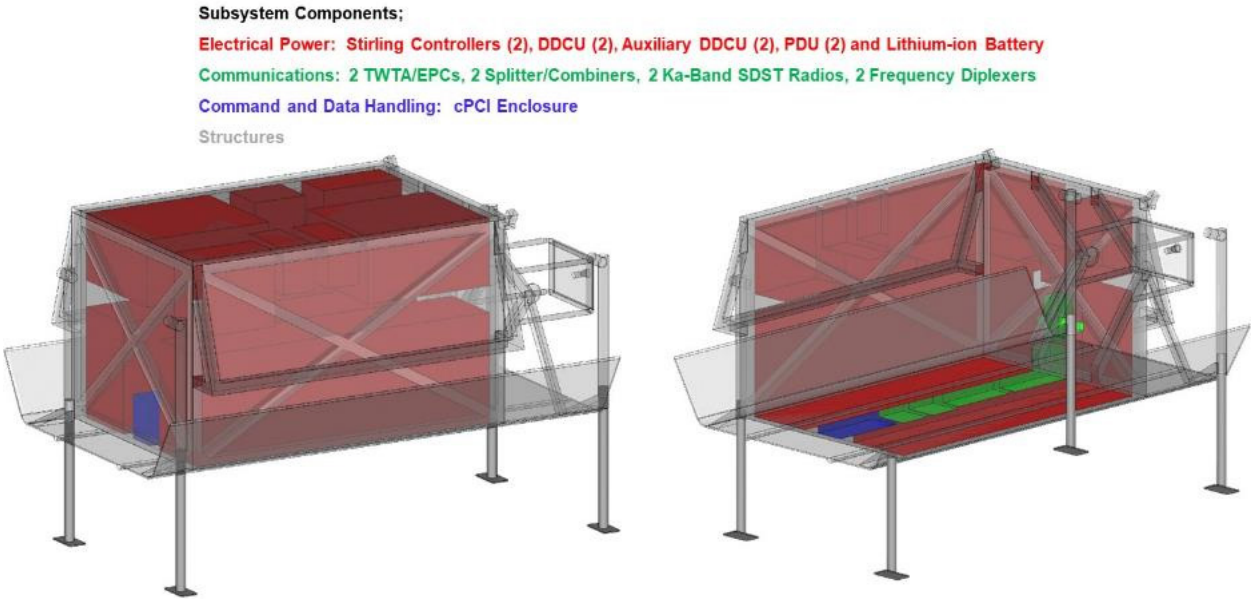

Figure 2.13.—Internal components on the control systems element.

Those communications system electronics located inside the box truss structure include two traveling wave tube amplifiers (TWTA) and electronic power conditioners (EPC), two splitter/combiners, two Ka-band small deep space transponder (SDST) radios, and two frequency diplexers. The two TWTA/EPC boxes and two SDST radios are mounted directly to the base of the sled structure between the two Stirling controllers, while the smaller combiner/splitters and frequency diplexers are mounted to the closeout panel on the spool end of the box truss.

Finally, the enclosure for the CDHS is mounted directly to the base of the sled structure in between the two Stirling converters. While placement of these boxes is not fully optimized, the locations were selected to pack them as tightly as possible to minimize the length of the box truss, and thus the overall length of the control systems element so that it can fit on the same rover chassis with the cable and spool systems element.

The stowed cable and spool systems element, complete with dimensions, is shown in Figure 2.14. As with the control systems element design, a box truss is used to provide space for the stacked electronics radiator panels stowed on top, and closeout panels are added to the box truss to assist in mounting the insulation required to provide an acceptable thermal environment for the electronics contained inside the truss. Those components that require deployment once deployed to the lunar surface include the double-sided electronics radiator and the 1 km of cabling that will be deployed as the rover transports the cable and spool systems element to the end user location 1 km away from the reactor system element. Again, the radiator design and deployment concept are based on the radiator wings currently flying on the ISS. The deployment concept for the cable and spool systems element is shown in Figure 2.15.

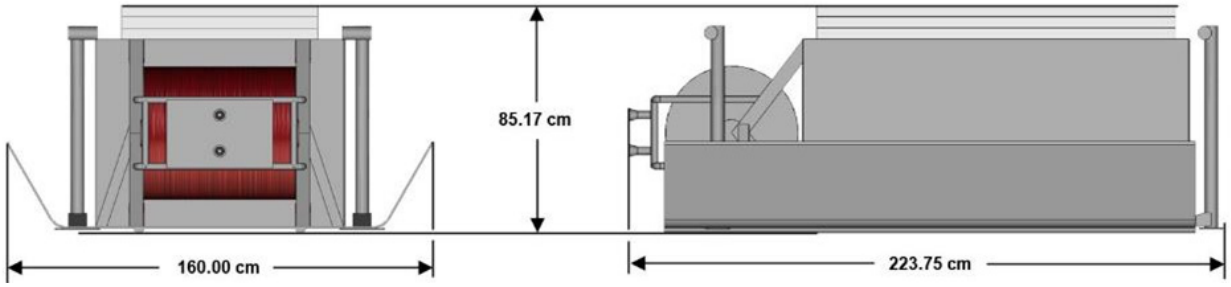

Figure 2.14.—Stowed dimensions of the cable and spool systems element.

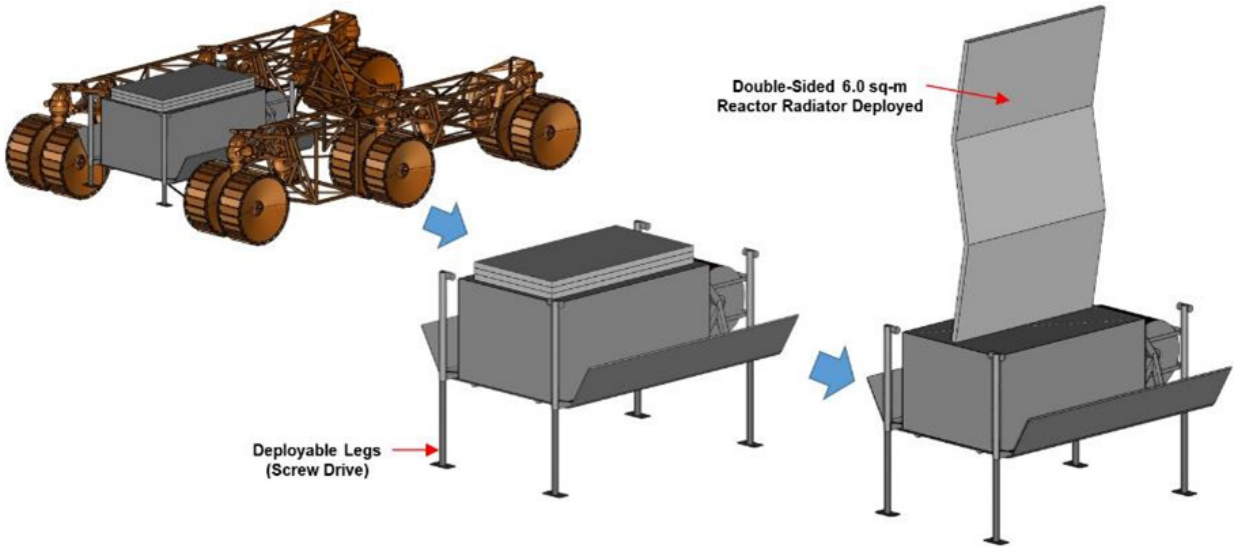

Figure 2.15.—Deployment concept for the cable and spool systems element.

Figure 2.16 shows the fully deployed dimensions for the cable and spool systems element. There are a total of three double-sided panels that when deployed create a wing that has a height 219.62 cm above the top of the closeout panel located on top of the box truss. Given a panel width of 135 cm, this provides the 6.0 m^2 effective radiator area required to reject the waste heat from the electronics located inside the box truss. Once again, a 20° angle between adjacent radiator panels is assumed due to limitations on a scissor jack mechanism to place all four panels in the same plane.

In addition to the electronics radiator, the only other component located on the outside of the box truss structure is the spool containing 1 km of cabling. All the external components can be seen in Figure 2.17.

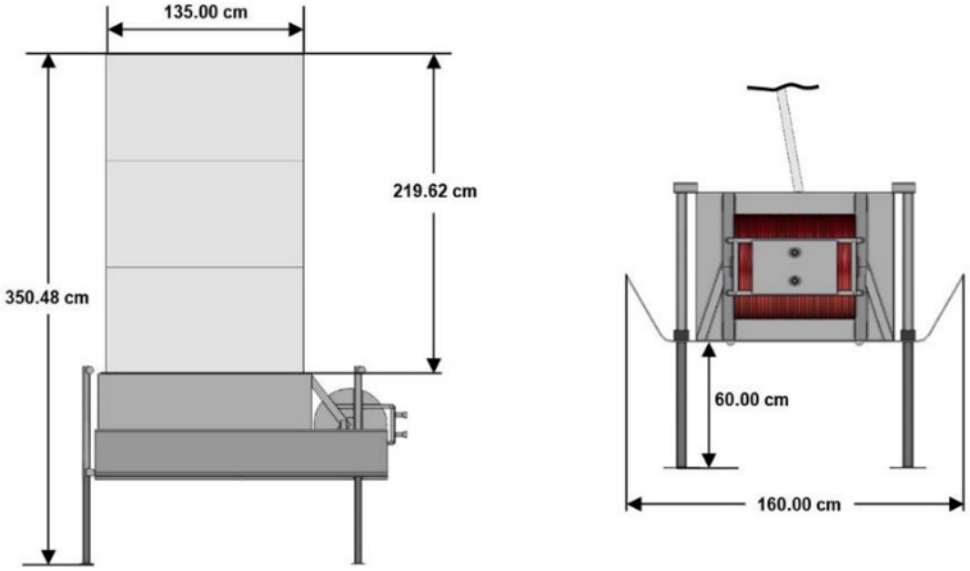

Figure 2.16.—Deployed dimensions for the cable and spool systems element.

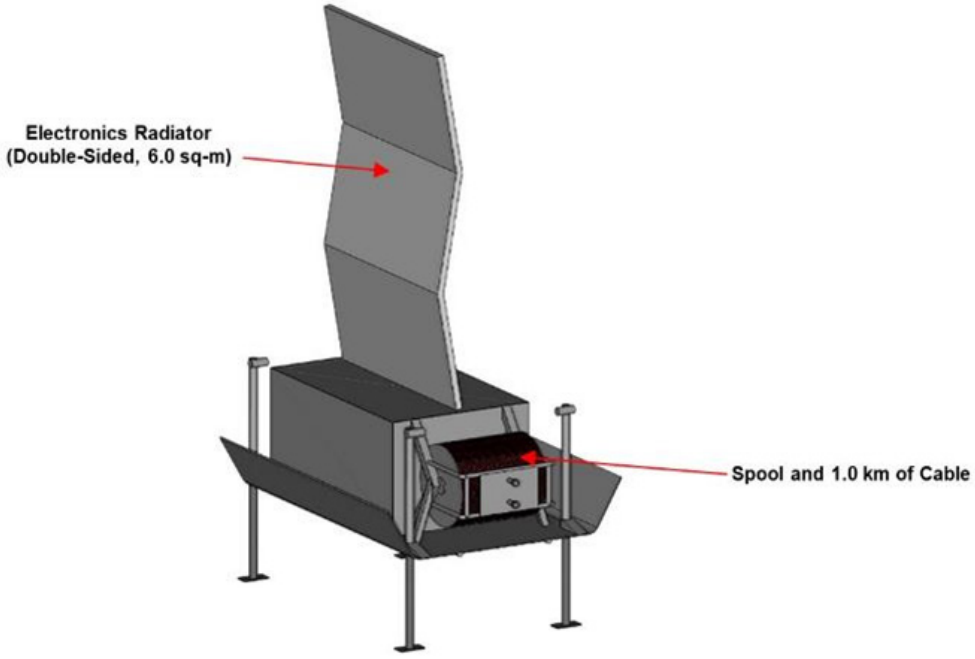

Figure 2.17.—External components on the cable and spool systems element.

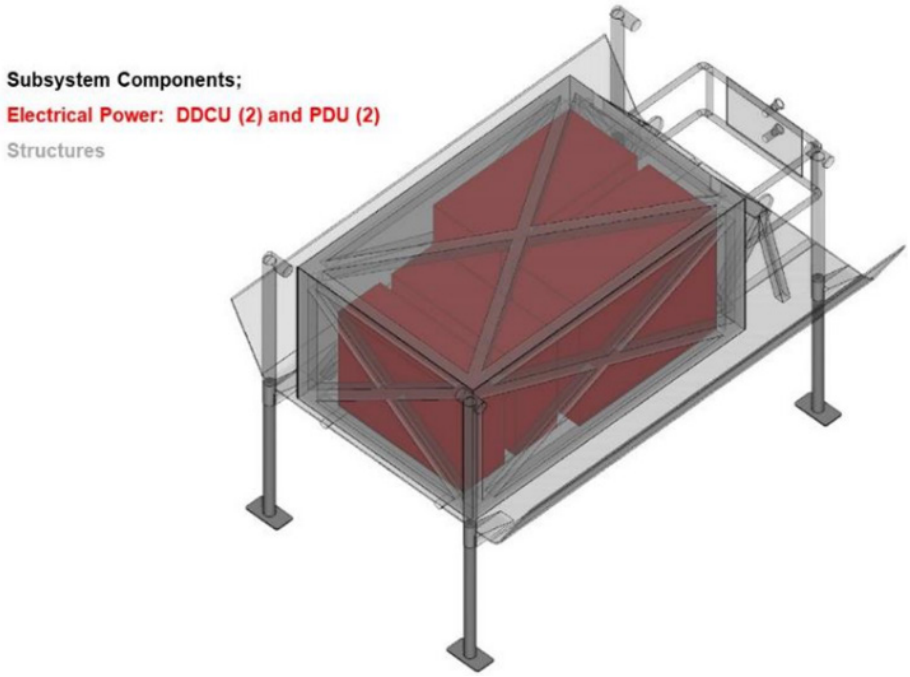

Figure 2.18.—Internal components on the cable and spool systems element.

The spool is sized to carry the 1 km of cable that runs between the control systems and cable and spool systems elements. To keep the overall length of the cable and spool systems element at a minimum, the diameter of the spool design was minimized, thus increasing the spool width. However, the larger width still fits within the distance between the two sled legs located on the same end of the sled. Additional structure is incorporated to the end of the box truss structure to support the spool and to tie it into the base of the sled structure for reinforcement.

Those components on the cable and spool systems element that are located inside the box truss structure are the two DDCUs and the two power distribution units (PDU) of the EPS. Figure 2.18 shows these components inside of the box truss structure. All four boxes are mounted directly to the sled base structure. Note that the top closeout panel for the cable and spool systems element is just a thin face sheet rather than a honeycomb panel as none of the electronics boxes are mounted to it, thus providing room for cross members to be added to the top of the box truss to provide the support for the stowed radiator panels.

2.3 Growth, Contingency, and Margin Policy

The mass growth, contingency, and mass margin policy used by the Compass Team is congruent with the standards described in American Institute for Aeronautics and Astronautics (AIAA) S–120A-2015 (Ref. 9). This methodology starts with the basic mass of the components and adds the mass growth allowance (MGA). This subtotal is defined as the predicted mass. Mass margin is then added to the predicted mass to calculate the allowable mass. The aerospace community typically refers to the mass margin as system level growth. This methodology is shown visually in Figure 2.19.

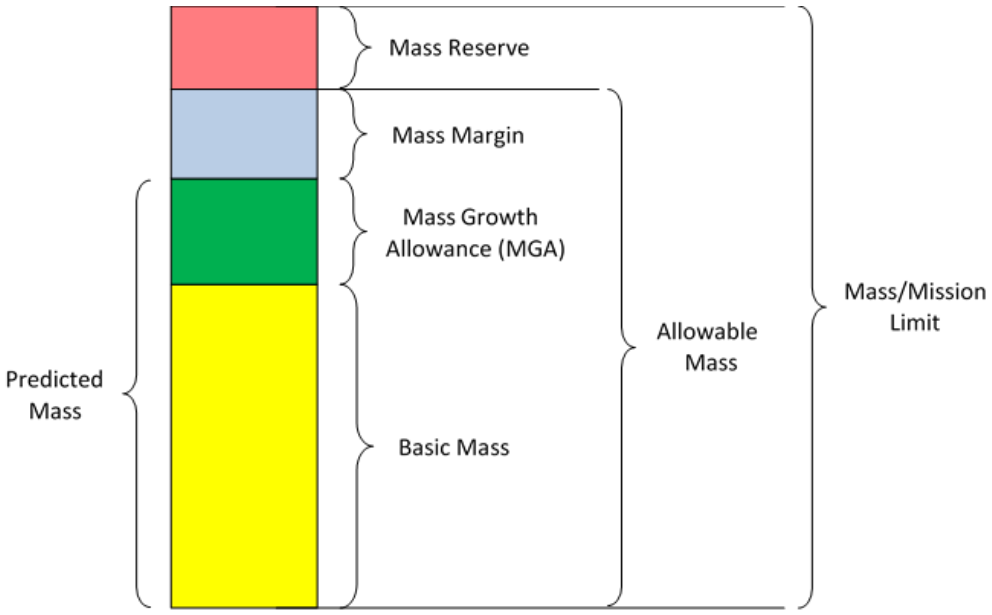

Figure 2.19.—Graphic of General Mass Definitions.

2.3.1 Terms and Definitions Regarding Mass

Mass — *The measure of the quantity of matter in a body.*

Basic Mass — *Mass data based on the most recent baseline design. This is the bottoms-up estimate of component mass, as determined by the subsystem leads.*

Note 1: This design assessment includes the estimated, calculated, or measured (actual) mass, and includes an estimate for undefined design details like cables, multi-layer insulation, and adhesives.

Note 2: The MGA and uncertainties are not included in the basic mass.

Note 3: Compass has referred to this as current best estimate (CBE) in past mission designs.

CBE Mass — *See Basic Mass.*

Dry Mass — *The dry mass is the total mass of the system or spacecraft (S/C) when no propellant or pressurants are added.*

Basic Dry Mass — *This is basic mass (i.e., CBE mass) minus the propellant, or wet portion of the S/C mass. Mass data is based on the most recent baseline design. This is the bottoms-up estimate of component mass, as determined by the subsystem leads. This does not include the wet mass (e.g., propellant, pressurant, cryo-fluids boil-off, etc.).*

CBE Dry Mass — *See Basic Dry Mass.*

MGA — *MGA is defined as the predicted change to the basic mass of an item based on an assessment of its design maturity, fabrication status, and any in-scope design changes that may still occur.*

Predicted Mass	*This is the basic mass plus the mass growth allowance for to each line item, as defined by the subsystem engineers.*
Predicted Dry Mass	*This is the predicted mass minus the propellant or wet portion of the mass. The predicted mass is the basic dry mass plus the mass growth allowance as the subsystem engineers apply it to each line item. This does not include the wet mass (e.g., propellant, pressurant, cryo-fluids boil-off, etc.).*
Mass Reserve (aka Margin)	*This is the difference between the allowable mass for the space system and its total mass. Compass does not set a mass reserve, it is arrived at by subtracting the total mass of the design from the design requirement established at the start of the design study, such as an allowable mass. The goal is to have a mass reserve greater than or equal to zero to arrive at a feasible design case. A negative mass reserve would indicate that the design has not yet been closed and cannot be considered feasible. More work would need to be completed.*
Mass Margin	*The extra allowance carried at the system level needed to reach the AIAA recommended "green" mass risk assessment level, which is currently set at >15 percent for the Authorization to Proceed program milestone. This value is defined as the difference between allowable mass and predicted mass, with the percentage being with respect to basic mass:*

*Percent Mass Margin = (Allowable Mass – Predicted Mass)/Basic Mass*100*

For the current Compass design process, a mass margin of 15 percent is applied with respect to the basic mass and added to the predicted mass. The resulting total mass is compared to the allowable mass as the design progresses. If the total mass is < than the allowable mass, then the mass margin is > 15 percent and the design closes while maintaining a "green" mass risk assessment level.

If total mass ≥ allowable mass, then the design does not close with the required 15 percent mass margin, and either the total mass needs to be reduced, or the mass risk posture reevaluated, and the mass margin reduced. However, depending on the numerical difference, the design may not close even if the mass margin is set to 0 percent.

System-Level Growth	*See Mass Margin*
Total Mass	*The summation of basic mass, applied MGA, and the mass margin (aka system-level growth).*
Allowable Mass	*The limits against which margins are calculated.*

Note: Derived from or given as a requirement early in the design, the allowable mass is intended to remain constant for its duration.

Table 2.3 expands definitions for the MEL column titles to provide information on the way masses are tracked through the MEL used in the Compass design sessions. These definitions are consistent with those above in Figure 2.9 and in the terms and definitions. This table is an alternate way to present the same information to provide more clarity.

For the conceptual level studies conducted by the Compass Team, a mass margin of 15 percent based on basic dry mass is used, which is recommended in the AIAA standard for a grade of "green" at the authorization to proceed milestone, as is shown in Table 2.4. It is worth noting that we assume 30 percent MGA + Mass Margin is suitable for a green rating, providing that there is more allowable mass that would fit to push the percentage slightly above 30 percent. For this study, a "green" rating was achieved across the board.

2.3.2 Mass and Power Growth

The Compass Team normally uses the in AIAA standard S–120A-2015 (Ref. 9) as the guideline for its mass growth calculations. Table 2.5 on the following page shows the percent mass growth of a piece of equipment based on both its level of design maturity and its functional subsystem.

The Compass Team typically uses a 30 percent growth on the bottoms-up power requirements of the bus subsystems when modeling the amount of required power. There is an exception, however, for the mobility subsystem. No additional margin is carried on top of this power growth.

TABLE 2.3.—DEFINITION OF MASSES TRACKED IN MEL

Item	Definition
Basic Mass	Mass data based on the most recent baseline design
	Basic Dry Mass
MGA (Growth)	Predicted change to the basic dry mass of an item phrased as a percentage of basic dry mass
	MGA% * Basic Dry Mass = Growth
Predicted Mass	The basic mass plus the mass growth allowance (MGA)
	Basic Dry Mass + Growth

TABLE 2.4.—MASS RISK ASSESSMENT

Program Milestone	Recommended MGA (%)	Recommended Mass Margin (%)	MGA + Mass Margin (%)	Grade
Authorization to Proceed	> 15	> 15	> 30	Green
	9 < MGA ≤ 15	10 < Mass Margin ≤ 15	19 < MGA + Mass Margin ≤ 30	Yellow
	≤ 9	≤ 10	≤ 19	Red

TABLE 2.5.—AIAA MASS GROWTH ALLOWANCE GUIDELINES FROM AIAA S-120A-2015 (REF. 9)

Maturity Code		Design Maturity (Basis for Mass Determination)	Percentage Mass Growth Allowance												
			Electrical/Electronic Components			Primary Structure	Secondary Structure	Mechanisms	Propulsion, Fluid Systems Hardware	Batteries	Wire Harnesses	Solar Array	ECLSS*, Crew Systems	Thermal Control	Instrumentation
			0-5 kg	5-15 kg	>15 kg										
E	1	Estimated	20-35	15-25	10-20	18-25	20-35	18-25	15-25	20-25	50-100	20-35	20-30	30-50	25-75
	2	Layout	15-30	10-20	5-15	10-20	10-25	10-20	10-20	10-20	15-45	10-20	10-20	15-30	20-30
C	3	Preliminary Design	5-20	3-15	3-12	4-15	8-15	5-15	5-15	5-15	10-25	5-15	5-15	8-15	10-25
	4	Released Design	5-10	2-10	2-10	2-6	3-8	3-4	2-7	3-7	3-10	3-5	3-8	3-8	3-5
A	5	Existing Hardware	1-5	1-3	1-3	1-3	1-5	1-3	1-3	1-3	1-5	1-3	1-4	1-3	1-3
	6	Actual Mass	Measured mass of specific flight hardware; no MGA; use appropriate measurement uncertainty.												
S	7	CFE or Specification Value	Typically, an NTE value is provided, and no MGA is applied.												

Expanded Definitions of Maturity Categories		
E1	Estimated	a. An approximation based on rough sketches, parametric analysis, or incomplete requirements.
		b. A guess based on experience.
		c. A value with unknown basis or pedigree.
E2	Layout	a. A calculation or approximation based on conceptual designs (layout drawings or models) prior to initial sizing.
		b. Major modifications to existing hardware.
C3	Preliminary Design	a. Calculations based on new design after initial sizing but prior to final structural, thermal, or manufacturing analysis.
		b. Minor modification of existing hardware.
C4	Released Design	a. Calculations based on a design after final signoff and release for procurement or production.
		b. Very minor modification of existing hardware.
A5	Existing Hardware	a. Measured mass from another program, assuming that hardware will satisfy program requirements with no changes.
		b. Values substituted based on empirical production variation of same or similar hardware or qualification hardware.
		c. Catalog values.

Note: The MGA percentage ranges in the above table are applied to the basic mass to arrive at the predicted mass.

* Environmental Control and Life Support System

3.0 Baseline Design

3.1 System-Level Summary

A system block diagram of the design is shown in Figure 3.1. The red boxes illustrate the separate elements which were designed, and the rover chassis (provided to the team) is shown in Figure 3.1. Each element configuration is described in the Section 2.2.

3.1.1 Master Equipment List (MEL)

Table 3.1 provides the MEL for the 40 kWe Deployable FSPS. It is a top-level summary of all the subsystem masses and each subsystem section provides details for these values. The masses include basic mass and subsystem margin as applied by each subsystem lead, but do not show the additional 15 percent mass margin added at the system level.

The team ran an additional case, assuming the system needed to be deployed at the lunar equator, instead of the poles. This was not a full design and should not be considered as such, but a top-level MEL was estimated and is shown in Table 3.2.

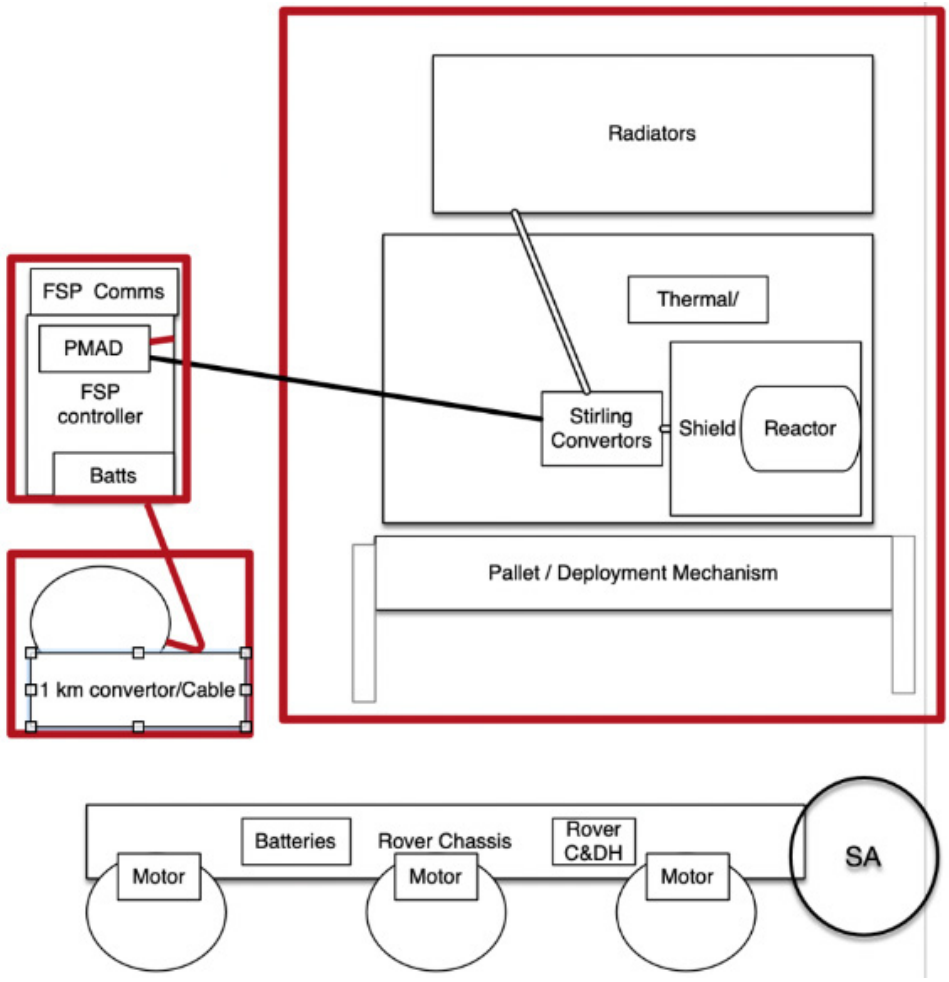

Figure 3.1.—System Block Diagram.

TABLE 3.1.—40 kWe DEPLOYABLE FSPS MEL

Description 40kW_Case 2_FSPS Deployability CD-2021-187	Basic Mass (kg)	Growth (%)	Growth (kg)	Total Mass (kg)
Deployable FSP System	7446	20%	1483	8929
Fission Surface Power System	5590	16%	905	6496
Fission Power Subsystem	3969.1	15%	595.4	4564.4
Thermal Control (Non-Propellant)	1100.6	18%	198.1	1298.8
Structures and Mechanisms	520.4	22%	112.0	632.4
Control Systems	1258	32%	401	1659
Command & Data Handling	46.4	30%	13.9	60.3
Communications and Tracking	25.6	11%	2.8	28.4
Electrical Power Subsystem	733.4	41%	300.2	1033.6
Thermal Control (Non-Propellant)	183.8	18%	33.1	216.9
Structures and Mechanisms	268.7	19%	51.1	319.9
Cable and Spool	597	30%	177	774
Electrical Power Subsystem	357.0	37%	131.2	488.1
Thermal Control (Non-Propellant)	68.1	18%	12.3	80.4
Structures and Mechanisms	172.3	19%	33.4	205.8

TABLE 3.2.—40 kWe DEPLOYABLE FSPS- EQUATOR MEL

Description 40kW_Equator_Case 3_FSPS Deployability CD-2021-187	Basic Mass (kg)	Growth (%)	Growth (kg)	Total Mass (kg)
Deployable FSP System	8315	20%	1640	9955
Fission Surface Power System	6257	16%	1025	7282
Fission Power Subsystem	3969.1	15%	595.4	4564.4
Thermal Control (Non-Propellant)	1706.2	18%	307.1	2013.3
Structures and Mechanisms	581.7	21%	123.0	704.7
Control Systems	1414	30%	429	1843
Command & Data Handling	46.4	30%	13.9	60.3
Communications and Tracking	25.6	11%	2.8	28.4
Electrical Power Subsystem	733.4	41%	300.2	1033.6
Thermal Control (Non-Propellant)	303.7	18%	54.7	358.4
Structures and Mechanisms	305.0	19%	57.7	362.7
Cable and Spool	644	29%	185	829
Electrical Power Subsystem	357.0	37%	131.2	488.1
Thermal Control (Non-Propellant)	114.6	18%	20.6	135.3
Structures and Mechanisms	172.3	19%	33.4	205.8

3.1.2 Architecture Details – Lander Payload and Rover Chassis Assumptions

The Human Class Cargo lunar Lander (Ref. 6) was assumed to be representative in this case. An estimated payload capacity of 12,000 kg delivered to the lunar surface was assumed. Deploying the FSPS from the lander to the surface/rover chassis was considered outside the scope of this design. Additionally, the design assumed the use of a rover chassis, based on the Space Exploration Vehicle Concept (Ref. 7), to carry and deploy the FSPS. Table 3.3 shows the assumed mass properties of this rover chassis. The rover is assumed to be able to transport 9,000 kg per trip.

3.1.3 Spacecraft Total Mass Summary

The MEL in Table 3.4 captures the bottoms-up CBE and growth percentage on the FSPS that was calculated for each subsystem by the subsystem team leads. Mass details per subsystem are provided in Section 4.0, Subsystem Breakdown. Table 3.5 shows the same table for the case on the equator.

To meet the AIAA MGA and margin recommendations (Ref. 9), an allocation is necessary for margin on basic dry mass at the system-level, in addition to the growth calculated on each individual subsystem. This additional margin is shown in the line “Recommended Mass Margin (Additional System Level Growth).”

TABLE 3.3.—ASSUMED MASS PROPERTIES
OF THE ROVER CHASSIS

MEL Summary: Case 1_FSPS Deployability CD-2021-187	Mobility System
Main Subsystems	Total Basic Mass(kg)
Element Dry Mass (no prop,consum)	1600.0
Element Mass Growth Allowance (Aggregate)	240.0
MGA Percentage	15%
Predicted Mass (Basic + MGA)	1840.0
System Level Mass Margin	240.0
System Level Growth Percentage	15%
Element Dry Mass (Basic+MGA+Margin)	2080.0

TABLE 3.4.—SUMMARY OF SYSTEM LEVEL MASS

MEL Summary: 40kW_Case 2_FSPS Deployability CD-2021-187	Fission Surface Power System	Control Systems	Cable and Spool	TOTAL to be carried by Lander
Main Subsystems	Basic Mass (kg)	Basic Mass (kg)	Basic Mass (kg)	Total Basic Mass(kg)
Fission Power System	3969	0.0	0.0	3969.1
Command & Data Handling	0.0	46.4	0.0	46.4
Communications and Tracking	0.0	25.6	0.0	25.6
Electrical Power Subsystem	0.0	733.4	357.0	1090.3
Thermal Control (Non-Propellant)	1100.6	183.8	68.1	1352.6
Structures and Mechanisms	520.4	268.7	172.3	961.5
Element Total	*5590.2*	*1257.9*	*597.4*	*7445.5*
Element Dry Mass (no prop,consum)	5590.2	1257.9	597.4	7445.5
Element Mass Growth Allowance (Aggregate)	905.4	401.1	176.9	1483.4
MGA Percentage	16%	32%	30%	20%
Predicted Mass (Basic + MGA)	6495.6	1659.1	774.3	8928.9
System Level Mass Margin	838.5	188.7	89.6	1116.8
System Level Growth Percentage	15%	15%	15%	15%
Element Dry Mass (Basic+MGA+Margin)	7334.1	1847.8	863.9	10045.8
	Mobility System Trip 1	Mobility System Trip 2		

TABLE 3.5.—SUMMARY OF SYSTEM LEVEL MASS FOR THE EQUATOR CASE

MEL Summary: 40kW_Equator_Case 3_FSPS Deployability CD-2021-187	Fission Surface Power System	Control Systems	Cable and Spool	TOTAL to be carried by Lander
Main Subsystems	Basic Mass (kg)	Basic Mass (kg)	Basic Mass (kg)	Total Basic Mass(kg)
Fission Power System	3969	0.0	0.0	3969.1
Command & Data Handling	0.0	46.4	0.0	46.4
Communications and Tracking	0.0	25.6	0.0	25.6
Electrical Power Subsystem	0.0	733.4	357.0	1090.3
Thermal Control (Non-Propellant)	1706.2	303.7	114.6	2124.6
Structures and Mechanisms	581.7	305.0	172.3	1059.1
Element Total	*6257.0*	*1414.2*	*643.9*	*8315.1*
Element Dry Mass (no prop,consum)	6257.0	1414.2	643.9	8315.1
Element Mass Growth Allowance (Aggregate)	1025.5	429.3	185.2	1639.9
MGA Percentage	16%	30%	29%	20%
Predicted Mass (Basic + MGA)	7282.5	1843.4	829.1	9955.0
System Level Mass Margin	938.6	212.1	96.6	1247.3
System Level Growth Percentage	15%	15%	15%	15%
Element Dry Mass (Basic+MGA+Margin)	8221.0	2055.5	925.7	11202.3
	Mobility System Trip 1	Mobility System Trip 2		

TABLE 3.6.—POWER MODE TITLES AND DESCRIPTIONS

Power Mode Title	Power Mode Duration	Power Mode Description
Launch and Transit to Moon (powered by lander)	150 days	Launch 20 min, 150 days transit
Landing and Offloading from Lander (powered by lander)	2 days	2 kW provided by lander
Load/Transport/Deploy Power Gen at FSPS Site (powered by rover)	1 day	Rover can move 5 km/h, moving 1 km from lander, minimum of 1 km from lunar base
Load/Transport/Mate Controller box pallet (Partially powered by rover)	8 h	(Also, load 1 km spool to deploy later) Mate while on rover power (control box is on rover power) (FSPS is on battery power)
Control Box Deployment (Partially powered by rover)	2 h	50 m to deploy control box, 2 h to deploy cables and control box then start reactor (control box powered by rover)
Reactor Startup	8 h	
Reactor Commissioning	24 h	begin running power through cable at this stage to a shunt on the rover – heats cable and verifies functionality
1 km Cable Deployment	2 days	
Nominal Operations	10 years	
FSPS Idle Operations	TBD days of cool down plus 2 days to move	TBD +2 days

3.1.4 Power Equipment List (PEL)

Table 3.6 provides definitions of the power system power modes. These power modes are used by the subsystem leads to identify the power requirements for each subsystem in each mode.

The power equipment list (PEL) top-level summary from the bottoms-up analysis on the FSPS is listed in Table 4.1. The power summary represents the sum of all power requirements estimated by individual subsystem team leads and include growth allowances assumed in the study. Further discussion of the power and energy requirements of this design can be found in Section 4.1, Electrical Power Subsystem.

4.0 Subsystem Breakdown

This section provides a detailed description of each major FSPS subsystem. In addition to the descriptions and diagrams, each subsection includes a subsystem MEL, which rolls up into the overall system level MEL and mass summary for each case.

4.1 Electrical Power Subsystem

The EPS is responsible for generating, storing, and distributing electrical power to the various loads around the spacecraft. Power generation is provided by a fission power system, which must provide no less than 40 kW to the end user 1 km away through the life of the system.

4.1.1 System Requirements

The driving requirement for the EPS is to provide 40 kW to the end user, 1 km away from the reactor. The EPS must account for any losses between the reactor and the end user to ensure that the end user always has access to 40 kW or more through the life of the system. These losses as well as the power needs of other subsystems are captured in the Compass PEL shown in Table 4.1.

The Compass PEL reflects the current best estimate of electrical loads throughout the spacecraft and breaks it down by subsystem. Electrical losses are captured within the EPS line in the Control System element and within the Cable and Spool element. In addition, the PEL breaks out the estimated electrical power consumption by power mode, capturing the various operational modes that will be seen throughout the life of the spacecraft. Note that the 40-kW user load is not included within the PEL but applies to Power Mode 9 ("Nominal Operations") over a 10-year period.

Power Modes 1 to 5 capture the events required to transfer the system to the Moon, deploy from the lander vehicle, and locate to the final deployment site. During these modes, any electrical power required by this system is provided by the lander or rover elements. Power Mode 6, the first mode where the system will be operating on its own power, encompasses the reactor startup and drives the requirement for energy storage in the system. In Power Mode 7, the reactor is assumed to be operational and performing checkout procedures, but is power positive, so no additional power is required from the energy storage. Similarly, Power Modes 8 to 10 assume the reactor is operating nominally and thus no additional power from the energy storage is required.

TABLE 4.1.—POWERED EQUIPMENT LIST (PEL)

Power Mode	1	2	3	4	5	6	7	8	9	10
Description	Launch/ Transit	Landing/ Offloading	Power Gen Setup at FSPS Site	Ctrl Box Pallet Setup	Ctrl Box Deploy-ment	Reactor Startup	Reactor Comm-issioning	1 km Cable Deployment	Nominal Ops	FSPS Idle Ops
Duration	150 days	2 days	1 day	8 h	2 h	8 h	24 h	2 days	10 year	x+2 days
Deployable FSPS	(W)	(W)	(W)	(W)	(W)	(W)	(W)	(W)	(W)	(W)
FSPS	0.0	0.0	0.0	0.5	6.8	706.8	206.8	206.8	206.8	6.8
Fission Power	0.0	0.0	0.0	0.0	0.0	500.0	0.0	0.0	0.0	0.0
Thermal Control (Non-Propellant)	0.0	0.0	0.0	0.0	6.8	206.8	206.8	206.8	206.8	6.8
Control Systems	0.0	0.0	0.0	0.0	6.8	1584.8	1236.2	1238.3	6290.9	1394.8
C&DH	0.0	0.0	0.0	0.0	0.0	24.0	24.0	26.0	24.0	24.0
Comm & Tracking	0.0	0.0	0.0	0.0	0.0	50.0	50.0	50.0	50.0	50.0
Electrical Power	0.0	0.0	0.0	0.0	0.0	1504.0	1155.4	1155.5	6210.1	1314.0
Thermal Control (Non-Propellant)	0.0	0.0	0.0	0.0	6.8	6.8	6.8	6.8	6.8	6.8
Cable & Spool	0.0	0.0	0.0	0.0	0.0	0.0	0.0	0.0	4532.7	470.1
Bus Power, Total	0.0	0.0	0.0	0.5	13.6	2291.6	1443.0	1445.1	11030.4	1871.7
30% Growth	0	0	0	0	4	687	433	434	3309	562
Total Requirement	0	0	0	1	18	2979	1876	1879	14340	2433

4.1.2 System Assumptions

EPS sizing assumptions regarding the mission and component design/operation are as follows:

Mission

- All EPS components are single-fault-tolerant excluding the main power transfer cable.
  - All single-fault-tolerant components excluding energy storage have one fully redundant unit.
    - Redundant EPS components are always powered on, consuming parasitic power, but not actively operating.
  - The energy storage (battery) includes 1 spare string of cells instead of a second battery unit.
- No EPS power is needed until Power Mode 6 (Reactor Startup).
  - Reactor startup power flows from the system's energy storage back through the Stirling controllers (not through the control system's auxiliary loads). This requires the bidirectional power transfer capability.
  - The auxiliary electrical loads (local to the reactor control system) operate at a nominal 120 Vdc.
- The fission reactor supplies system power and recharges the battery starting with Power Mode 7 (Reactor Commissioning).
- The cable/spool system and end user do not require power until Power Mode 9 (Nominal Operations).
  - The end user requires 40 kW of power at a nominal 120 Vdc.

Fission System

- Eight Stirling generators convert reactor thermal output into single-phase 240 Vac, 50 Hz electrical power.
- Each Stirling generator is paired with two controllers to provide single-fault tolerance.
- The Stirling generators and their controllers are separated by a 50 m power cable to reduce the radiation exposure to the downstream electronics.
- Each Stirling controller rectifies the 240 Vac signal from the Stirling generators into a nominal 400 DC.

Energy Storage

- The energy storage uses a rechargeable Li-ion battery chemistry.
- Battery cells are commercial off-the-shelf (COTS).
- A raw battery output of 4 kW for 1 h (4 kWh) provides sufficient reactor startup power.
- The maximum depth of discharge is 80 percent.

Power Management and Distribution (PMAD)

- The Metcalf Model (Ref. 10) provides mass, volume, efficiency, and parasitic power estimates for several major system components.
- Metcalf Model mass outputs are reduced by 25 percent to account for technology modernization, as the model is based on the ISS PMAD components.
- EPS harnessing between the various electrical components is 25 percent of the total EPS electronics mass (excluding the power transfer cable).
- The main power transfer cable operates at ±2800 Vdc to minimize losses; has an efficiency of 95 percent; and is 1 km in length.

4.1.3 System Trades

Possible system trades include:

- Stirling controller design: a wide variety of strategies have been proposed and demonstrated to accomplish Stirling control, but all utilize similar power conversion hardware, which is the focus of the sizing efforts in this study.
- Power transfer cable sizing, which is determined by the operating power level and operating voltage. In a final FSPS design, transmission voltage and form (AC vs. DC) are set by lunar-grid-level trades that consider system mass minimization, reliability, radiation-hardened component availability, and program risk. While this study used DC cabling, an AC system has the advantage of easier implementation using currently available field effect transistor (FET) switching devices. In an AC system, voltage boost and buck can be addressed using a transformer, virtually eliminating the need for high voltage FETs (Ref. 11).

4.1.4 Analytical Methods

Many of the PMAD components in the power system are sized using the Metcalf Model(Ref. 10). The Metcalf Model contains a number of PMAD models developed to quickly assess candidate architectures for NASA's various Space Exploration Initiative missions in the early 1990s and is designed to generate "ballpark" component mass estimates to support conceptual PMAD system design studies. The model has been validated against the as-built ISS PMAD components. For this design, the Metcalf Model is used to quickly generate sizing estimates for the Stirling controllers (AC/DC static rectifier model), 400 to 120 Vdc bidirectional converter (DC/DC converter model), 400 Vdc to ±2800 Vdc converter (DC/DC converter model), ±2800 to 120 Vdc converter (DC/DC converter model), and 40 kW end user power distribution unit (DC remote bus isolator switchgear model).

The remaining auxiliary PDU is sizing using NASA's Advanced Modular Power System (AMPS) (Ref. 12) technology developed at NASA Glenn Research Center (GRC). The AMPS model is based on real modular PMAD components that are being developed and tested at GRC. Each PMAD box contains a variety of "cards" that serve different functions and can be combined into a single PMAD box depending on the user's needs. For this Compass design, the AMPS components are used to create a low-power 120 Vdc PDU.

4.1.5 Risk Inputs

Two major risks are identified for the EPS: power transfer cable single-point failure and high-voltage electronics development.

While the rest of the EPS assumes single-fault tolerance for all components, the 1 km power transfer cable has no redundancy. Failure of this cable would result in a complete loss of power at the end user. While power cables have high reliability, external sources such as micrometeoroid or orbital debris (MM/OD) strikes or extra-vehicular robotics /extra-vehicular activity near the cable may cause damage. Critical components such as this cable should include redundancy to prevent a full system failure. Ideally, such a redundancy should include a physically separate cable, not just a redundant connection within the existing power transfer cable, to mitigate risks such as MM/OD. The risk card is shown in Table 4.2.

The other major risk for the EPS is with high-voltage electronics development. The main power transfer cable operates at ±2800 Vdc relative to ground, but this high voltage has not been demonstrated on the lunar surface and may require significant development challenges. While terrestrial power grid technologies have implemented high voltage power conversion equipment, space applications have yet to demonstrate these same voltages in space due to the increased radiation exposure. There is significant interest in high-voltage

power electronics for use in lunar or Mars power architectures, but these technologies continue to be developed. In the near term, it therefore may not be practical to utilize a ±2800 Vdc power transfer cable. Based on recent developments in the space power electronics sector, voltages above 600 Vdc will be difficult to achieve today and may require significant development, driving the cost and schedule of any programs seeking high-voltage power electronics. This risk card is shown in Table 4.3.

4.1.6 System Design

The FSPS design consists of three components: the fission reactor, the reactor control systems, and the downstream cable/spool system. The end-to-end efficiency between the Stirling terminals and the end user load is approximately 78 percent.

4.1.6.1 Reactor Design

A previous NASA analysis developed a highly enriched uranium (HEU) fueled fast-spectrum reactor (175 kWth) to meet these same functional needs (Ref. 4). Recently, Los Alamos National Laboratory undertook a preliminary assessment of alternatives to develop a high-assay low-enriched uranium (HALEU) fueled reactor design. Results indicate that YH-moderated HALEU fueled reactors could be used to achieve the required functionality. This HALEU FSPS reactor will need to provide ~250 kWth to supply the required 40 kWe for 10-year operation. The basic HALEU design would use ~20 percent enriched UN pellets with Na–Mo (steel-wick) heat pipes and a YH moderator.

Reactor shielding is a major portion of the reactor mass but can be reduced by situating the power conversion, control electronics, and indeed the crew, at appropriate distances. Table 4.4 shows the assumptions used in this analysis.

Assuming the 1 km distance and the requirement for less than 5 rem/year for permanently present crew, a shadow shield approach is taken. This eliminates a heavy, four-pi-shield, but would require the crew to remain in a 1 km wide area swath, 1 km from the reactor. A mass breakdown of the fission power subsystem for the 40 kWe design can be seen in Table 4.5. Note that these are basic masses and do not include MGA or margin.

TABLE 4.2.—POWER TRANSFER CABLE SINGLE-POINT FAILURE RISK

Risk Title:	Power Transfer Cable Single-Point Failure						Risk Owner:	EPS
Risk Statement:	The main 40 kW power transfer cable does not include redundancy, creating a single point failure within the overall electrical power subsystem.							
Likelihood:	2	Consequence Scores:						
		Safety:	1	Performance:	5	Schedule:	1	Cost:	3
Mitigation Strategy:	Include redundant cable lines to prevent single-point failure in power delivery.							

TABLE 4.3.—HIGH-VOLTAGE ELECTRONICS DEVELOPMENT RISK

Risk Title:	High-Voltage Electronics Development						Risk Owner:	EPS
Risk Statement:	The main 40 kW power transfer cable operates at ±2800 Vdc relative to ground. This high voltage has not yet been demonstrated on the lunar surface and may require significant development challenges.							
Likelihood:	4	Consequence Scores:						
		Safety:	1	Performance:	3	Schedule:	4	Cost:	4
Mitigation Strategy:	Redesign the system for a reduced power transfer cable voltage that may be achievable near-term or invest in the development of high voltage power electronics for the lunar surface.							

TABLE 4.4.—DISTANCE/ RADIATION TOLERANCE ASSUMPTIONS

Item	Distance	Radiation Tolerance
Stirling Components	1 m	n: 5×10^{14} n/cm^2 (>100 keV) Gamma: 25 Mrad (rad Si)
Electronics	10 m	n: 5×10^{11} n/cm^2 Gamma: 25 krad
Humans (Crew)	1 km	Total 5 rem/yr (gamma + neutron); 100% occupancy; 1 km wide swath

TABLE 4.5.— FISSION POWER SUBSYSTEM MASS BREAKDOWN.

Name	Quantity	Unit Mass (kg)	Basic Mass (kg)
Primary Heat Exchanger	1	497	497
Shielding-Li H and W	1	1250	1250
Reactor Control and Instrumentation	1	6	6
Reactor Control Mechanism	1	18	18
Stirling Convertors – gas bearing	8	110	878
Stirling Convertor to Reactor Structure	8	12	93
Balance of Core Assembly	1	1000	1000
Assembly Structure and Cold Plate	1	228	228

4.1.6.2 Power Conversion Design

Stirling convertors are used to convert heat energy from the reactor into reciprocating motion in the linear alternator and then into electrical energy. The flow of heat energy from the reactor into the engine is constant on the time scale of the engine reciprocating frequency and therefore constant electrical energy must be drawn from the alternator to prevent an energy imbalance in the Stirling convertor, which would manifest as the acceleration and overstroke of the piston. The electrical energy drawn from the engine must be equal to the thermal energy into the engine minus losses averaged over the full piston stroke. It is impossible for the user load to perfectly match the constant heat input, and therefore a controller is required to continuously regulate engine operation independent of both the user load and the precise thermal input.

Based upon development efforts during the KiloPower program, thermal losses from the reactor are estimated to be 18 percent. Additionally, thermal losses from the reactor to the Stirling convertor hot end interface are 2 percent based upon recent work at GRC. Significant research and development have gone into the development of 6 kWe-class Stirling convertors, both in and outside of NASA. Because of this, a configuration of eight 6.2 kWe convertors operating as dual opposed pairs are selected after the downstream power management and distribution system losses are estimated. No spare convertors are included for this architecture, and if Stirling convertors fail (forced to fail in pairs), power output from the system would degrade by approximately ¼ for each lost pair.

A hot end temperature of 700 °C (973 K) is set by material limits of the superalloy used for Stirling convertors designed for long-duration operation. Normally, a spectrum of cold end temperatures is traded with the final cold end temperature selected based on which provides the best specific mass (W/kg). Because reactors scale [specific power (Wth/kg)] very efficiently with increasing power, the overall system tends to have lower temperature ratios than radioisotope power systems. Therefore, an optimal temperature ratio of about 2.0 maximizes specific power. Due to limitations in alternator organics development, the cold end temperature is limited to 150 °C (420 K) rather than the best specific system power cold end temperature of 460 K.

Overall end-to-end thermal to electric efficiency is 18.1 percent. Convertor efficiency is 26.1 percent, while downstream power management and distribution (PMAD) efficiency is 87 percent. Radiator inlet/outlet temperatures via a pumped fluid are 420 and 370 K, respectively.

4.1.6.3 Reactor Control System

The EPS architecture of the reactor and reactor control system are shown in Figure 4.1, with the efficiency of each component labeled in red. The "x2" annotation specifies complete unit redundancy (e.g., only 8 Stirling controllers are required, but each controller has a redundant unit to satisfy single-fault tolerance), so there are 16 total controllers in the system (two per generator).

The fission system outputs single-phase electrical power at 240 Vac/50 Hz, which is converted to the nominal 400 Vdc bus; a large capacitive bank is required to buffer the rippling AC power into DC. The 400 Vdc electrical power is then boosted by a DC-DC converter to ±2800 Vdc (5600 Vdc L-L) for power transfer via the 1 km cable (see Section 4.1.7 Cable/Spool System).

The auxiliary electrical system is local to the reactor control system and provides support to the reactor's operation; it includes reactor-related auxiliary loads such as thermal control. The system also includes onboard energy storage needed to start up the fission reactor. During reactor startup, battery power flows downstream to the auxiliary loads as well as back upstream to the controllers. After startup, the reactor power flowing downstream to the 400 Vdc bus supports the auxiliary system operation and recharges the battery. Thus, the power transfer between the 400 Vdc main bus and the 120 Vdc auxiliary bus is bidirectional.

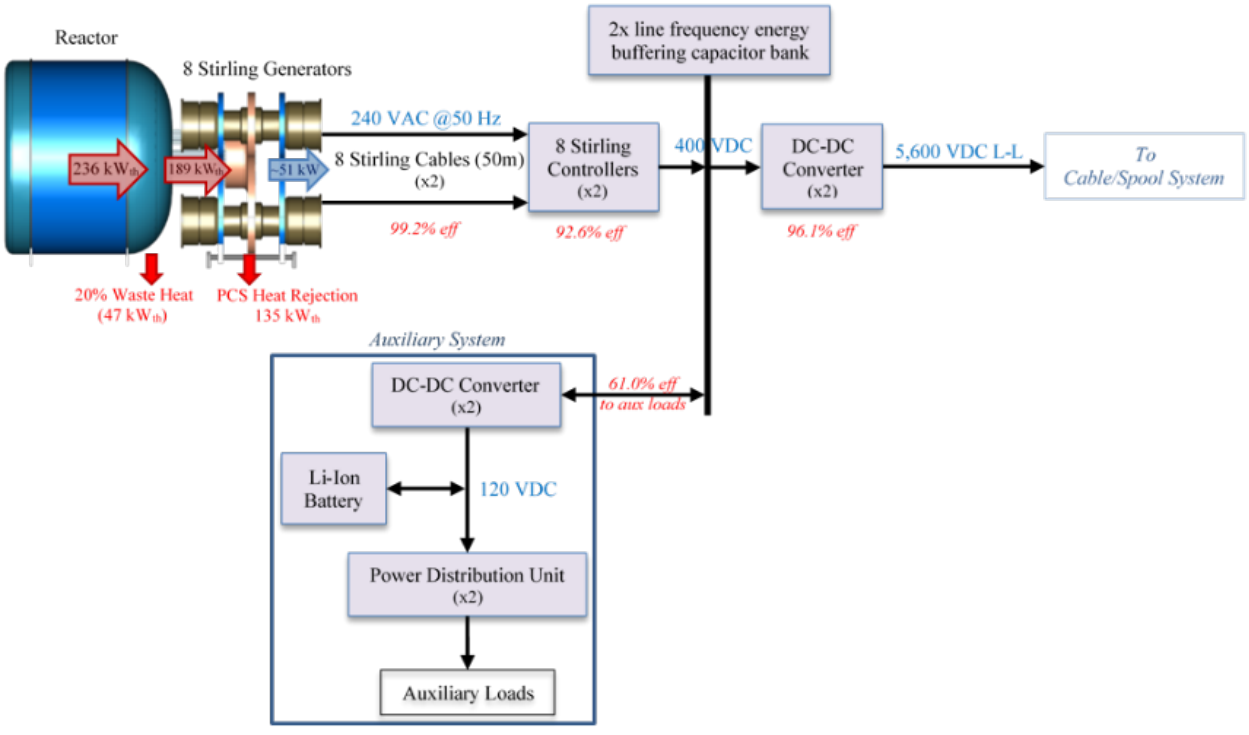

Figure 4.1.—Reactor Control System EPS Design.

The Li-ion battery is tied directly to the 120 Vdc auxiliary bus (battery-on-bus architecture). A dedicated battery charge/discharge regulator is not included. Charge regulation is managed by the upstream auxiliary DC-DC converter unit. The battery is sized to a total energy of 4 kWh and power output of 4 kW to provide reactor startup and auxiliary system power, the maximum battery requirement. Using COTS LG 18650 MJ1 battery cells (Ref. 13), this results in a 34S-13P cell configuration (with one spare string included).

The Metcalf Model is used to size the Stirling controllers and DC-DC converters in the reactor control system. The auxiliary PDU is sized using GRC's Advanced Modular Power Systems (AMPS) technology. Each PDU box consists of 1 controller module (CTLM), 1 housekeeping module (HKPM), two bus switchgear modules (BSGMs), and 5 load switchgear modules (LSGMs) that can support up to 20 total independent loads.

4.1.7 Cable/Spool System

The cable/spool system is shown in Figure 4.2 and starts with the 1-km-long power transfer cable at ±2800 Vdc. A DC-DC converter converts the high voltage from the cable to a nominal 120 Vdc, which is distributed to the end user by a PDU. As before, the "x2" indicates complete unit redundancy (e.g., there are 2 PDUs in the system). The cable/spool system does not begin drawing power until Power Mode 9 (Nominal Operations).

The Metcalf Model is used to size the DC-DC down converter and 40 kW power distribution unit.

In this study, the cable efficiency is held at 95 percent, and an optimization was performed to trade the mass of Al conductors versus the mass of wire insulation over the cable operating voltage. This design only allocated mass for a vacuum-rated, insulated cable without considering micrometeor shielding or redundancy. The minimum wire gauge is capped at 16 AWG for mechanical strength.

Figure 4.3 shows the mass vs. voltage for a 1 km cable carrying 43.5 kWe of power at 95 percent efficiency. Under the assumptions of limited cable protection, this design reaches a mass minimization of ~45 kg at ±2800 Vdc. A similar sweep can be performed for an AC design, resulting in an overall cable that is slightly heavier due to the need for increased insulation thickness based on the increased insulation degradation caused by the AC voltage waveform.

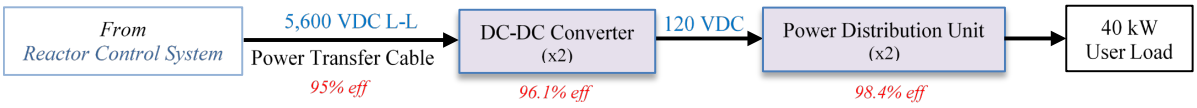

Figure 4.2.—Cable/Spool System EPS Design.

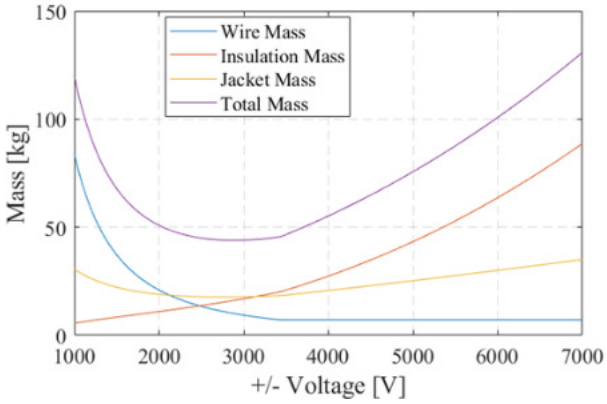

Figure 4.3.—Transmission Voltage vs. Wire Mass for a DC-Insulated Al Cable (1 km, 95% Efficient).

4.1.8 Recommendation(s)

The Team made several assumptions about the operating voltage of various components in the EPS. This is required because of the rapid conceptual design process used by the Compass team. In the future, more detailed assessments of the power system architecture should be made by designers to assess the impact of operating voltage throughout the power system. These operating voltages should be traded against the technology state-of-the-art as well as net system efficiency, factoring in any losses within the main power transfer cable as well as the DC-DC converters on each end of the cable. In addition, the mass of these units should also be weighed as part of this trade since low-voltage units, while technically feasible, may not be a valid solution if they become overly massive.

In addition, many of the EPS PMAD components are designed using the Metcalf Model. While this model is excellent for quick conceptual design analyses, a detailed engineering design should be completed to fully assess and design the various PMAD components in the EPS. In particular, the Stirling controllers are designed using the AC/DC static rectifier model, which does not have a real-world counterpart on the ISS to validate the Metcalf Model. Further design and analysis of these components is needed to continue to assess the feasibility of this design.

4.1.9 Technology Readiness Levels (TRLs)

Table 4.6 provides the TRLs of the various EPS components.

4.1.10 Master Equipment List

Table 4.7, Table 4.8, and Table 4.9 provide the MELs related to the EPS subsystem.

TABLE 4.6.—EPS COMPONENT TRLS

Component	TRL	Reason
Stirling controllers	4	New technology for space, which will require significant design and development for this application.
Stirling controller cables	8	Standard space-rated cable harnessing (AC)
DC-DC converters (400 ↔ ±2800 Vdc)	4	High-voltage boost/buck capabilities are still under development for space applications. High-voltage electronics are challenging to implement in space due to the radiation environment.
DC-DC converter (auxiliary)	6	Non-standard, but feasible operating voltage range will require some development and qualification for the space environment.
PDUs (auxiliary and end user)	6	Similar components exist for space applications but will require significant modification for this design.
Power transfer cable	6	Similar components used for power harnessing in space but will require significant modification for this design.
Li-ion battery	8	Cell qualification testing recently completed by ABSL / Quallion (EnerSys) (Ref. 14)
Harnessing	9	Standard space-rated cable harnessing (DC)

TABLE 4.7.—ELECTRICAL POWER SYSTEMS: CABLE AND SPOOL

Description 40kW_Case 2_FSPS Deployability CD-2021-187	QTY	Unit Mass	Basic Mass	Growth	Growth	Total Mass
Electrical Power Subsystem			**357.0**	**37%**	**131.2**	**488.1**
Power Management & Distribution			**357.0**	**37%**	**131.2**	**488.1**
Power Transfer Cable	1	73.0	73.0	50%	36.5	109.5
DC-DC Converter Unit	2	83.6	167.2	25%	41.8	209.0
Power Distribution Unit	2	42.6	85.2	25%	21.3	106.5
Harness	1	31.6	31.6	100%	31.6	63.1

TABLE 4.8.—ELECTRICAL POWER SYSTEMS: CONTROL SYSTEMS

Description 40kW_Case 2_FSPS Deployability CD-2021-187	QTY	Unit Mass	Basic Mass	Growth	Growth	Total Mass
Electrical Power Subsystem			**733.4**	**41%**	**300.2**	**1033.6**
Energy Storage			**32.5**	**20%**	**6.5**	**39.0**
Lithium-Ion Battery	1	32.5	32.5	20%	6.5	39.0
Power Management & Distribution			**700.9**	**42%**	**293.7**	**994.6**
Stirling Controllers	2	141.5	283.0	25%	70.8	353.8
DC-DC Converter Unit	2	68.2	136.4	25%	34.1	170.5
Auxilary DC-DC Converter Unit	2	19.9	39.8	25%	10.0	49.8
Power Distribution Unit	2	13.5	27.0	25%	6.8	33.8
Harness	1	129.7	129.7	100%	129.7	259.4
Stirling Controller Cable	1	85.0	85.0	50%	42.5	127.5

TABLE 4.9.— ELECTRICAL POWER SYSTEMS: FSPS

Description 40kW_Case 2_FSPS Deployability CD-2021-187	QTY	Unit Mass	Basic Mass	Growth	Growth	Total Mass
Fission Power Subsystem			**3969.1**	**15%**	**595.4**	**4564.4**
FPS Group 1			**2752.4**	**15%**	**412.9**	**3165.2**
Balance of Core Assembly	1	1000.0	1000.0	15%	150.0	1150.0
Primary Heat Exchanger	1	496.4	496.4	15%	74.5	570.8
Shielding- LiH & W	1	1250.0	1250.0	15%	187.5	1437.5
Reactor Control and Instrumentation	1	6.0	6.0	15%	0.9	6.9
FPS Group 2			**988.7**	**15%**	**148.3**	**1137.0**
Reactor Control Mechanism	1	17.5	17.5	15%	2.6	20.1
Stirling Convertors - gas bearing	8	109.8	878.4	15%	131.8	1010.2
Stirling Convertor to Reactor Structure	8	11.6	92.8	15%	13.9	106.7
FPS Group 3			**228.0**	**15%**	**34.2**	**262.2**
Assembly Structure and Cold Plate	1	228.0	228.0	15%	34.2	262.2

4.2 Thermal Control System

The fission reactor system is used to provide power for science and or a human mission at the lunar poles. The landing system consists of the main lander housing the fission reactor. All components of the thermal system are located on the lander. The thermal system addresses the thermal control for the reactor and the electrical components on the lander used to operate the reactor. There are three main components

to the reactor system. Each has a thermal control system needed for their operation on the lunar surface. The thermal system is broken down into three separate systems:

- Reactor thermal control
- Electronics thermal control including a shunt radiator for rejecting waste power from the reactor
- Power distribution thermal control

For the thermal system there is a worst case hot and worst case cold environment. Both are used to size different aspects of the system for each of the three components (reactor, electronics, and distribution). Solar Intensity and view angle as well as the view to warm bodies such as the sunlit lunar surface along with the internal heat generation are used to determine the worst case hot and cold conditions. Operating on the lunar surface means that the thermal environment will change considerably from daytime to nighttime or from sunlit to shadow operation. Therefore, the worst case warm conditions occur while sunlit when all internal components are operating maximizing the waste heat generated. Whereas the worst case cold operating conditions occur while in shadow and worst case nonoperational cold conditions occur during night. The thermal system main components are listed below. Each of these will be described in detail in the following sections.

- Deployable Radiator Panels for each of the Main Systems
- Fixed Shunt Radiator Panel
- Cold Plates
- Heat Pipes
- Pump Loop Coolant System
- Multi-Layer Insulation (MLI)
- Heaters
- Temperature Sensors, Controllers, Switches, Data Acquisition

4.2.1 Operational Environment

The operational environment is a critical aspect to the thermal system design. The surrounding surface temperature is used to determine both the heat loss and heat rejection to the surroundings. The day and nighttime temperature swings on the lunar surface are severe and can fluctuate over 300 °C. During daytime operation near the equator the surface regolith will reach a temperature of ~385 K. Nighttime temperatures at the equator are similar to those at other latitudes including the poles, dropping below 100 K at nighttime. Due to the large temperature swings the equator has the worst operational thermal environment. At higher latitudes the temperature variation between day and night lessens and becomes colder for both the day and nighttime periods. This temperature variation as a function of latitude is shown in Figure 4.4.

The fission reactor system operates primarily at the lunar south pole in both sunlight and shadow conditions. The Team also examined operation at the equator to see how this change in daylight environmental conditions affected the radiator sizing and other aspects of the system. In Figure 4.4 the temperature curve for 89° N latitude, near the lunar pole, shows a maximum temperature of ~150 K and a minimum temperature of ~50 K. There is also a long period of time where at this latitude there is continual darkness (from day 95 to day 230). This is seen by the flat, slowly descending temperature curve over this period. Operation within a crater or previously shadowed region (PSR) in the polar region provides extremes in temperature. These range from the PSR (estimated to be maintained at 30 to 50 K), to the sunlit portion which, depending on the latitude, can achieve temperatures up to approximately 240 K.

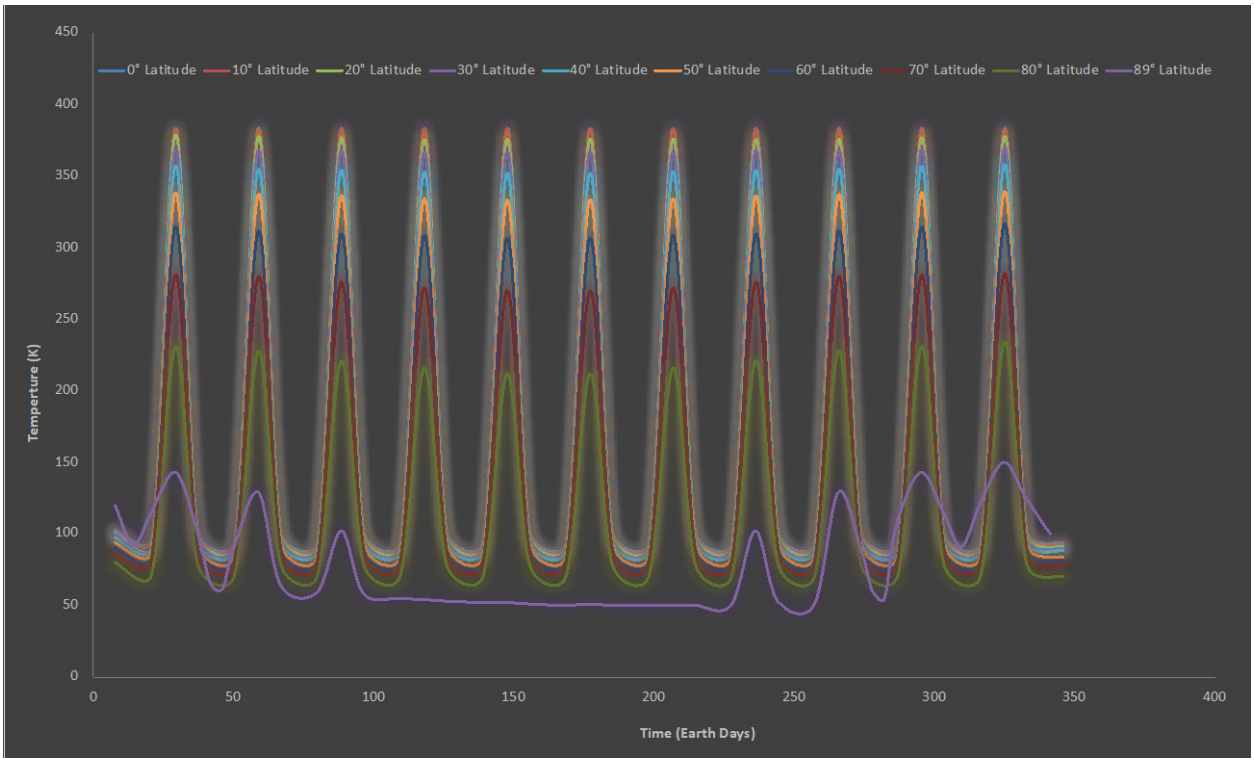

Figure 4.4.—Lunar Surface Temperature for Latitudes from the Equator to the Pole over 1 Earth Year.

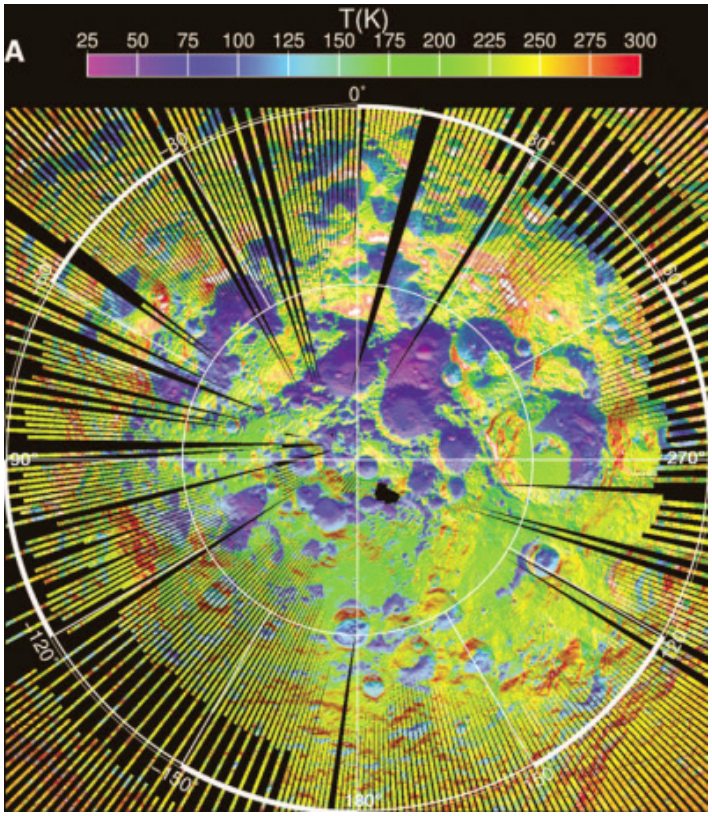

Figure 4.5.—LRO Surface Temperature Distribution for the Lunar South Pole.

The temperature curves shown in Figure 4.5 represent average surface temperature at the latitudes shown. However, the actual surface temperature will vary significantly, particularly at the poles, depending on surface elevation and slope. This variation is shown in Figure 4.6 for the lunar south pole.

As shown in Figure 4.6, surface temperatures outside of the craters at the South pole under sunlit conditions will achieve temperatures in the range of 130 to 275 K depending on their elevation and angle to the Sun. Whereas temperature variation within a crater during daytime ranges from less than 50 to 275 K. Based on the average surface temperatures and an assumed view factor to the surroundings of 0.5, the effective sink temperature at the pole for an object in sunlight is approximately 235 K.

Even though the lunar declination angle is small at 1.5°, there still are seasonal effects for the craters at or near the polar location. These effects are shown in Figure 4.6. Quadrants A and C show the maximum temperature variation between the summer and winter. This variation is on the order of 30 to 40 K where the permanently shadowed region of the crater would vary between 70 K in the summer and 40 K in the winter. The amplitude of the temperature, shown in quadrants B and D, represent the day and night temperature variation for the summer and winter respectively. This shows that the day and night temperature fluctuations are low and are comparable to or less than the variation between the maximum summer and winter temperatures. Table 4.10 summarizes the environmental conditions at the lunar pole.

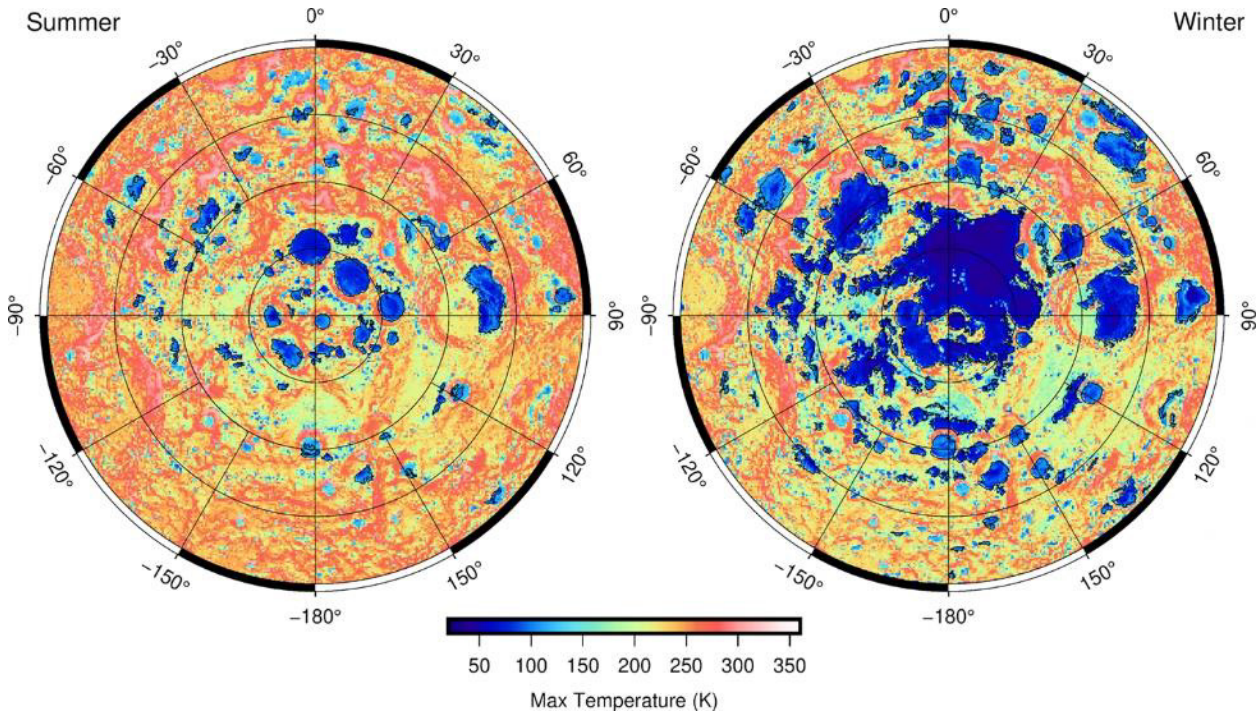

Figure 4.6.—Maximum Surface Temperature and Amplitude for PSRs at the Lunar South Pole (Ref. 15, Creative Commons CC BY-SA 4.0 license, https://creativecommons.org/licenses/by/4.0/)).

TABLE 4.10.—ENVIRONMENTAL CONDITIONS

	Surface	PSR
Sky Temperature	4 K (–269 °C)	4 K (–269 °C)
Surface Temperature Sunlit	254 K (–19°C)	NA
Surface Temperature Shadow	60 K (–213°C)	60 K (–213 °C)
Average Sink Temperature Sunlit (horizontal Surface)	133 K (–140 °C)	NA
Average Sink temperature sunlit (6-sided cube)	235 K (–38 °C)	NA
Average Sink Temperature in Shadow	50.5 K (–222.5 °C)	50.5 K (–222.5 °C)
Solar Heat Input	1370 W/m^2	NA

TABLE 4.11.—THERMAL SYSTEM REQUIREMENTS

Specifications		Value/Description
Waste heat:	Fission Reactor	126,400 W
	Electronics	5,100 W
	Power Distribution	2,000 W
	Shunt Power	40,000 W
Operating Temperature		Average reactor operating temperature 395 K (420 K inlet, 50 K Temperature drop across the radiator with exit temperature at 370 K) Electronics ~ 271 K to 310 K (–3 to 37 °C) Shunt Radiator 800 K
Enclosure Dimensions: Reactor Electronics Power Distribution		 Length (l_e) 1.5 m, Width (w_e) 0.75 m, Height (h_e): 0.6 m Insulation surface area: 5.0 m^2 Length (l_e): 1.0 m, Width (w_e) 0.75 m, Height (h_e) .6 m, Surface Area 3.6 m^2
Insulation (MLI)		25 layers of MLI are used to cover all external surfaces for the electronics enclosure and back side of the shunt radiators.
Environment		Lunar polar operation 50 to 220 K surface temperature range
Radiators		Fission Reactor: Accordion Deployable Double Sided Electronics: Fixed Single Sided Shunt: Fixed Single Sided
Cooling		Fission Reactor: Pump Loop Cooling System Electronics: Heat Pipe Cooling System Shunt: Electrical Heaters
Heating		Electric heaters are used to provide heating to the internal components as needed.

4.2.2 Thermal System Requirements

The system requirements are based on the waste heat generated by the various components and systems. This waste heat is used to size the radiators for rejecting the heat to the surroundings. In addition to the waste heat power level the operating temperature of the components is used to determine the rejection temperature of the radiator. Table 4.11 identifies the FSPS enclosure specification, assumptions and requirements for the thermal system design and operation.

4.2.3 Radiator System Design and Sizing

The sizing of the system is based on the heat load that must be rejected and the heat transfer from the radiator by radiation to the surroundings. The radiation heat transfer (Q_r) on the lunar surface is based on the view the radiator must both the surface (F_{sur}) and the sky (F_{sky}) as well as the input heat flux from the Sun. These two views compose the total view of the radiator to the surroundings as given by Equation (1).

$$1 = F_{sur} + F_{sky} \tag{1}$$

The total radiative heat transfer from the radiator to the surface and sky is dependent on the emissivity of the radiator (e) as given by Equation (2).

$$Q_r = A_r \varepsilon \sigma \left[F_{sky} \left(T_r^4 - T_{sky}^4 \right) + F_{sur} (T_r^4 - T_{sur}^4) \right] - \alpha \phi_s [\cos(\beta) + a \cos(\gamma)] \tag{2}$$

Where the Stefan-Boltzmann constant (s) is:

$$\sigma = 5.670367 \times 10^{-8} \ [\mathrm{W/m^2K^4}] \tag{3}$$

An estimate of the radiator mass (M_r) can be made based on its required area. The radiator structure is separated into a number of components with a scaling coefficient for each component to linearly scale the mass based on the required A_r. These coefficients, listed in Table 4.12, are derived from satellite and spacecraft radiator mass data. The total M_r is given by Equation (4).

$$M_r = C_p A_r + C_c A_r + C_t A_r + C_h A_r + C_a A_r + C_s A_r + C_{at} A_r + C_{ds} A_r \tag{4}$$

It should be noted that louvers are not used on the radiators. Louvers are generally required to reduce the heat loss to the environment during times of low power output or during nighttime operation. However, since the reactor system is designed to operate continuously once started, the addition of the louvers is not needed during normal operation. The main concern with not having louvers on the radiator is that if the system needs to shut down during a nighttime period, the radiators will cool rapidly and freeze the coolant loop coolant. This can become an issue during restart of the system. The risk and mitigation approaches to a nighttime shutdown of the system will need to be addressed in future work.

TABLE 4.12.—RADIATOR MASS SCALING COEFFICIENTS

Radiator component	Value, g/m^2
Panels, C_p	3.30
Coating, C_c	0.42
Tubing, C_t	1.31
Header, C_h	0.23
Adhesives, C_a	0.29
Stingers, C_s	1.50
Attachment, C_{at}	0.75
Deployment and Structure, C_{ds}	6.84

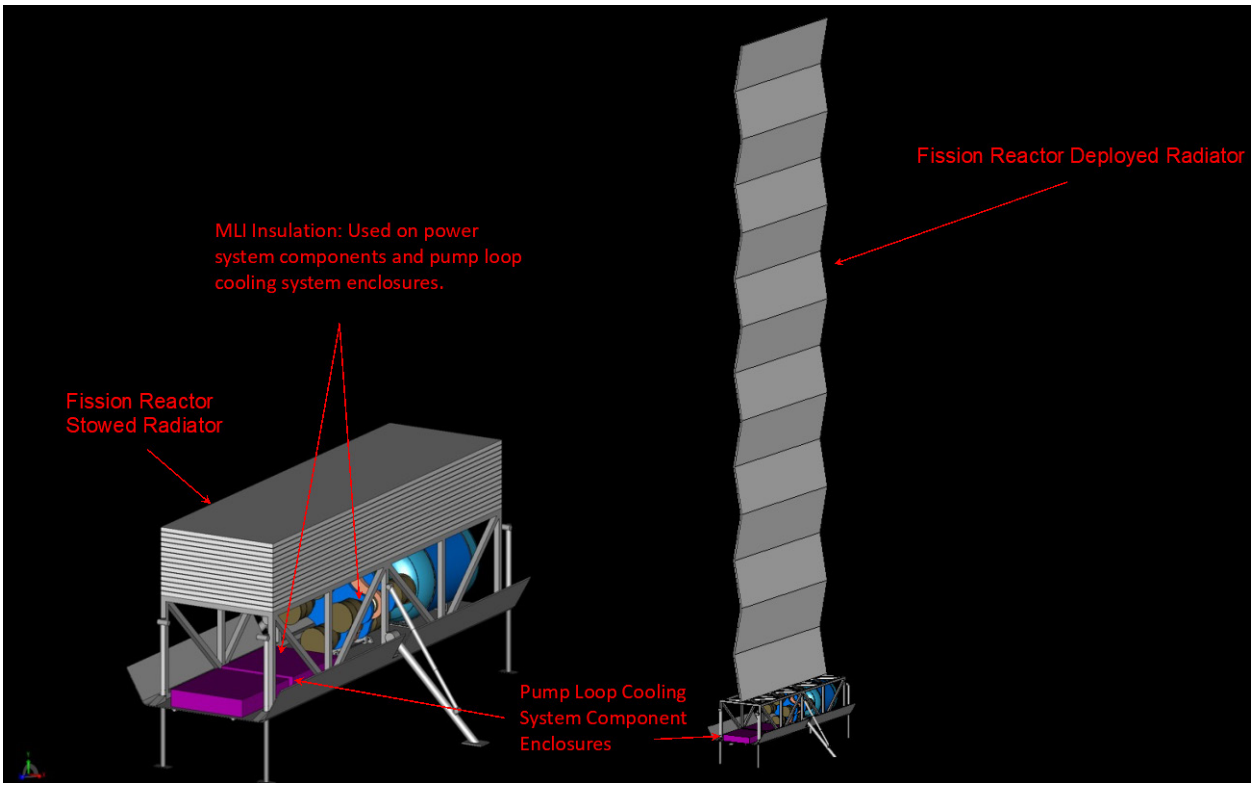

Figure 4.7.—Reactor Waste Heat Radiator Illustration.

4.2.3.1 Reactor Waste Heat Radiator

The radiator is deployed vertically on the top deck of the transport sled with both the front and back sides acting as radiating surfaces as illustrated in Figure 4.7. This provides a good view to deep space and the surrounding lunar surface. The Team assumed a 0.5 view factor to deep space and a 0.5 view factor to the lunar surface.

The Team assumed a worst-case Sun angle onto the radiator. It is assumed that the solar flux is normal to one side of the radiator. However due to the dual sided operation of the radiator, the opposite side only had a view to deep space and the surface. This situation is approximated by a 45° Sun angle to the total radiator area. The radiator sizing is based on an energy balance analysis of the area needed to reject the identified heat load to space. From the area, a series of scaling equations, given by Table 4.12, are used to determine the mass of the radiator. The radiator is sized to remove the waste heat from the fission reactor during worst-case hot operational conditions, which occur while sunlit on the lunar surface under full power operation. A pump loop cooling system is baselined as the means of moving heat from the Stirling engines to the radiator.

The radiator is sized using a power balance between the heat input from the surroundings and the heat rejection to the surroundings based on the desired operating temperature for the radiator. This power balance is illustrated in Table 4.17. The Team assumed that the radiator has a 50 percent view to the surrounding surface and a 50 percent view to the sky. The main heat load on the radiator is from the Sun which is just above the horizon for operation at the south pole.

The overall mission and corresponding thermal design are for operation at the lunar south pole. However, the reactor radiator is sized to determine how operations at different lunar locations would affect the radiator size. The worst-case operational conditions for the radiator sizing would be at the equator. This can be seen by the temperature data in Figure 4.4 where the surface temperatures at the

equator reach the highest level compared to other latitudes. Figure 4.8 shows the radiator sizing and surface conditions for operation at the equator.

Figure 4.9 shows the required size for the radiator from the beginning of the lunar day until just past noon. This size is needed to reject the waste heat from the 10-kW reactor as the rises and the surface temperature increases. The maximum surface temperature occurs after solar noon as the surface will continue to heat until the Sun angles drop low enough so that the radiative temperature balance begins to decrease. Figure 4.9 also shows the effective sink temperature for the radiator for two different orientations, normal to the Sun and parallel to the Sun. Initially the sink temperatures vary considerably with the radiator oriented normal to the rising Sun being approximately 70 °C warmer than that for the array parallel to the Sun. As the Sun increases in elevation the effect of the radiator orientation diminishes and the sink temperatures between the two radiator orientations get closer together. At noon when the Sun is directly overhead, the sink temperature is equal for both the normal and parallel radiators as expected. The sink temperatures continue to rise as the Sun passes noon because the surface temperature is still increasing and reaches a maximum of approximately 325 K for the parallel radiator and approximately 330 K for the normal radiator when the surface temperature reaches its maximum temperature of approximately 385 K. The worst-case or greatest required radiator area for operation at the equator occurs at this maximum surface temperature and corresponding maximum sink temperature during the day for each radiator orientation. This represents a 62 percent increase in radiator surface area between operating at the pole to operating at the equator. Table 4.13 summarizes the specifications for the operation and sizing for both at the pole and equator.

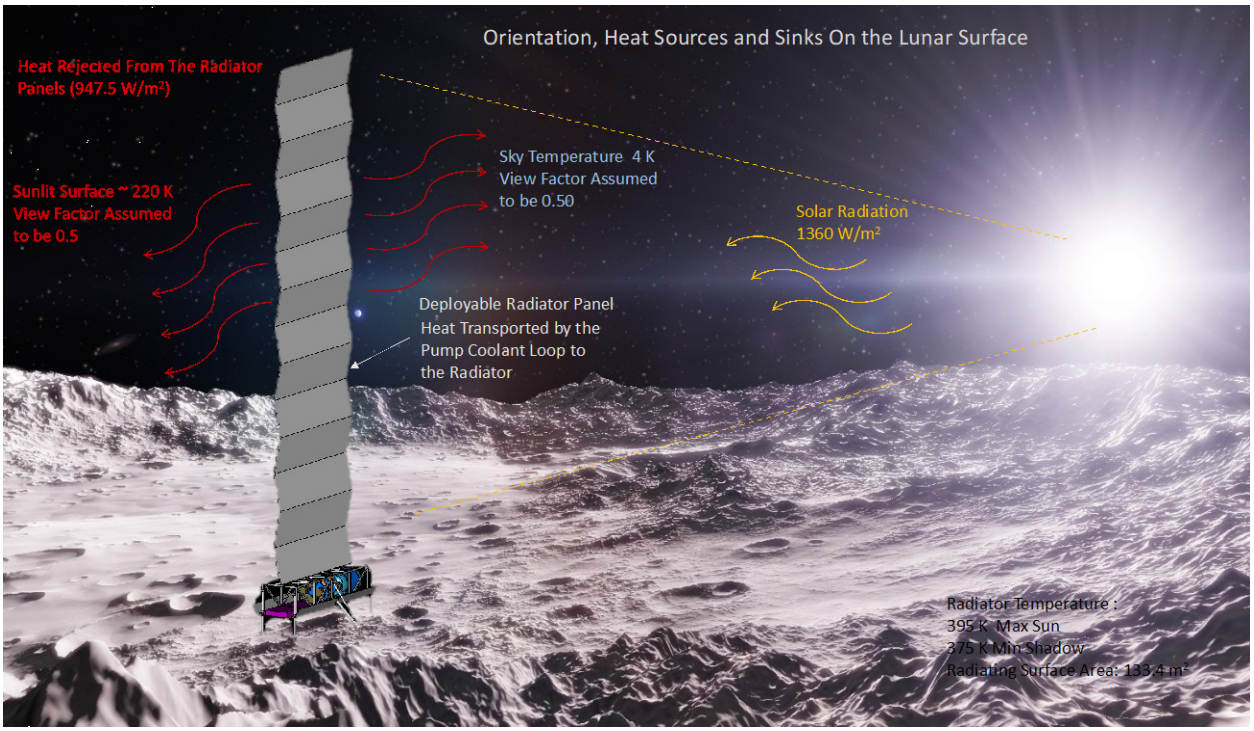

Figure 4.8.—Reactor Radiator Thermal Power Balance Illustration.

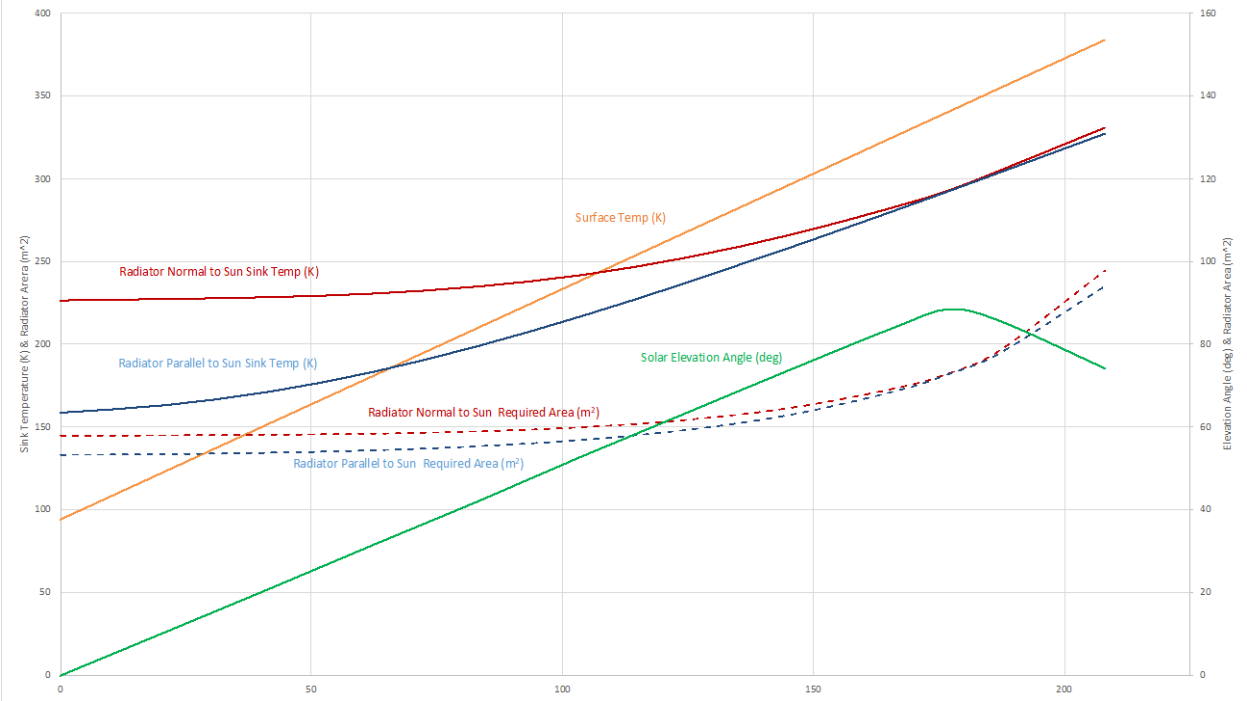

Figure 4.9.—Environmental Conditions and Radiator Sizing for Operation at the Equator.

TABLE 4.13.—REACTOR WASTE HEAT RADIATOR SPECIFICATIONS

Variable	Value
Radiator Solar Absorptivity	0.14
Radiator Emissivity	0.84
Max Radiator Sun Angle	45°
View Factor lunar surface	0.5
View Factor to Deep Space	0.5
Radiator Operating Temperature	In Sunlight 395 K nominal (420 K inlet, 370 K exit)
	In Shadow: 375 K nominal
Power Dissipation and Radiator Area (operation at the pole)	126,400 W
	133.4 m^2 (Accordion Deployable)
Power Dissipation and Radiator Area (operation at the equator)	126,400 W
	216.2 m^2 (Accordion Deployable)

The radiator configuration is based on the international space station accordion radiator. This type of radiator has panels that fold out in an accordion fashion to deploy as shown in Figure 4.10. Basing the reactor main radiator on the ISS radiator system provides the ability to utilize space qualified hardware and flight heritage in the radiator and coolant system design. The ISS radiator panel has several characteristics that would be applicable to the FSPS main reactor radiator.

- Accordion Deployable Panels
- Pump Loop Cooling System
- Rotatable Panels
- Comparable Radiator Area (79 m^2 Per Panel)

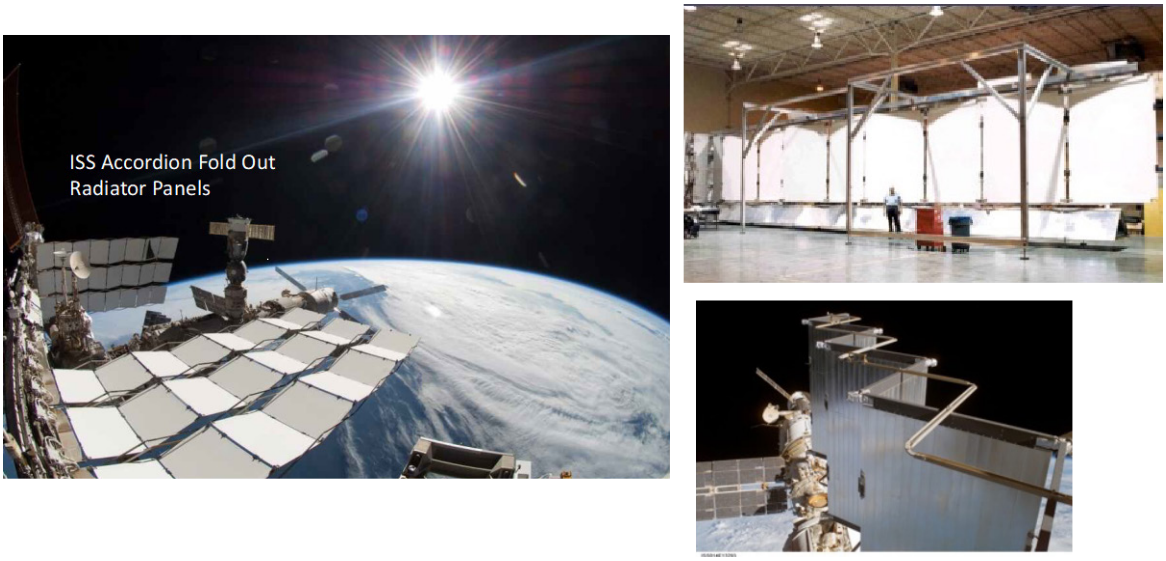

Figure 4.10.—ISS Deployable Radiator.

Because of the high heat load and the required radiator size for operation at the equator or lower latitudes on the lunar surface, alternate radiator approaches can be considered. One alternate approach that may provide benefits is a liquid droplet radiator. This radiator concept is not new, but the technology is at a very low level for space applications. A liquid droplet radiator sprays the cooling fluid in droplets which then reject heat to the surroundings. The droplets then drop down into a collector and the fluid is pumped through the cooling system to heat up again. Figure 4.11 illustrates this approach.

The advantages to this type of radiator system include:

- Compact size: the rejection area is based on the number of droplets sprayed and the time they stay aloft.
- Reduced weight: since radiator panels are not needed, the cooling fluid is used directly for cooling.
- Scales to large thermal power levels.
- Lunar surface operation provides benefits due to the gravitational field.

The disadvantages in addition to being at a low development level are that the fluid loss to the surroundings through evaporation can be significant and that it would be easy to containment the system with lunar dust since the coolant fluid is exposed to the surroundings.

4.2.3.2 Reactor Electronics Waste Heat Radiator

An accordion deployable radiator is also utilized to provide cooling for the electronic components of the fission power system. The radiator is located on the upper deck of the electronics sled above the electronics enclosure. But unlike the reactor waste heat radiator, a heat pipe system is used to move the heat from the electronics to the radiator. Figure 4.12 illustrates this radiator placement.

As with the reactor waste heat radiator, the reactor electronics radiator is sized based on an energy balance analysis of the area needed to reject the identified heat load to space. From the area a series of scaling equations, given by Table 4.12, are used to determine the mass of the radiator.

The radiator is oriented vertically and radiated to the surroundings from both sides of the radiator. The electronics are operated at a temperature up to 300 K. The radiator is sized to remove the waste heat from the fission reactor electronics during worst case hot operational conditions, which occur while sunlit on the lunar surface under full power operation. This power balance is illustrated in Figure 4.13. It is assumed that the radiator had a 50 percent view to the surrounding surface and a 50 percent view to the sky. The main heat load on the radiator is from the Sun, which is just above the horizon for operation at the south pole.

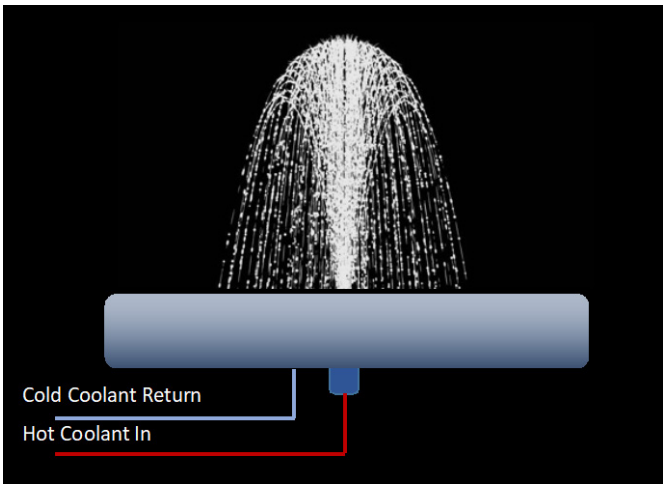

Figure 4.11.—Liquid Droplet Radiator Illustration.

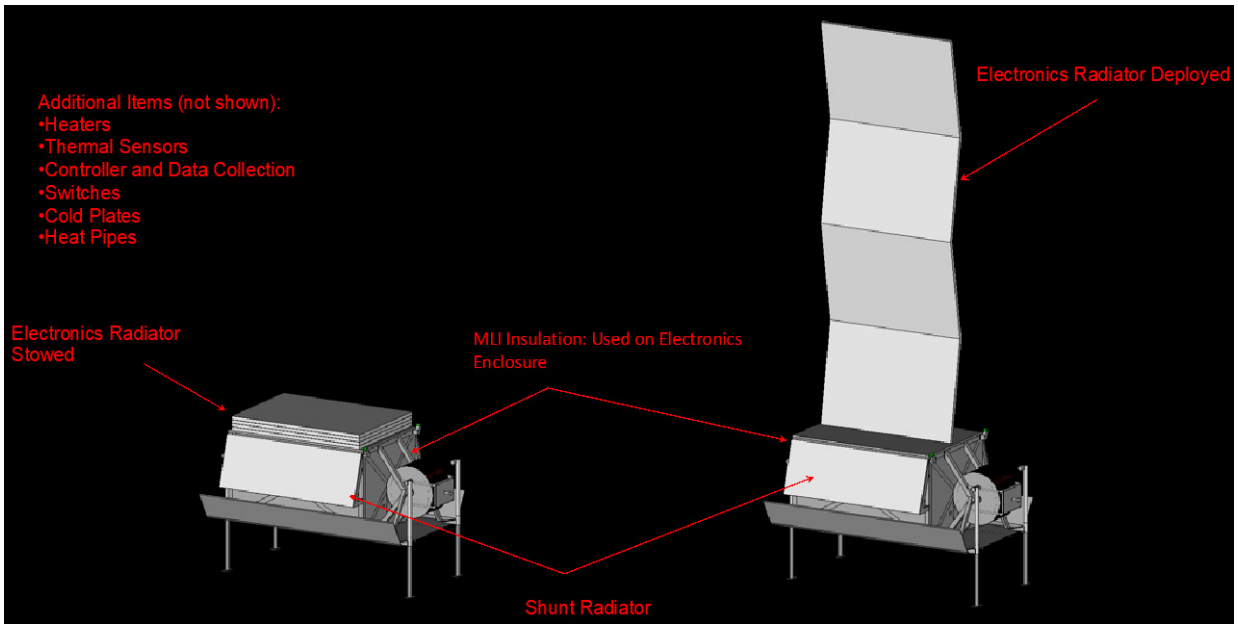

Figure 4.12.—Reactor Electronics Radiator Illustration.

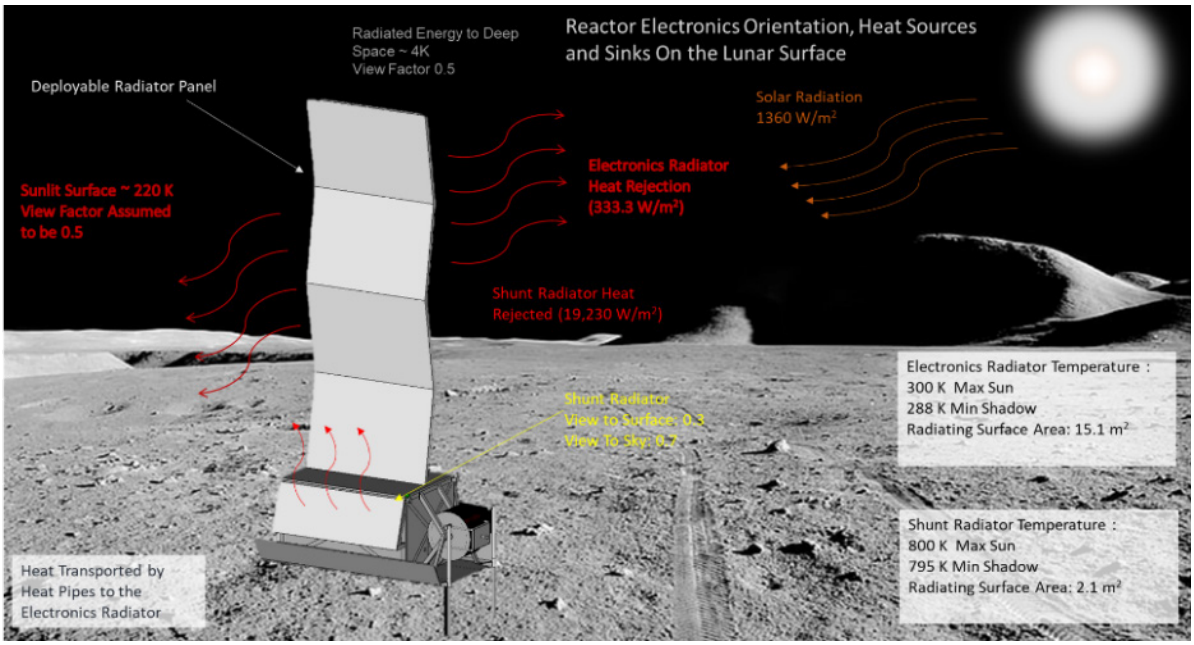

Figure 4.13.—Reactor Radiator Thermal Power Balance Illustration.

TABLE 4.14.—REACTOR ELECTRONICS RADIATOR SPECIFICATIONS

Variable	Value
Radiator solar absorptivity	0.14
Radiator emissivity	0.84
Max radiator Sun angle	45°
View factor to lunar surface	0.5
View factor to deep space	0.5
Radiator operating temperature	Electronics: 288 to 300 K
Power dissipation and radiator area (Operation at the pole)	5,100 W
	15.3 m^2 (double-sided, deployable)
Power dissipation and radiator area (operation at equator)	No solution, radiation configuration must be changed

During shadow, and if the electronics system thermal output decreases, heaters will be used to maintain the internal temperature of the electronics enclosure. Louvers are not used on the radiator since the reactor will be operating continuously once started and the electronics will provide sufficient waste heat during operation. The radiator orientation also provides the best operating conditions for the heat pipe system by locating the condenser section above the evaporator section thereby returning the fluid in the direction of the gravity field. Due to the low heat rejection temperature, this radiator cannot operate at the lunar equator with the current configuration. To work at the equator the orientation of the radiator must change to a single-sided horizontal radiator to reduce the ambient sink temperature by eliminating the view of the radiator to the lunar surface. The electronics radiator specifications are given in Table 4.14.

4.2.3.3 Power Shunt Radiator

A shunt radiator is used to absorb excess power and convert it to heat. This type of radiator is essentially a resistor that heats up as current is passed through it.

Under conditions where the load demand on the reactor is less than the output produced and there is a desire to maintain a higher output power level, the shunt radiator is used to reject this excess power. This

type of power rejection is used as a means of regulation of the reactor and the power conversion system. This radiator allows the reactor to operate within its design output power limits when the load demands are too low. It can also be used as a means of testing the reactor by providing a load to which the reactor can send power to verify its operation. The shunt radiator is sized to reject the full 40 kW output of the reactor.

The shunt radiator is located on the side of the electronics sled and is angled toward the sky to provide a better view to deep space and to minimize its view of any surrounding equipment. This will minimize the heat load from the shunt radiator onto that equipment. The positioning of the shunt radiator on the electronics sled is illustrated in Figure 4.12. The radiator is divided into two segments on opposite sides of the electronics sled. The radiator sizing is based on an energy balance analysis of the area needed to reject the identified heat load to space, as illustrated in Figure 4.13.

The radiator is designed to operate at 800 K. This high operating temperature enables the shunt radiator to be compact and fit on the sides of the electronics sled without the need for deployment. The back side of the shunt radiator panels are insulated to minimize the heat flux from the radiator to the electronics enclosure. The shunt radiator specifications are given in Table 4.15.

4.2.3.4 Power Distribution Electronics Waste Heat Radiator

As with the reactor waste heat and electronics, an accordion deployable radiator is utilized to provide cooling for the power distribution electronics. The radiator is located on the upper deck of the power distribution sled above the conditioning electronics enclosure. As with the reactor electronics radiator, a heat pipe system is used to move the heat from the power distribution and conditioning electronics to the radiator. This radiator placement is illustrated in Figure 4.14.

As with the other radiators, the power distribution electronics radiator is sized based on an energy balance analysis of the area needed to reject the identified heat load to space. From the area a series of scaling equations, given by Table 4.12, are used to determine the mass of the radiator.

The radiator is oriented vertically on top of the power distribution sled and radiated to the surroundings from both sides of the radiator. The power distribution electronics are operated at a temperature up to 300K. The radiator is sized to remove the waste heat from the power distribution electronics during worst case hot operational conditions, which occur while sunlit on the lunar surface under full power operation. This power balance is illustrated in Figure 4.15. It is assumed that the radiator had a 50 percent view to the surrounding surface and a 50 percent view to the sky. The main heat load on the radiator is from the Sun, which is just above the horizon for operation at the south pole.

During shadow, and if the distribution electronics system thermal output decreases, heaters will be used to maintain the internal temperature of the electronics enclosure. As with the other radiators, louvers are not used on the radiator since the reactor will be operating continuously once started and the distribution electronics will provide sufficient waste heat during operation. The radiator orientation also

TABLE 4.15.—SHUNT RADIATOR SPECIFICATIONS

Variable	Value
Radiator solar absorptivity	0.14
Radiator emissivity	0.84
Max radiator Sun angle	45°
View factor to lunar surface	0.3
View factor to deep space	0.7
Radiator operating temperature	795 to 800 K
Power dissipation and radiator area	40,000 W
	2.1 m^2 (single-sided, fixed-body mounted)

provides the best operating conditions for the heat pipe system by locating the condenser section above the evaporator section thereby returning the fluid in the direction of the gravity field. Due to the low heat rejection temperature, this radiator cannot operate at the lunar equator with the current configuration. To work at the equator the orientation of the radiator must change to a single-sided horizontal radiator to reduce the ambient sink temperature by eliminating the view of the radiator to the lunar surface. The shunt radiator specifications are given in Table 4.16.

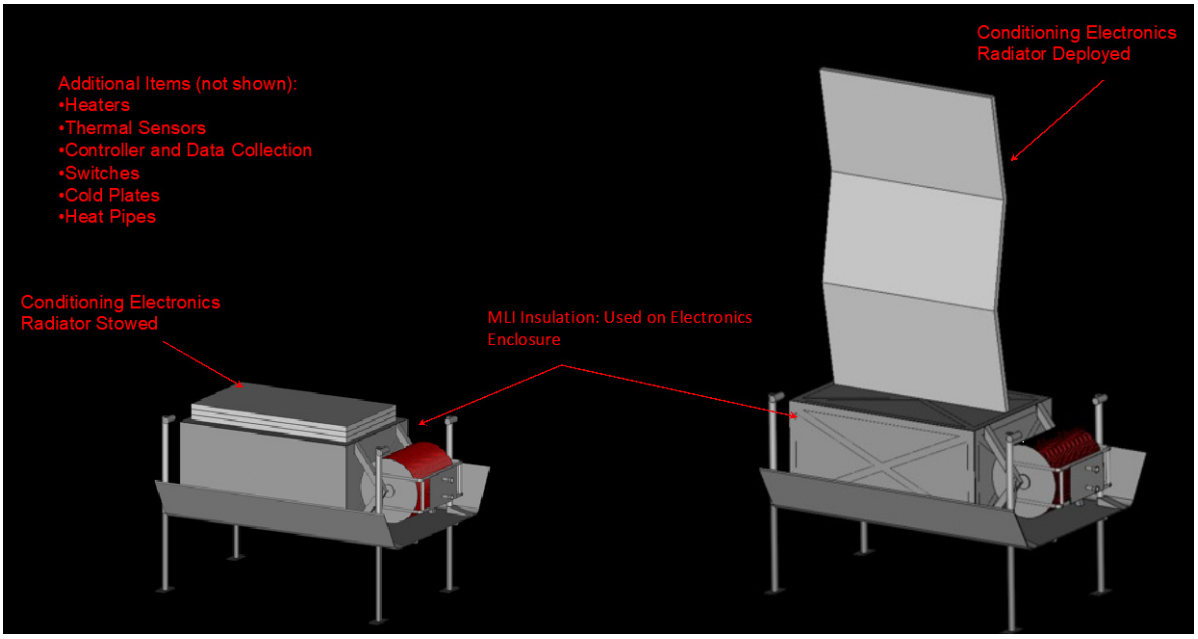

Figure 4.14.—Power Distribution Electronics Radiator Illustration.

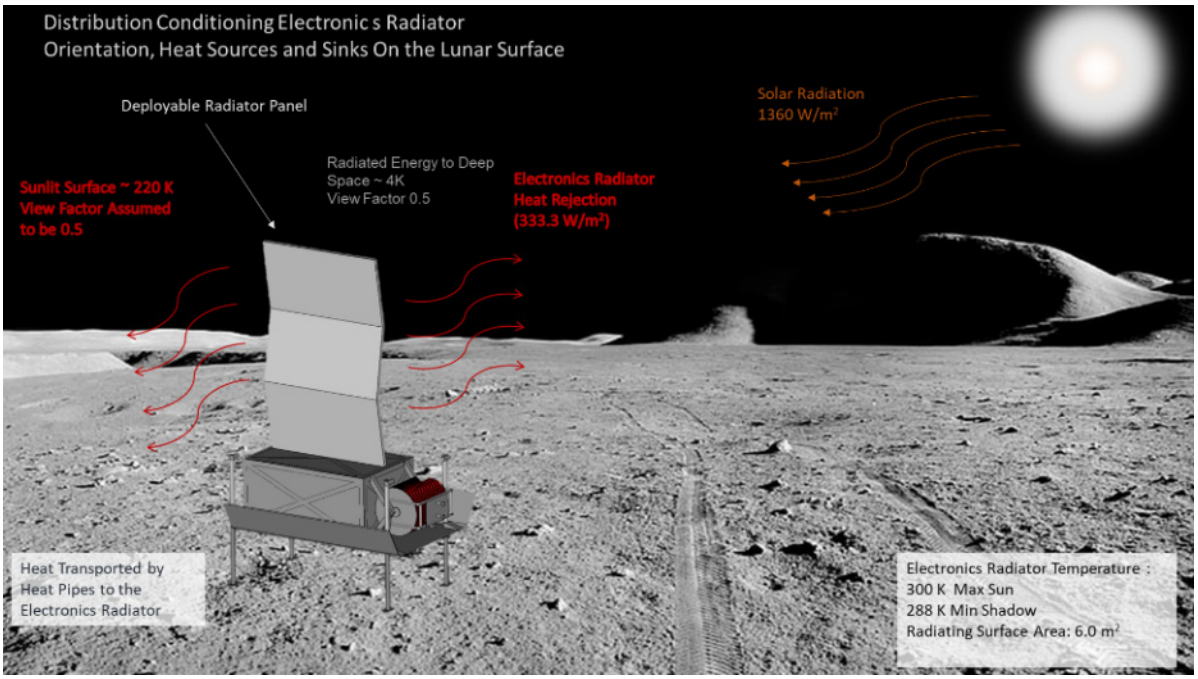

Figure 4.15.—Reactor Radiator Thermal Power Balance Illustration.

TABLE 4.16.—POWER DISTRIBUTION ELECTRONICS RADIATOR SPECIFICATIONS

Variable	Value
Radiator Solar Absorptivity	0.14
Radiator Emissivity	0.84
Max Radiator Sun Angle	45°
View factor to lunar surface	0.5
View factor to deep space	0.5
Radiator operating temperature	Electronics: 288 to 300 K
Power dissipation and radiator area (operation at the pole)	2,000 W
	6.0 m^2 (double-sided, deployable)
Power dissipation and radiator area (operation at equator)	No solution, radiation configuration must be changed

4.2.3.5 Pump Loop Coolant System

The coolant system for the reactor radiator is similar to that used for the ISS radiator. It is a pump loop system that uses a fluid to collect heat from the cold end of the Stirling converters and pumps that fluid to the radiators to reject the heat to the surroundings. This system is illustrated in Figure 4.16.

Figure 4.16 represents a generalized approach to the coolant system components for the reactor radiator pump loop coolant system. Utilizing a coolant design similar to that of the ISS radiator coolant system provides development benefits since that system has space heritage. Changes to the ISS coolant system will be necessary to accommodate the differences between the heat load integration and operating environment. The main differences include:

- Operation within the 1/6 g lunar environment versus 0 g orbital environment
- The ability to shunt a portion of the coolant fluid around the radiator to provide thermal control for the reactor during startup and shutdown.
- The integration of the Stirling engine cold end heat removal cold plates.
- The radiator operating temperature for the reactor is 395 K (122 °C). The ISS has two coolant loops operating at 277 K (4 °C) and 290 K (17 °C).
- The ISS utilizes Ammonia as the coolant fluid. At the higher operating temperature of the reactor a different coolant fluid would be utilized.

In the baseline design shown above, the coolant flows through tubes integrated into the radiator. This is similar to the ISS design approach. An alternative approach that can be considered is to flow the coolant into a manifold that transfers the heat from the coolant loop to heat pipes. The heat pipes are then integrated into the radiator panel. Both arrangements are illustrated in Figure 4.17 and the advantages and disadvantages to these two approaches are listed in Table 4.17.

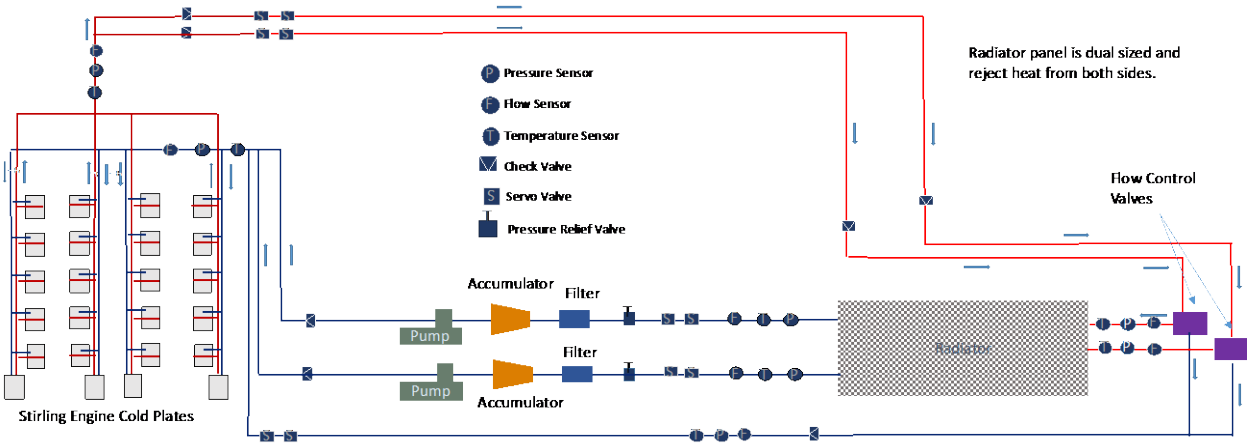

Figure 4.16.—Reactor Radiator Coolant Loop System.

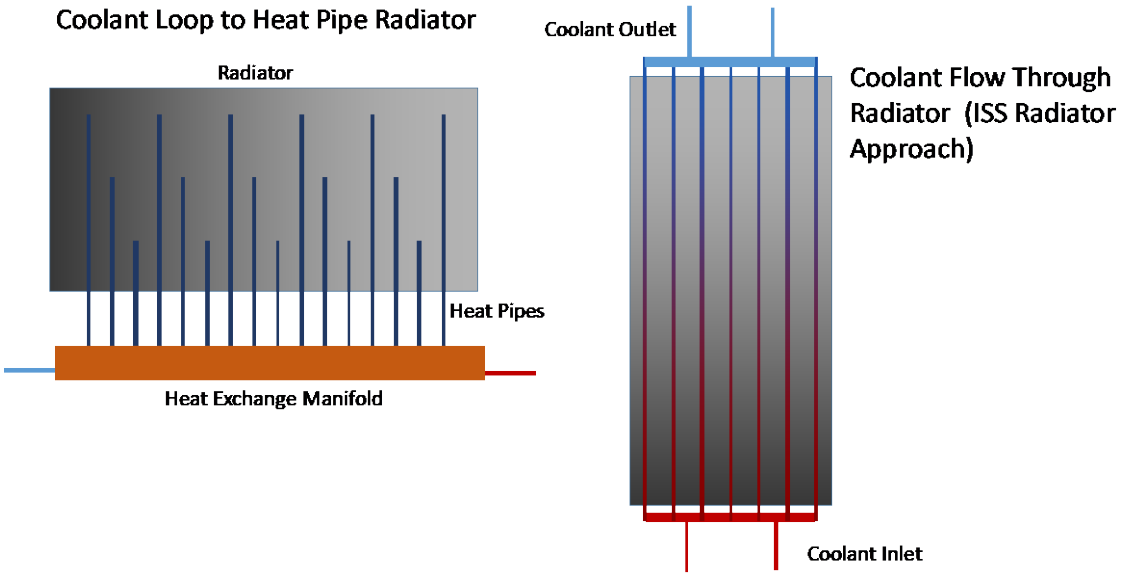

Figure 4.17.—Coolant / Radiator Interface Options.

TABLE 4.17.—COOLANT / RADIATOR INTERFACE ADVANTAGES AND DISADVANTAGES

Coolant / Radiator Method	Advantages	Disadvantages
Coolant Flow Through	Simplified design utilizing less components Has heritage with the ISS radiator design	Greater temperature gradient across the radiator
Heat pipe Radiator with Coolant Heat Exchange Manifold	More uniform radiator temperature distribution. Increased reliability. Individual heat pipe failures would not significantly affect the radiator performance.	Requires an additional heat exchange manifold and the integration of heat pipes into the radiator panels.

4.2.3.6 Heat Pipes

Heat pipes operate by boiling a liquid fluid when the heat pipe is subjected to heat at a design operating temperature. The fluid vapor then moves to the opposite end of the heat pipe (radiator) where the heat is rejected, and the fluid condenses back to a liquid. A wick structure in the absence of gravity is used to help move the fluid back to the heating section through capillary forces. Once back to the heat input section the fluid will boil again repeating the process. Variable conductance heat pipes operate in a similar fashion but use a varying volume, non-condensable gas to adjust the amount of heat that the heat pipe can move while maintaining a fixed operating temperature.

The temperature dependent saturation pressure of the working fluid increases at high heat loads. This increase in pressure compresses the non-condensable gas into a reservoir at the end of the heat pipe provide a larger active condenser area. Thereby enabling more heat to be moved to the radiator by the heat pipe. As the heat load decreases the pressure decreases and the non-condensable gas fills up a greater volume of the heat pipe reducing the condenser area and thereby reducing the heat flow. A variable conductance heat pipe is a passive device that adjusts automatically to varying heat load inputs maintaining a constant operating temperature.

The working fluid for the heat pipe is chosen based on the desired operating temperature of the heat pipe and the heat removal requirement. To size the heat pipe and select the best working fluid a factor termed the Merit Number is utilized. The Merit number (N) is based on the properties of the working fluid as given by Equation (5). These properties include the latent heat of vaporization (H_v), the density (ρ_{wf}), surface tension (σ_{wf}) and the dynamic viscosity (μ_{wf}).

$$N = \frac{H_v \rho_{wf} \sigma_{wf}}{\mu_{wf}} \tag{5}$$

Figure 4.18 plots this number for various fluids. The higher the Merit number the greater the performance of the heat pipe. From this figure it can be seen for the desired operating temperature of 300 K water provides the best choice.

Using the Merit number, the heat pipe thermal power (P_{hp}) transfer capacity can be calculated as given by Equation (6) which is based on the heat pipe wick cross sectional area (A_w), the wick material permeability (K_w), the wick pore radius (r_{wp}) and the heat pipe length (L_{hp}).

$$P_{hp} = \frac{2NA_wK_w}{r_{wp}L_{hp}} \tag{6}$$

Using Equation (6) the heat pipes are sized for the heat produced by each of the loads. The required heat pipe size and specific mass are given in Table 4.18.

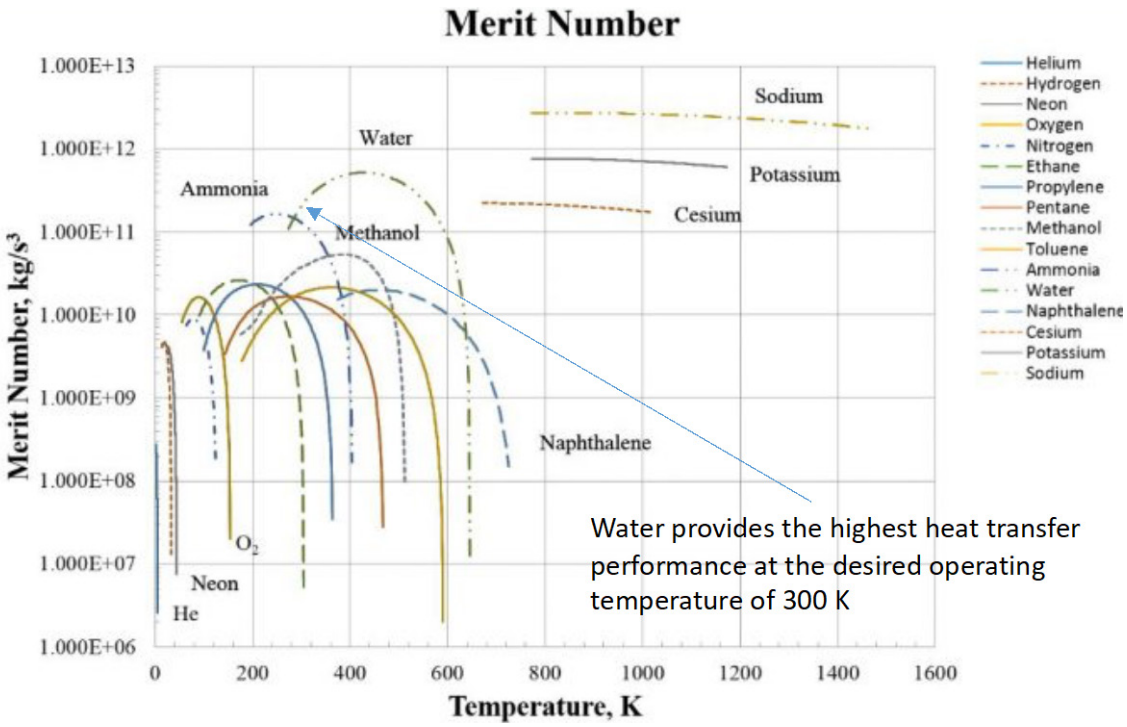

Figure 4.18.—Heat Pipe Merit Number Comparison for Various Working Fluids.

TABLE 4.18.—HEAT PIPE SIZING SPECIFICATIONS FOR THE REACTOR ELECTRONICS AND DISTRIBUTION CART

Characteristic	Value
Heat Pipe Radius	1.7 cm (Reactor Electronics) 1.35 cm (Power Distribution Electronics)
Wick Thickness	1.0 cm (Reactor Electronics) 0.8 cm (Power Distribution Electronics)
Heat Pipe Length	2.5 m (Reactor Electronics) 2.0 m (Power Distribution Electronics)
Heat Transfer Capability	322 W (Reactor Electronics) 255 W (Power Distribution Electronics)
Heat Pipe Mass	1.41 kg (0.564 kg/m)/ heat pipe (Reactor Electronics) 0.874 kg (0.437 kg/m)/ heat pipe (Power Distribution Electronics)

4.2.3.7 Cold Plates

Cold plates are used to interface the heat pipes to the loads. These plates come in a number of shapes and sizes depending on the heat source configuration. They are used to provide a good thermal connection between the heat source and the heat pipe evaporator section. The heat source is mounted to the cold plate, which in turn has the heat pipe either mounted to it or incorporated into it. This provides a good thermal contact between the cold plate and the heat pipe.

The number of cold plates and heat pipe runs that are used is dependent on the distribution of the loads and the desired redundancy for the thermal system. The electronics cold plates have two heat pipe runs per plate. The heat pipes share the load from each cold plate although each heat pipe can carry the full heat load from the cold plate. The two heat pipe runs are used to provide a redundant heat flow path in case of a failure of one of the heat pipes. Table 4.19 summarizes the cold plate specifications.

TABLE 4.19.—COLD PLATE SPECIFICATIONS

Variable	Value
Cooling Plate and Line Material	Al
Cooling Plate and Line Material Density	2,770 kg/m^3
Number of Cooling Plates	8 (Reactor Electronics)
	8 (Power Distribution Electronics)
Cooling Plate Length	0.2 m electronics
Cooling Plate Width	0.2 m electronics
Cooling Plate Thickness	5 mm
Heat Pipes Per Cold Plate	3 (Reactor Electronics)
	2 (Power Distribution Electronics)

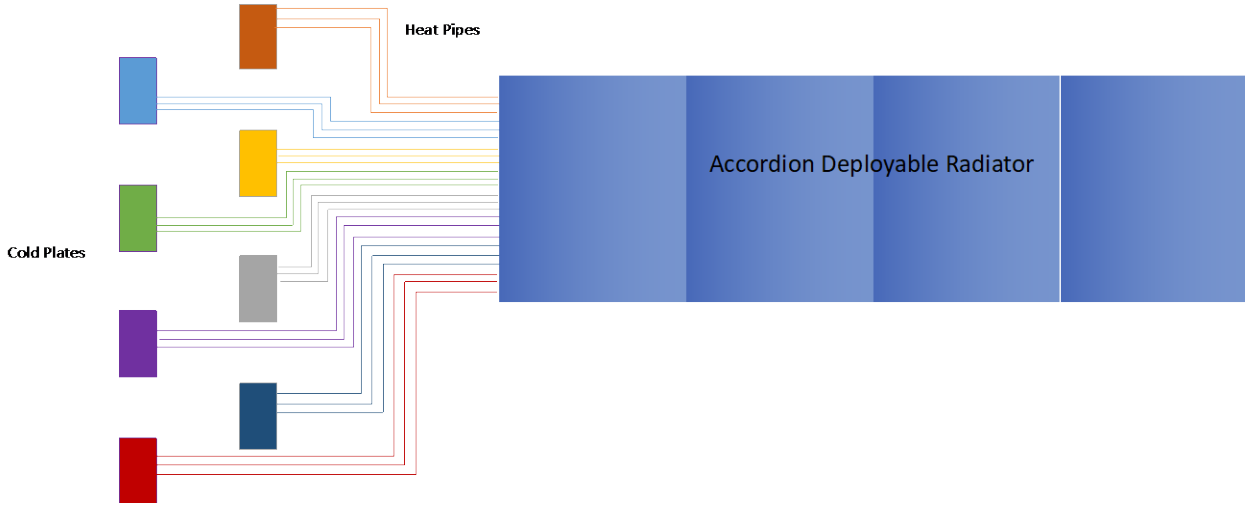

Figure 4.19.—Cold Plate and Heat Pipe Layout for the Reactor Electronics Thermal Control System.

The heat pipe/cold plate configuration for the reactor electronics have three heat pipes going from each cold plate to the radiator as illustrated in Figure 4.19. There are a total of eight cold plates to remove the 5.1 kW of waste heat from the electronics enclosure. This is assumed to be evenly distributed between the cold plates at 638 W per cold plate. The three heat pipes from each cold plate share the total heat load on that cold plate. For each of cold plates, two of the three heat pipes are needed to transfer the full heat load to the radiator. This provides a redundant path in case of a heat pipe failure. The heat pipes are distributed evenly between each of the deployed panels. It should be noted that due to the waste heat level and size of the radiator a pump loop coolant system similar to that for the reactor waste heat may also be considered instead of the heat pipe-based coolant system.

The power distribution electronics have two heat pipes are run from each cold plate to the radiator as illustrated in Figure 4.20. There are a total of eight cold plates to remove the 2.0 kW of heat from the electronics enclosure. It is assumed that the heat is evenly distributed between these cold plates at 250 W per cold plate. The two heat pipes from each cold plate share the thermal load and heat distribution to the radiator. However, the heat pipes are sized so that either of the two heat pipes can transfer the full heat load to the radiator. This provides a redundant path in case of a heat pipe failure. The heat pipes are distributed evenly between each of the deployed panels.

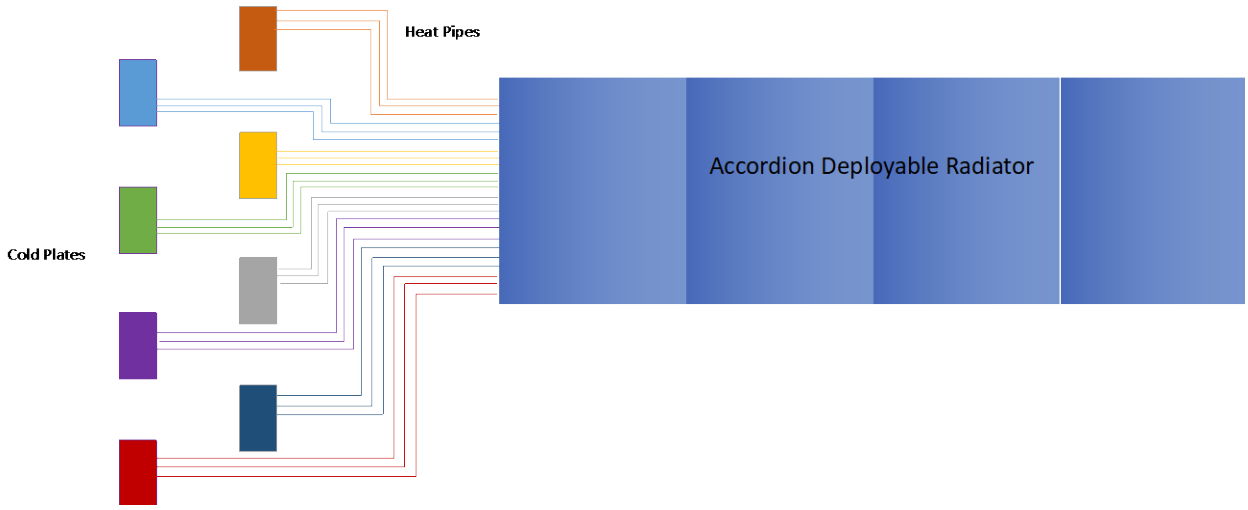

Figure 4.20.—Cold Plate and Heat Pipe Layout for the Power Distribution Electronics Thermal Control System.

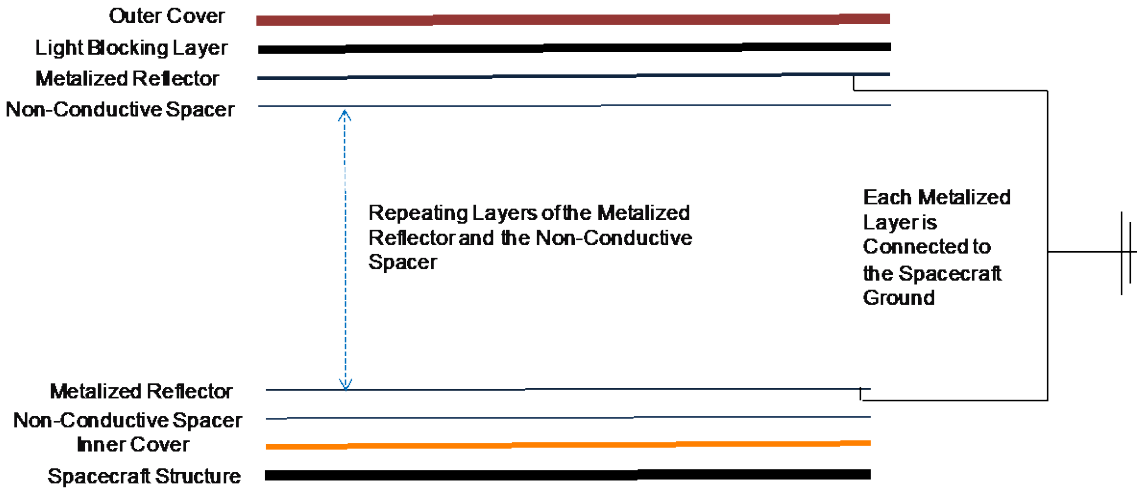

Figure 4.21.—Illustration of MLI Construction Layout and Component Layers.

4.2.3.8 Insulation

The Moon has no appreciable atmosphere. Therefore, in the vacuum of space radiation heat transfer is the main mechanism for heat leak from the electronics enclosure to the surroundings. MLI provides the best method for reducing this heat leak to the surroundings. MLI is constructed of a number of layers of metalized material with a nonconductive spacer between the layers. The metalized material has a low absorptivity which resists radiative heat transfer between the layers. MLI can be conformed to fit over various shapes. It is typically held in place with Velcro, glue or tack welding the layers together (see Figure 4.21).

MLI is used to insulate the electronics enclosure on the reactor electronics sled as well as the power distribution sled. The Team performed an analysis of the heat loss that would occur during daytime and nighttime operation. This analysis is used to determine the required worst case heater power that would be required during nighttime operation. The heat loss paths from the electronics enclosures considered in the analysis include the following:

- Heat loss through the MLI
- Heat loss from passthroughs and seams in the MLI

- Heat loss through the support structure

The amount of heat lost through the insulation is dependent on the enclosure surface area, environmental temperatures (desired internal temperature T_{ei} and the nighttime sink temperature T_{sn}) and the type and number of layers of insulation (n). The heat loss from the enclosure through the insulation is given by Equation (7). The heat loss is based on the surface area of the enclosure (A_e) and the emissivity of both the enclosure wall surface (ε_{ew}) and MLI layers.

$$Q_{hi} = \frac{A_e \sigma (T_{ei}^4 - T_{sn}^4)}{\left(\frac{1}{\varepsilon_{ew}}\right) + \left(\frac{2n_l}{\varepsilon_l}\right) - (n_l + 1)} \tag{7}$$

The surface area for the enclosure is dependent on the dimensions given in Table 4.11 as given by Equation (8).

$$A_h = h_e l_e w_e \tag{8}$$

The MLI is very good at resisting heat flow. However, the majority of heat leak through the insulation occurs from passthroughs and seams (Q_{ps}) in the insulation covering. This heat leak is approximated by Equation (9) which is based on the mean insulation temperature (T_m) given by Equation (10) and constants f_p and f_n, given by Equations (11) and (12), respectively.

$$Q_{ps} = 0.664 \left(\frac{0.000136}{4\sigma T_m^2} + 0.000121 T_m^2 \right) f_p f_n A_h \sigma (T_{hi}^4 - T_{sn}^4) \tag{9}$$

$$T_m = \left(\frac{(T_{hi}^2 + T_{sn}^2)(T_{hi} + T_{sn})}{4} \right)^{\frac{1}{3}} \tag{10}$$

The passthrough constant (f_p) is based on the present of passthrough area (A_{pt}) of items such as wires or tubes that pass through the insulation. This area is given in percent value, for example if the estimated passthrough area is ½ percent, 0.5 is used as the percent passthrough area.

$$f_p = 0.73 + 0.27 A_{pt} \tag{11}$$

$$f_n = 4.547 - 0.501 n_l \tag{12}$$

The MLI specifications used for the variables in determining the heat loss through the passthroughs and seams are given in Table 4.20.

There will be heat leak through conduction from items that pass through the enclosure and are exposed to the surroundings such as the heat pipe connections to the radiator. Also, the support structure that secures the electronics enclosure to the frame is in direct contact with the external frame and subsequent surface. This support structure path will conduct heat to the surface. The heat leak (Q_{cp}) through conduction from these sources is given by Equation (13), which is dependent on the number of conductive paths (n_{cp}), the thermal conductivity of the material (k), the cross-sectional area of the material normal to the direction of the heat flow (A_{cp}), and the length of the conductive path (L_{cp}).

$$Q_{cp} = \frac{n_{cp} k A_{cp} (T_{hi} - T_{sn})}{L_{cp}} \tag{13}$$

The cross-sectional area for the conductive paths is given by Equation (14). It is assumed that all of the paths considered could be represented by a hollow cylinder shape with a specified inner diameter (d_{icp}) and wall thickness (t_{cp}) where the cross-sectional area of that shape is normal to the flow of heat from the interior of the habitat to the surroundings.

$$A_{cp} = \pi\left(\left(\frac{d_{icp}}{2} + t_{cp}\right)^2 - \left(\frac{d_{icp}}{2}\right)^2\right) \tag{14}$$

The variables used to determine the heat leak for each of the identified conductive paths is summarized in Table 4.21.

TABLE 4.20.—ENCLOSURE PASSTHROUGH AND SEAMS HEAT LEAK VARIABLES

Variable	Value
Insulation Emissivity (e_i)	0.07
Enclosure Wall Emissivity (e_{hi})	0.07
Number of Layers of insulation (n_l)	25
Percent of passthrough Area (A_{pt})	5 percent
Spacecraft MLI Material	Aluminumized Kevlar
Spacecraft MLI Material Aerial Density	
Outer Covering	0.11 kg/m^2
Inner Covering	0.05 kg/m^2
Spacer	0.0063 kg/m^2
Reflective Layer	0.055 kg/m^2
Attachment and Seals Percentage	10 percent
MLI Thickness	1 cm Spacecraft Bus and heat shield
MLI Layer Spacing	0.2 mm
MLI Density	20 kg/m^3
Effective Thermal Conductivity	0.00016 W/mK

TABLE 4.21.—ENCLOSURE CONDUCTIVE PATH HEAT LEAK VARIABLES

Variable	Sensor and Power Wires	Enclosure Support Structure
Number of Conductive Paths (n_{cp})	20	4
Thermal Conductivity (k)	400 W/mK (Copper)	6.7 W/mK (Ti-6Al-4V)
Inner Diameter (d_{icp})	1 mm	3.5 cm
Thickness (t_{cp})	NA	0.5 cm
Length (L_{cp})	0.5 m	25 cm
Interior Temperature (T_{hi})	300 K	300 K
Surrounding Sink Temperature (T_{sn})	50.5 K Nighttime / Shadow 235 K Sunlight	50.5 K Nighttime / Shadow 235 K Sunlight

The total heat loss from the enclosure to the surroundings during nighttime operation (Q_e) is given by Equation (15) and summarized in Table 4.22 and illustrated in Figure 4.22.

$$Q_e = Q_i + Q_{ps} + Q_{ss} + Q_w \tag{15}$$

Under normal operation the heat loss is less than the power consumed by the electronics and systems within the enclosure. Therefore, the waste heat from these systems can be used to maintain the enclosure temperature during normal operations.

TABLE 4.22.—ENCLOSURE HEAT LOSS SUMMARY

Heat Loss Path	Heat Loss Sunlight (W)	Heat Loss Nighttime (W)	Heat Loss Sunlight (W)	Heat Loss Nighttime (W)
	Power Distribution Electronics Enclosure		Reactor Electronics Enclosure	
Insulation (Q_i)	0.8	1.3	1.1	1.8
Passthroughs and Seams (Q_{ps})	14.4	23.0	20.2	32.4
Support Structure (Q_{ss})	3.28	12.6	3.28	12.6
Wiring (Q_w)	1.5	3.1	1.5	3.1
Total (Q_h)	19.1	38.8	24.9	48.1

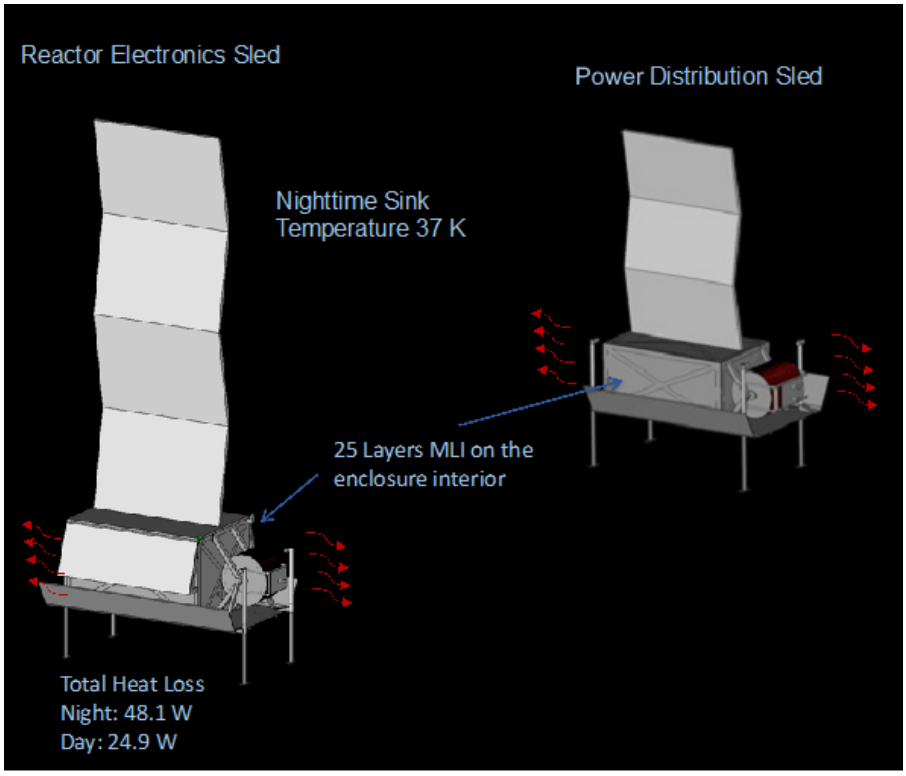

Figure 4.22.—Heat Loss from Electronics Enclosure within a PSR.

4.2.3.9 Heaters

Electric heaters are incorporated onto the cold plates as well as on critical components as needed. These heaters are used to maintain the temperature of these components above their minimum operating temperature throughout the mission. Waste heat from the internal components as well as electric heaters are used to provide heat to the spacecraft electronic components if needed. The flexible strip and plate heaters are used to provide heat to the electronic and mechanical components within the spacecraft. Flat plate heaters are used on each of the cold plates to provide heat to the mounted electronics and or packaging if necessary.

Thermal control within the electronics enclosure is accomplished using a network of thermocouples whose output is used to control the power to the various heaters and a data acquisition and control computer is used to operate the thermal system. During normal operation it is estimated that the waste heat from the electronics components will be sufficient to maintain the temperature of the components within the spacecraft within their desired operating temperature range. Therefore, the heater power will be minimal during normal operations. Heater power will vary with the mission operation from 0.0 W when the electronics are operational to the heat loss given in Table 4.22 for the power distribution sled electronics and the reactor electronics during sunlight or nighttime operation.

4.2.3.10 Estimated TRL for the Thermal System

The technology readiness level (TRL) for the thermal components is estimated in Table 4.23. These estimates are based on the current space use and heritage of the technology and the modifications needed for this mission application.

TABLE 4.23.—TRL ESTIMATE FOR THERMAL SYSTEM COMPONENTS

Component	TRL	Comments
Electric Heaters	9	Commonly used in spacecraft. Commercially available in various shapes and sized.
Thermocouples	9	Commonly used in spacecraft. Commercially available.
Heater switches	9	Commonly used in spacecraft. Commercially available.
Pump loop system (includes Servo Valves, Flow Diverter Valves, Check Valves, Coolant Pumps, Vent Valves, Filters, Accumulators, Temperature Sensors, Pressure Sensors, Flow Sensors, Coolant and Coolant lines)	6 to 9	Used in spacecraft pump loop system and commercially available. May need to be modified due to the high radiation environment.
Reactor Accordion Deployed Radiator	6*	Used for heat rejection on high power satellites and the international space station. However, design will need to be modified to meet the requirements of this mission application.
Radiator line micro meteoroid and orbital debris (MMOD)	6*	MMOD has been used for spacecraft applications. A custom design will be needed.
Shunt Radiator	6*	A custom design will be needed.
Multi-Layer Insulation (MLI)	6*	A custom design will be needed.
Electronics Radiator (fixed, single sided flat plate)	6*	Commonly used for heat rejection on spacecraft. A custom radiator design will be needed.
Electronics Heat Pipes (water working fluid)	6*	Heat pipe design and working fluid are commonly used for heat rejection on spacecraft. A custom heat pipe design will be needed.
Cold Plates	6*	Cold plates are integrated with the heat pipes for heat removal. A custom design for this application will be needed.

* Component or technology has flight heritage, the TRL represents the need to construct a custom design for this application.

4.2.4 Master Equipment List

Table 4.24 to Table 4.26 detail the thermal control system for the polar case, whereas Table 4.27 to Table 4.29 detail a quick look at an equator deployment.

TABLE 4.24.—THERMAL CONTROL: CABLE AND SPOOL MEL

Description 40kW_Case 2_FSPS Deployability CD-2021-187	QTY	Unit Mass	Basic Mass	Growth	Growth	Total Mass
Thermal Control (Non-Propellant)			**68.1**	**18%**	**12.3**	**80.4**
Passive Thermal Control			**68.1**	**18%**	**12.3**	**80.4**
Electronics MLI	1	6.6	6.6	18%	1.2	7.7
Electronics Radiator	1	46.5	46.5	18%	8.4	54.9
Electronics Heat Pipes	16	0.9	14.0	18%	2.5	16.5
Electronics Cold Plates	8	0.1	1.1	18%	0.2	1.3

TABLE 4.25.—THERMAL CONTROL: CONTROL SYSTEMS MEL

Description 40kW_Case 2_FSPS Deployability CD-2021-187	QTY	Unit Mass	Basic Mass	Growth	Growth	Total Mass
Thermal Control (Non-Propellant)			**183.8**	**18%**	**33.1**	**216.9**
Active Thermal Control			**1.4**	**18%**	**0.2**	**1.6**
Heaters	8	0.1	0.4	18%	0.1	0.5
Thermal Control/Heaters Circuit	2	0.2	0.4	18%	0.1	0.5
Data Acquisition	2	0.3	0.5	18%	0.1	0.6
Thermocouples	8	0.0	0.1	18%	0.0	0.1
Passive Thermal Control			**182.4**	**18%**	**32.8**	**215.3**
Radiators	1	119.9	119.9	18%	21.6	141.5
Electronics MLI Insulation	1	9.4	9.4	18%	1.7	11.0
Thermal Coatings/Paint	1	0.9	0.9	18%	0.2	1.0
Electronics Heat Pipes	24	1.4	33.9	18%	6.1	40.0
Electronics Cold Plates	8	0.3	2.4	18%	0.4	2.8
Shunt Radiator	1	16.0	16.0	18%	2.9	18.9

TABLE 4.26.—THERMAL CONTROL: FSPS MEL

Description 40kW_Case 2_FSPS Deployability CD-2021-187	QTY	Unit Mass	Basic Mass	Growth	Growth	Total Mass
Thermal Control (Non-Propellant)			**1100.6**	**18%**	**198.1**	**1298.8**
Active Thermal Control			**8.2**	**18%**	**1.5**	**9.7**
Heaters	8	0.1	0.4	18%	0.1	0.5
Thermal Control	2	0.2	0.4	18%	0.1	0.5
Thermocouples	8	0.0	0.1	18%	0.0	0.1
Data Acquisition	2	0.3	0.5	18%	0.1	0.6
Switches	8	0.1	0.8	18%	0.1	0.9
Servo Valves	12	0.5	6.0	18%	1.1	7.1
Passive Thermal Control			**110.7**	**18%**	**19.9**	**130.6**
colling System insulation	1	3.3	3.3	18%	0.6	3.9
Enclosure	2	7.5	15.0	18%	2.7	17.7
Flow Diverter Valve	2	1.0	2.0	18%	0.4	2.4
Check Valve	7	0.3	2.1	18%	0.4	2.5
Coolant Pump	4	1.5	6.0	18%	1.1	7.1
Vent Valve	2	0.1	0.2	18%	0.0	0.2
Filter	2	0.4	0.8	18%	0.1	0.9
Accumulator	2	4.0	8.0	18%	1.4	9.4
Heat Exchanger	1	6.8	6.8	18%	1.2	8.0
Temperature Sensor	8	0.1	0.8	18%	0.1	0.9
Pressure Sensor	7	0.1	0.7	18%	0.1	0.8
Flow Sensor	6	0.3	1.8	18%	0.3	2.1
Coolant Lines	1	11.0	11.0	18%	2.0	13.0
Coolant	1	52.2	52.2	18%	9.4	61.6
Semi-Passive Thermal Control			**981.8**	**18%**	**176.7**	**1158.5**
Reactor Radiator	1	976.7	976.7	18%	175.8	1152.5
Radiator Lines MMOD	1	5.1	5.1	18%	0.9	6.0

TABLE 4.27.—THERMAL CONTROL: CABLE AND SPOOL: EQUATOR MEL

Description 40kW_Equator_Case 3_FSPS Deployability CD-2021-187	Basic Mass	Growth	Growth	Total Mass
Thermal Control (Non-Propellant)	**114.6**	**18%**	**20.6**	**135.3**
Passive Thermal Control	**114.6**	**18%**	**20.6**	**135.3**
Electronics MLI	6.6	18%	1.2	7.7
Electronics Radiator	93.0	18%	16.7	109.7
Electronics Heat Pipes	14.0	18%	2.5	16.5
Electronics Cold Plates	1.1	18%	0.2	1.3

TABLE 4.28.—THERMAL CONTROL: CONTROL SYSTEMS: EQUATOR MEL

Description 40kW_Equator_Case 3_FSPS Deployability CD-2021-187	Basic Mass	Growth	Growth	Total Mass
Thermal Control (Non-Propellant)	**303.7**	**18%**	**54.7**	**358.4**
Active Thermal Control	**1.4**	**18%**	**0.2**	**1.6**
Heaters	0.4	18%	0.1	0.5
Thermal Control/Heaters Circuit	0.4	18%	0.1	0.5
Data Acquisition	0.5	18%	0.1	0.6
Thermocouples	0.1	18%	0.0	0.1
Passive Thermal Control	**302.4**	**18%**	**54.4**	**356.8**
Radiators	239.8	18%	43.2	283.0
Electronics MLI Insulation	9.4	18%	1.7	11.0
Thermal Coatings/Paint	0.9	18%	0.2	1.0
Electronics Heat Pipes	33.9	18%	6.1	40.0
Electronics Cold Plates	2.4	18%	0.4	2.8
Shunt Radiator	16.0	18%	2.9	18.9

TABLE 4.29.—THERMAL CONTROL: FSPS: EQUATOR MEL

Description 40kW_Equator_Case 3_FSPS Deployability CD-2021-187	Basic Mass	Growth	Growth	Total Mass
Thermal Control (Non-Propellant)	**1706.2**	**18%**	**307.1**	**2013.3**
Active Thermal Control	**8.2**	**18%**	**1.5**	**9.7**
Heaters	0.4	18%	0.1	0.5
Thermal Control	0.4	18%	0.1	0.5
Thermocouples	0.1	18%	0.0	0.1
Data Acquisition	0.5	18%	0.1	0.6
Switches	0.8	18%	0.1	0.9
Servo Valves	6.0	18%	1.1	7.1
Passive Thermal Control	**110.7**	**18%**	**19.9**	**130.6**
colling System insulation	3.3	18%	0.6	3.9
Enclosure	15.0	18%	2.7	17.7
Flow Diverter Valve	2.0	18%	0.4	2.4
Check Valve	2.1	18%	0.4	2.5
Coolant Pump	6.0	18%	1.1	7.1
Vent Valve	0.2	18%	0.0	0.2
Filter	0.8	18%	0.1	0.9
Accumulator	8.0	18%	1.4	9.4
Heat Exchanger	6.8	18%	1.2	8.0
Temperature Sensor	0.8	18%	0.1	0.9
Pressure Sensor	0.7	18%	0.1	0.8
Flow Sensor	1.8	18%	0.3	2.1
Coolant Lines	11.0	18%	2.0	13.0
Coolant	52.2	18%	9.4	61.6
Semi-Passive Thermal Control	**1587.3**	**18%**	**285.7**	**1873.1**
Reactor Radiator	1582.3	18%	284.8	1867.1
Radiator Lines MMOD	5.1	18%	0.9	6.0

4.3 Structures

The FSPS structures must contain the necessary hardware for various systems. The main FSPS unit has a thermal control system. The control systems unit must accommodate C&DH, communications and tracking, electrical power, and a thermal control system. The cable and spool unit must contain electrical power and thermal control systems. The structural components must be able to withstand applied mechanical and thermal loads. In addition, the structures must provide minimum mass and deflections, sufficient stiffness, and vibration damping. The loads include an approximate maximum axial acceleration of 6 g acceleration from the launch vehicle. Figure 4.23 shows the deployed FSPS.

4.3.1 System Requirements

The bus is to support the mounted hardware bearing launch and operational mechanical and thermal loads without failure. The structures shall not degrade for the extent of the mission in the Earth, lunar, and deep space environments.

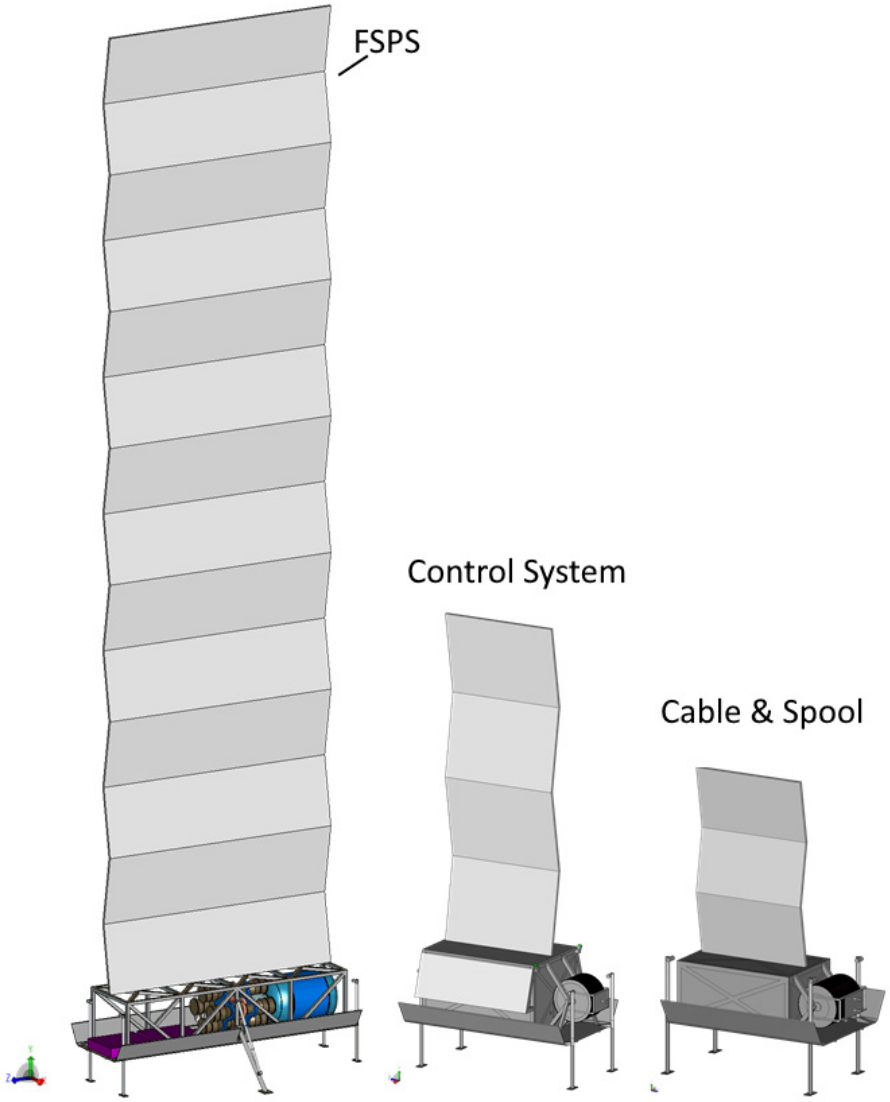

Figure 4.23.—Deployed FSPS.

4.3.2 System Assumptions

The sled/truss provides the backbone for the mounted hardware. The primary material for the sled/truss is Al. The Al alloy is 7075-T6 as described in the Federal Aviation Administration's Metallic Materials Properties Development and Standardization (MMPDS-16) (Ref. 16). The material is at a minimum Technology Readiness Level of 6 (TRL6) as presented by Mankins (Ref. 17). Components are of shells and tubular members. Joining of components is by threaded fasteners or riveting.

Secondary structures include tubes and decks for supporting equipment. Other secondary structures are the components for installation hardware.

4.3.3 System Trades

Outriggers were added to the FSPS to increase the tip over angle of the deployed unit.

4.3.4 Analytical Methods

Analytical methods were by hand calculations and spreadsheet to conduct preliminary stress analysis. In addition, the tip over angle for the FSPS main unit is determined.

4.3.5 Risk Inputs

A potential risk for the structural system may be excessive g loads or impact from operational loads or a foreign object or excessive slope leading to tip over at the landing site which may cause too much deformation, vibrations, or fracture of sections of the support structure. Consequences include lower performance from mounted hardware to loss of mission.

The likelihood is a medium ranking of three. Consequences may be relatively high with a ranking of four for cost, schedule, and performance. Safety would be ranked very low at one.

For risk mitigation the structure is to be designed to NASA standards to withstand expected g loads, a given impact, and to have sufficient stiffness and damping to minimize issues with vibrations. Trajectories and operations are to be planned to minimize the probability of impact with foreign objects, tipping over, and to minimize excessive loads.

There are potential risks with the mechanisms. Lunar dust may infiltrate mechanisms and reduce the performance or incapacitate the unit. Consequences include an inability to level the sled, deploy the radiators, or deploy the cable resulting in diminished performance or loss of mission.

The likelihood is low at a ranking of two. Consequences would be high for cost, schedule, and performance at a ranking of four. Effects on safety would be low at a ranking of one.

To reduce the effects of mechanism risks, the effort is to design the mechanisms to minimize lunar dust infiltration and/or to operate with the dust.

4.3.6 System Design

The main bus material is Al 7075-T6. Per the MMPDS (Ref. 16), the ultimate strength is 524 MPa (76 ksi) and the yield strength is 469 MPa (68 ksi). Applying safety factors of 1.4 on the ultimate strength and 1.25 on the yield strength and selecting the lower value, as per NASA Standard 5001B (2016), results in an allowable stress of 374 MPa (54.3 ksi) at room temperature. The Young's modulus is 71.7 GPa (10.4×10^6 psi), the density is 2.80 g/cm^3 (0.101 lb/in^3), and the Poisson's ratio is 0.33.

The FSPS unit Al space frame supports a 1000 kg radiator on top. It is assumed that the load is distributed evenly among the vertical members of the space frame. With a launch load of 6 g the resulting stress is 5.2 MPa (0.75 ksi) providing a margin of 71.

The screw jacks of the FSPS unit support approximately 950 kg per leg. With an acceleration of 1/6 g the resulting peak axial stress in each leg if 13.4 MPa (1.95 ksi). The FSPS unit is slid off the rover during

deployment. The two legs that are slid across the rover deck have rollers to provide an approximate friction coefficient of 0.2. The resulting drag force is 0.69 kN (154 lb). The resulting bending stress in each of the two deployed screw jacks is 158 MPa (22.9 ksi). The total stress is 172 MPa (24.9 ksi) resulting in a margin of 1.2.

The tall radiator over the FSPS unit required a check for the tip over angle for the assembly. The mass of the radiator is 976 kg with the center of gravity being approximately 9.7 m above the ground. The bus section is 5024 kg without the radiator mass. The center of gravity is approximately 1.07 m above the ground. The combined bus and radiator mass is 6000 kg with the center of gravity being 2.47 m above the ground. The resulting tip over angle is approximately 28.6°. Figure 4.24 illustrates the FSPS unit and the calculated location of the center of gravity.

The structural integrity of the scissor for the FSPS unit radiator was checked. It is assumed that the radiator is tilted 25.5° in the direction normal to the radiator surface. There are 14 radiator panels for a radiator assembly height of 16 m. A single panel is 1.14 m tall. It is assumed that the radiator panels are nearly fully deployed in a single plane. The scissor brace to panel attachment is assumed to be at the midpoint for each component which is at a height of 0.57 m for the base panel. Figure 4.25 illustrates the radiator and scissors layout. It is assumed that the scissor brace attachment to the bus is 0.298 m from the radiator panel. The resulting maximum stress in the scissor brace is 72.3 MPa with a margin of 4.2.

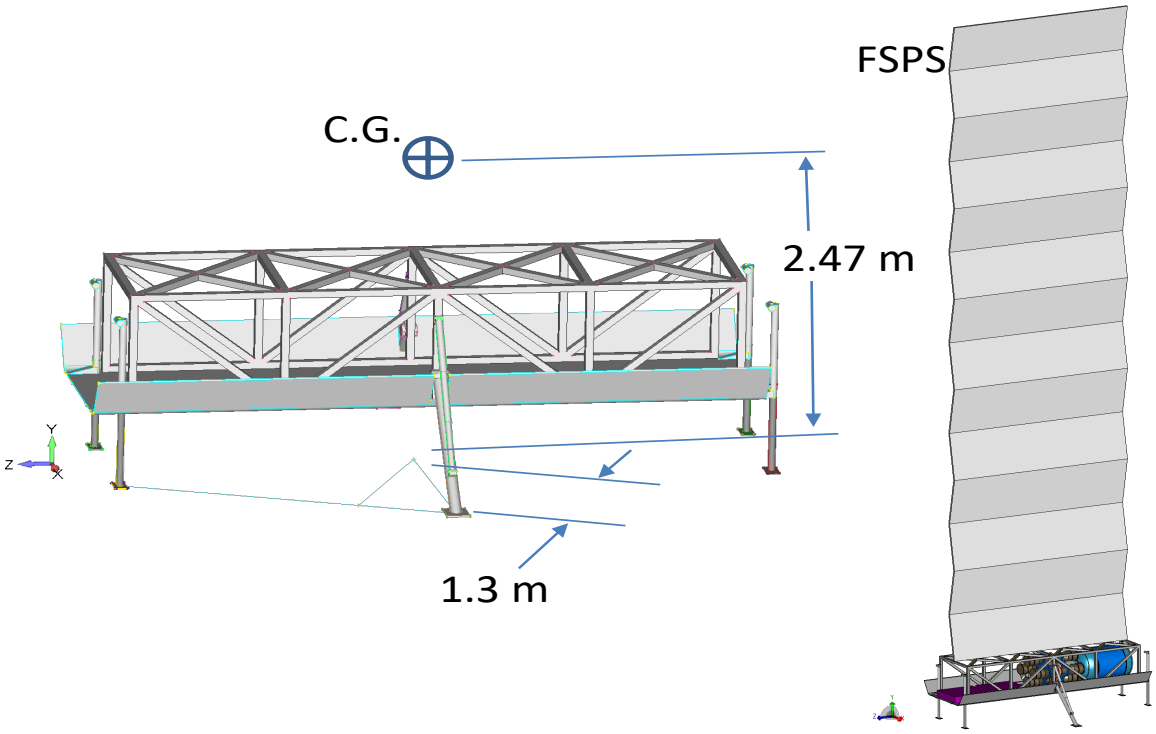

Figure 4.24.—FSPS unit center of gravity (C.G.) location.

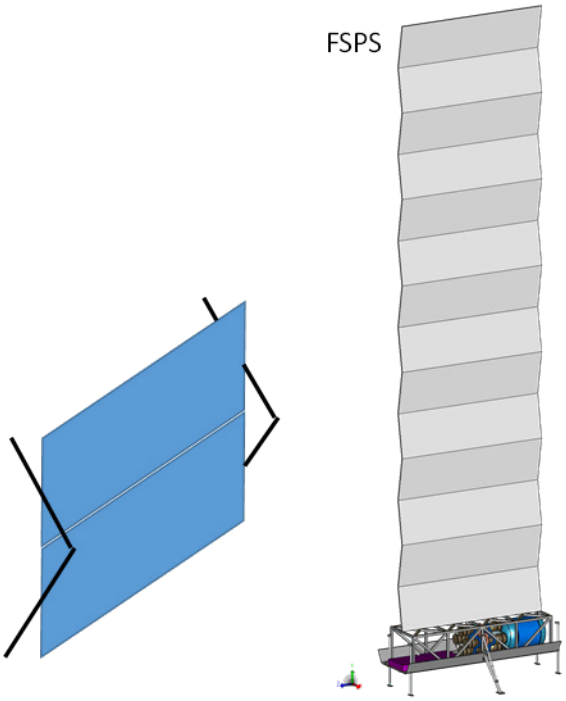

Figure 4.25.—FSPS unit radiator layout.

Installation hardware mass is estimated by taking 4 percent of the installed hardware mass. The installation hardware represents fasteners, small brackets, and other hardware used to attach main system components to the bus. Heineman (Ref. 18) has shown that past spacecraft have shown that the 4 percent is a good approximation for the mass. The 4 percent installation hardware mass is applied to the thermal control and science (reactor) of the FSPS main unit. It is applied to the command and data handling, communication and tracking, electrical power, and thermal control systems for the Control Systems unit. Lastly, it is applied to the electrical power and thermal control systems of the Cable and Spool unit.

The FSPS system utilized a few mechanisms. The mechanisms include motorized screw jacks, motorized outriggers, and a spool hub motor.

4.3.7 Cable and Spool Designs

The three units making up the FSPS system utilize two spool mounted cables to transfer power and data. The first is a 1 km long high voltage power transfer cable. The second is a 50 m long multi-use data and instrumentation cable that has conductors for the spool deployment motors, radiator deployment motors, screw jack motor, coolant pumps, heaters, flow diverter valves, servo valves, miscellaneous sensors, and power. Figure 4.26 shows this cables cross section and the specifics of its numerous conductors.

The spools for these two cables are designed using both the geometric constraints of the system and the geometric relationships between the spool's dimensions for a given cable length and diameter. The dimensions of the cable spools used in this design are defined in Figure 4.27.

For both the 1 km power cable and the 50 m multi-use data and instrumentation cable, a set of curves are developed that represented the correlations between each spool's geometric dimensions given each cables length, diameter, and corresponding winding efficiency. The inner diameter of each spool, however, is set by the cables anticipated minimum allowable bend radius. The results for both spools are shown in Figure 4.28 and Figure 4.29.

Type	Gauge	Qnty.
Spool Deployment Motors	26	3
Radiator Deployment Motors	20	6
Screw Jack Motor	20	12
Coolant Pumps	20	12
Heaters	26	16
Flow Diverter Valves	26	6
Servo Valves	26	36
Misc. Sensors	20	42
Power	8	16

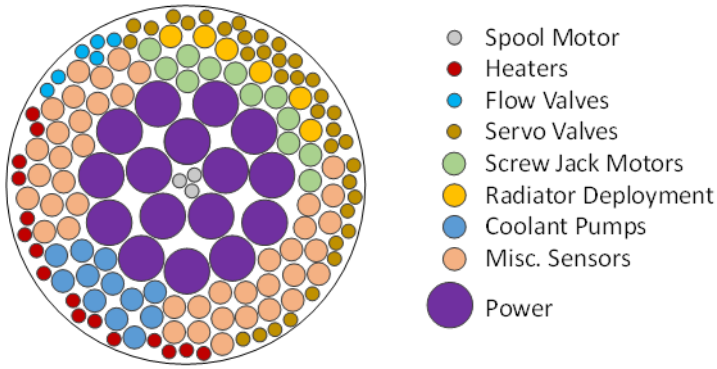

Figure 4.26.—Multi-Use Cable Cross Section.

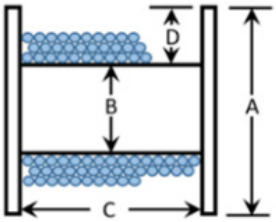

Dimension	Definition
A	Outer Spool Hub Diameter
B	Inner Spool Diameter
C	Inner Spool Width
D	Spool Hub Height

Figure 4.27.—Cable Spool Dimension Definitions.

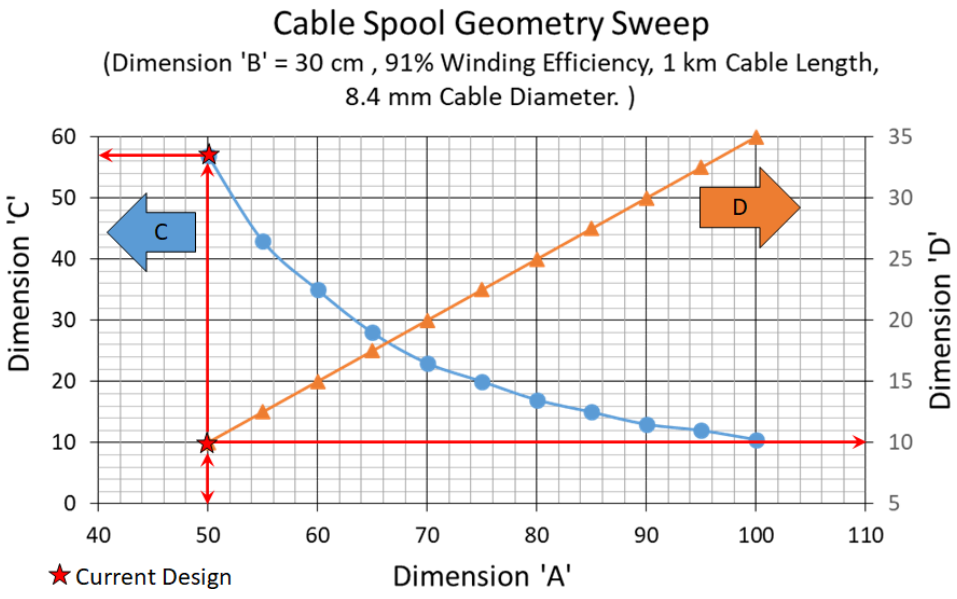

Figure 4.28.—Power Cable Spool Geometry Sweep.

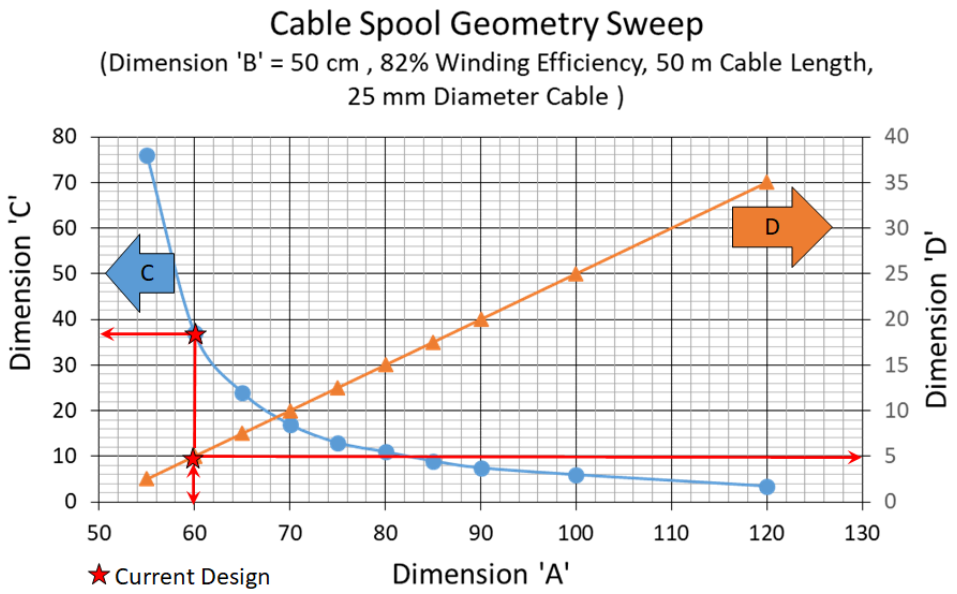

Figure 4.29.—Multi-Use Data and Instrumentation Cable Spool Geometry Sweep.

TABLE 4.30.—STRUCTURES: CABLE AND SPOOL MEL

Description 40kW_Case 2_FSPS Deployability CD-2021-187	QTY	Unit Mass	Basic Mass	Growth	Growth	Total Mass
Structures and Mechanisms			172.3	19%	33.4	205.8
Structures			137.8	18%	24.8	162.6
Primary Structures			137.8	18%	24.8	162.6
Sled	1	69.0	69.0	18%	12.4	81.4
Truss Assy	1	57.7	57.7	18%	10.4	68.1
Spool	1	5.8	5.8	18%	1.0	6.8
Spool mount	1	5.3	5.3	18%	1.0	6.3
Mechanisms			34.6	25%	8.6	43.2
Power System Mechanisms			17.6	25%	4.4	21.9
Spool hub motor	1	2.5	2.5	25%	0.6	3.1
Screw Jack	4	2.3	9.1	25%	2.3	11.3
Screw Jack Motor	4	1.5	6.0	25%	1.5	7.5
Installations			17.0	25%	4.3	21.3
Electrical Power Installation	1	14.3	14.3	25%	3.6	17.8
Therrmal Control Installation	1	2.7	2.7	25%	0.7	3.4

4.3.8 Recommendation(s)

Higher fidelity structural analysis would provide more details in the structural response of the assemblies. Different operational loads may be evaluated. That would provide information for optimizing the structure for high stiffness and strength along with a low mass. Greater use of advanced materials and architectures may further enhance the structure's performance. The application of orthogrid or isogrid panels would be worth investigating for the sleds.

4.3.9 Master Equipment List

Table 4.30 to Table 4.32 detail the Structures for the polar case, whereas Table 4.33 to Table 4.35 detail a quick look at an equator deployment.

TABLE 4.31.—STRUCTURES: CONTROL SYSTEMS MEL

Description 40kW_Case 2_FSPS Deployability CD-2021-187	QTY	Unit Mass	Basic Mass	Growth	Growth	Total Mass
Structures and Mechanisms			268.7	19%	51.1	319.9
Structures			211.6	18%	38.1	249.7
Primary Structures			211.6	18%	38.1	249.7
Sled	1	86.3	86.3	18%	15.5	101.9
Truss Assy	1	69.1	69.1	18%	12.4	81.5
Truss Top Panel, Orthogrid	1	26.3	26.3	18%	4.7	31.1
Spool Mount	1	11.9	11.9	18%	2.1	14.0
Spool	1	6.5	6.5	18%	1.2	7.7
Shunt Radiator Support	2	5.7	11.4	18%	2.1	13.5
Mechanisms			57.1	23%	13.1	70.2
Power System Mechanisms			17.6	18%	3.2	20.7
Screw Jack	4	2.3	9.1	18%	1.6	10.7
Screw Jack Motor	4	1.5	6.0	18%	1.1	7.1
Spool Hub Motor	1	2.5	2.5	18%	0.5	3.0
Installations			39.6	25%	9.9	49.5
C&DH installation	1	1.9	1.9	25%	0.5	2.3
Comm. & Tracking installation	1	1.0	1.0	25%	0.3	1.3
Electrical Power installation	1	29.3	29.3	25%	7.3	36.7
Thermal Control installation	1	7.4	7.4	25%	1.8	9.2

TABLE 4.32.—STRUCTURES: FSPS MEL

Description 40kW_Case 2_FSPS Deployability CD-2021-187	QTY	Unit Mass	Basic Mass	Growth	Growth	Total Mass
Structures and Mechanisms			520.4	22%	112.0	632.4
Structures			288.8	19%	55.2	344.0
Primary Structures			288.8	19%	55.2	344.0
Sled	1	155.8	155.8	18%	28.0	183.8
Truss Assy	1	87.4	87.4	18%	15.7	103.2
Radiator Scissor Assy	1	45.6	45.6	25%	11.4	57.0
Mechanisms			231.6	25%	56.8	288.4
Radiator Support			2.4	25%	0.6	3.0
Radiator Support Hinges	26	0.1	2.4	25%	0.6	3.0
Radiator Deployment			1.1	18%	0.2	1.3
Radiator Deployment Motor	2	0.5	1.1	18%	0.2	1.3
ScrewJacks and Outrigger			25.4	21%	5.3	30.7
screw jack	4	2.3	9.1	18%	1.6	10.7
screw jack motor	4	1.5	6.0	18%	1.1	7.1
Outrigger Assy	2	3.7	7.3	25%	1.8	9.2
Outrigger Assy Motor	2	1.5	3.0	25%	0.8	3.8
Installations			202.8	25%	50.7	253.5
Thermal Control Installation	1	44.0	44.0	25%	11.0	55.0
FSP Installation	1	158.8	158.8	25%	39.7	198.5

TABLE 4.33.—STRUCTURES: CONTROL SYSTEMS: EQUATOR MEL

Description 40kW_Equator_Case 3_FSPS Deployability CD-2021-187	Basic Mass	Growth	Growth	Total Mass
Structures and Mechanisms	**305.0**	**19%**	**57.7**	**362.7**
Structures	**247.9**	**18%**	**44.6**	**292.6**
Primary Structures	247.9	18%	44.6	292.6
Sled	86.3	18%	15.5	101.9
Truss Assy	69.1	18%	12.4	81.5
Truss Top Panel, Orthogrid	26.3	18%	4.7	31.1
Spool Mount	11.9	18%	2.1	14.0
Spool	6.5	18%	1.2	7.7
Shunt Radiator Support	11.4	18%	2.1	13.5
Radiator Support	36.3	18%	6.5	42.9
Mechanisms	**57.1**	**23%**	**13.1**	**70.2**
Power System Mechanisms	17.6	18%	3.2	20.7
Screw Jack	9.1	18%	1.6	10.7
Screw Jack Motor	6.0	18%	1.1	7.1
Spool Hub Motor	2.5	18%	0.5	3.0
Installations	39.6	25%	9.9	49.5
C&DH installation	1.9	25%	0.5	2.3
Comm. & Tracking installation	1.0	25%	0.3	1.3
Electrical Power installation	29.3	25%	7.3	36.7
Thermal Control installation	7.4	25%	1.8	9.2

TABLE 4.34.—STRUCTURES: CABLE AND SPOOL: EQUATOR MEL

Description 40kW_Equator_Case 3_FSPS Deployability CD-2021-187	Basic Mass	Growth	Growth	Total Mass
Structures and Mechanisms	**172.3**	**19%**	**33.4**	**205.8**
Structures	**137.8**	**18%**	**24.8**	**162.6**
Primary Structures	137.8	18%	**24.8**	**162.6**
Sled	69.0	18%	12.4	81.4
Truss Assy	57.7	18%	10.4	68.1
Spool	5.8	18%	1.0	6.8
Spool mount	5.3	18%	1.0	6.3
Mechanisms	**34.6**	**25%**	**8.6**	**43.2**
Power System Mechanisms	17.6	25%	**4.4**	**21.9**
Spool hub motor	2.5	25%	0.6	3.1
Screw Jack	9.1	25%	2.3	11.3
Screw Jack Motor	6.0	25%	1.5	7.5
Installations	17.0	25%	**4.3**	**21.3**
Electrical Power Installation	14.3	25%	3.6	17.8
Therrmal Control Installation	2.7	25%	0.7	3.4

TABLE 4.35.—STRUCTURES: FSPS: EQUATOR MEL

Description 40kW_Equator_Case 3_FSPS Deployability CD-2021-187	Basic Mass	Growth	Growth	Total Mass
Structures and Mechanisms	**581.7**	**21%**	**123.0**	**704.7**
Structures	**350.1**	**19%**	**66.2**	**416.3**
Primary Structures	350.1	19%	66.2	416.3
Sled	155.8	18%	28.0	183.8
Truss Assy	148.7	18%	26.8	175.5
Radiator Scissor Assy	45.6	25%	11.4	57.0
Mechanisms	**231.6**	**25%**	**56.8**	**288.4**
Radiator Support	2.4	25%	0.6	3.0
Radiator Support Hinges	2.4	25%	0.6	3.0
Radiator Deployment	1.1	18%	0.2	1.3
Radiator Deployment Motor	1.1	18%	0.2	1.3
ScrewJacks and Outrigger	25.4	21%	5.3	30.7
screw jack	9.1	18%	1.6	10.7
screw jack motor	6.0	18%	1.1	7.1
Outrigger Assy	7.3	25%	1.8	9.2
Outrigger Assy Motor	3.0	25%	0.8	3.8
Installations	202.8	25%	50.7	253.5
Thermal Control Installation	44.0	25%	11.0	55.0
FSP Installation	158.8	25%	39.7	198.5

4.4 Communications

The FSPS communications system provides all the necessary components to communicate between the surface elements and the Lunar Orbital Gateway Power and Propulsion Element (PPE).

4.4.1 Communications Requirements and Assumptions

The communications requirement for the for the 40 kWe Deployable FSPS is to provide Ka-band communications data link to and from the FSPS lander to the Lunar Orbital Gateway Power and Propulsion Element (PPE) Platform. The communication distance ranges approximately 70,000 km from the platform with passes three times per day, Gateway/PPE dependent. A minimum 5 kbps data rate and 3 dB margin, which is typical for communication design applications due to the uncertainty of the components' performance and available real effective isotropic radiated power, are included in the communications system link budget analysis.

Further, the design assumption for the communications link consists of single-fault tolerant hardware and a conventional flight proven radio configured for K-band operations at (26 GHz) and a 10 W radio frequency (RF) Tx power for the Lander (30 W TWTA); the PPE platform uses a Steerable High Gain 2-m-antenna, which is mounted external to the spacecraft (see Figure 4.30).

The data will be collected on the C&DH storage element and transmitted via the Ka-band communications system when a suitable link is available.

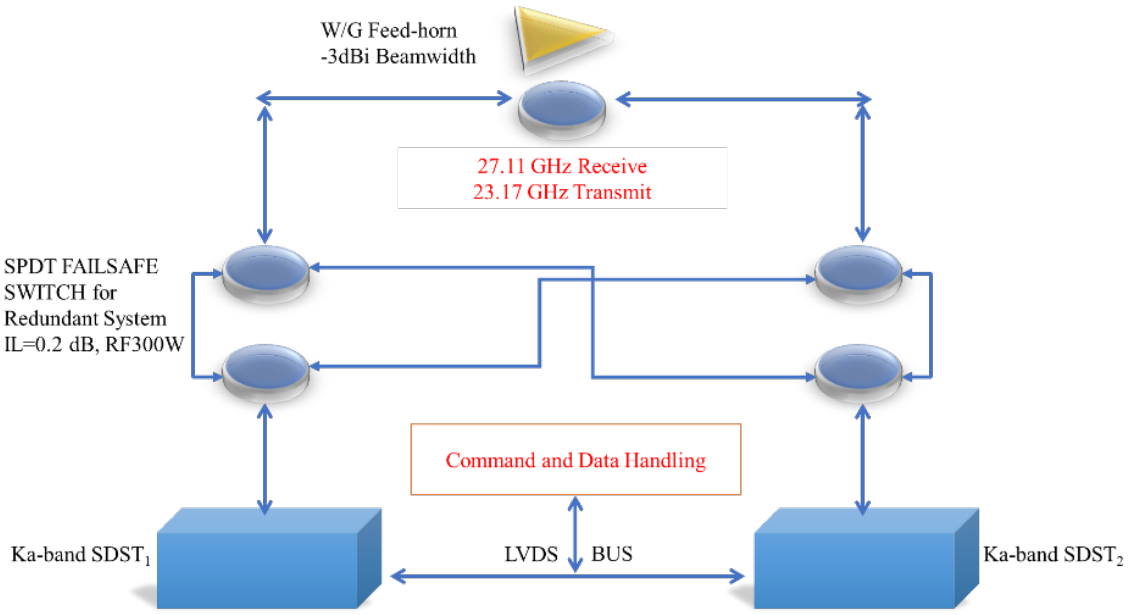

Figure 4.30.—Ka-band Block Diagram for Communications Subsystem.

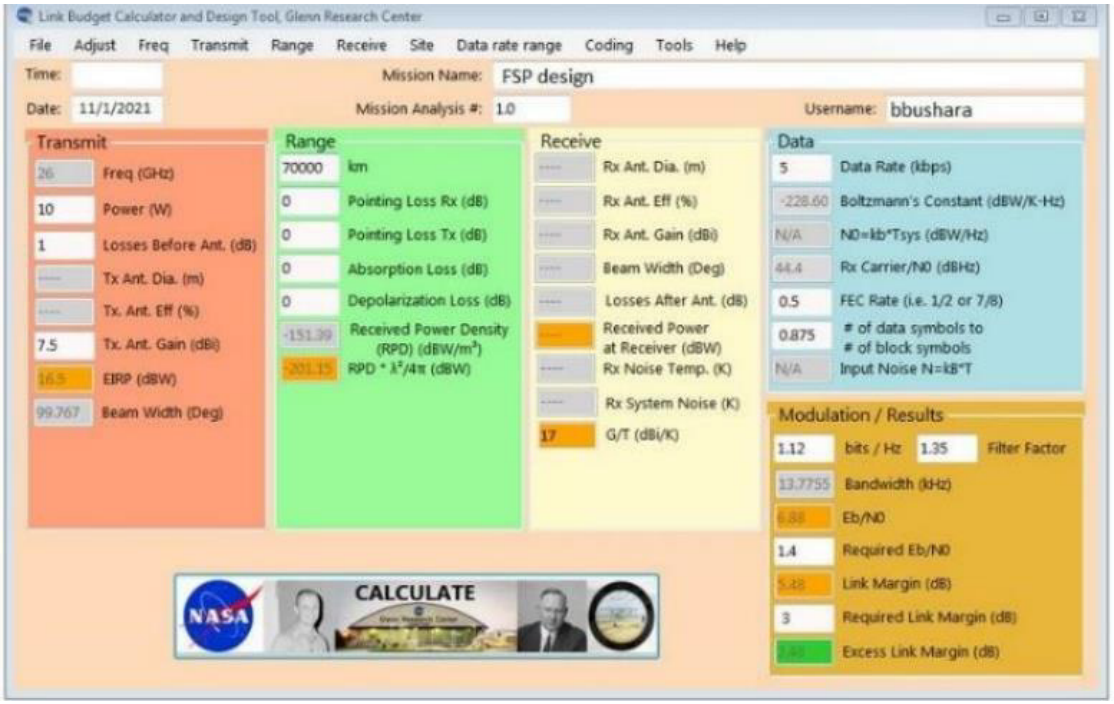

Figure 4.31.—Link Budget Analysis of Ka-band Subsystem.

4.4.2 Communications Design

The design consists of a flight proven Ka-band SDST compatible with the antenna system and different envelope constraints. The required power is less than 10 W with the final SDST radio configuration that can be procured to user specifications. A Ka-band antenna will be mounted on opposite direction on the lander surface toward the Lunar Gateway Orbit. The communications system has reasonable dimensions and mass less than 26 kg.

4.4.3 Communications Analytical Methods

The link budget analysis of the Ka-band to the lander shows 10 W of RF power in Figure 4.31 at the range of 70,000 km for the link and provides 5 kbps data rate. More details of the link budget analysis for PPE platform are found in Table 4.36 to achieve better data rate with plenty of link margin.

4.4.4 Communications Recommendation

The provided Ka-band link analysis shows that the communications system can transmit the required data rate from the lander to the Lunar Gateway platform and from the Lunar Gateway Platform to DSN ground stations with plenty of power and within the system envelope constraints. Other options (i.e., Direct Link to Earth ground stations) are not considered due to power and availability option for coverage with independent location affiliated node on NASA's Deep Space Network as an alternative.

4.4.5 Master Equipment List

Table 4.37 and Table 4.38 provide the MELs related to the communications subsystem. Both the polar and equatorial cases are assumed to have comparable communication systems.

TABLE 4.36.—LINK BUDGET ANALYSIS OF Ka-BAND SUBSYSTEM

	Node	Parameter	Value
1	Lunar System	Transmit Power	10.0 dBW
2	Lunar System	Circuit Loss	0.0 dB
3	Lunar System	Antenna Gain	7.5 dB
4	Lunar System	Antenna Pointing Loss	0.0 dB
5	Lunar System	EIRP	50.0 dBW
6	Channel	Distance	70000.0 km
7	Channel	Center Frequency	26995.0 MHz
8	Channel	Free Space Loss	–218.0 dB
9	Channel	Polarization Loss	0.0 dB
10	Channel	Total Atmospheric Loss	dB
11	Channel	RFI Losses	0.0 dB
12	Gateway	Total Received Power at Antenna	–168.0 dBW
13	Gateway	Antenna Pointing Loss	0.0 dB
14	Gateway	Antenna Gain	46.0 dB
15	Gateway	Circuit Loss	0.0 dB
16	Gateway	System Noise Temperature (T)	29.0 dBK
17	Gateway	Receive G/T	17.0 dB/K
18	Gateway	Total Received Power at Input (Prec)	–122.0 dBW
19	Gateway	Noise Spectral Density (No)	–199.6 dBW/Hz
20	Gateway	Received Rec/No	77.6 dB/Hz
21	Gateway	Modulation Loss	0.0
22	Gateway	Receive Symbol Rate	20.0 Msps
23	Gateway	Receive Symbol Rate Bandwidth	73.0 dB/Hz
24	Gateway	Received Es/NO	4.6 dB
25	Gateway	Implementation Loss	–3.0 dB
26	Gateway	Available Es/NO at Symbol Sync.	1.6 dB
27	Gateway	Effective Code Rate Including ASM	–3.0 dB
28	Gateway	Available Eb/NO at Decoder	4.7 dB
29	Gateway	Required Eb/NO	1.4 dB
30	Gateway	Required Es/NO	–1.6 dB
		Margin	3.3 dB

TABLE 4.37.—40 kW_CASE 3_FSPS - CONTROL SYSTEMS:
COMMUNICATIONS AND TRACKING MEL

Description 40kW_Equator_Case 3_FSPS Deployability CD-2021-187	Basic Mass	Growth	Growth	Total Mass
Communications and Tracking	**25.6**	**11%**	**2.8**	**28.4**
Ka band Communications System	**25.6**	**11%**	**2.8**	**28.4**
Ka-band Option SDST Radio	8.0	10%	0.8	8.8
Low Gain Antenna	1.0	10%	0.1	1.1
TWTA/EPC	12.0	10%	1.2	13.2
Frequency Diplexer	2.4	10%	0.2	2.6
Splitter/Combiner	1.2	10%	0.1	1.3
High Performance Cables	1.0	30%	0.3	1.3

TABLE 4.38.—40 kW_CASE 2_FSPS - CONTROL SYSTEMS:
COMMUNICATIONS AND TRACKING MEL

Description 40kW_Case 2_FSPS Deployability CD-2021-187	QTY	Unit Mass	Basic Mass	Growth	Growth	Total Mass
Communications and Tracking			**25.6**	**11%**	**2.8**	**28.4**
Ka band Communications System			**25.6**	**11%**	**2.8**	**28.4**
Ka-band Option SDST Radio	2	4.0	8.0	10%	0.8	8.8
Low Gain Antenna	2	0.5	1.0	10%	0.1	1.1
TWTA/EPC	2	6.0	12.0	10%	1.2	13.2
Frequency Diplexer	2	1.2	2.4	10%	0.2	2.6
Splitter/Combiner	2	0.6	1.2	10%	0.1	1.3
High Performance Cables	1	1.0	1.0	30%	0.3	1.3

4.5 Command and Data Handling

The command and data handling system provides control functions for the deployed system. To reduce shielding requirements, the components are located 50 m away from the reactor.

4.5.1 System Requirements

The C&DH subsystem is required to perform the following:

- Withstand 100 krad Total Ionizing Dose (TID) radiation over expected mission lifetime
- Detection and reset capability for Single Event Effects (SEE)
- Immunity to latch up SEE
- Dual fault tolerance reliability
- Avionics provide commanding, control and health management to the following subsystems:
- Fission Power Control Unit
- Fission Power Heat Rejection Unit
- Avionics provides data interfacing to all digital systems onboard

4.5.2 System Assumptions

This design assumes that the radiation analysis performed on the selected parts is applicable to the radiation environment of the mission. The qualification tests for avionics are based on solar radiation

while the radiation environment of the mission is from a close proximity power system. Differences in these environments may impact TID and SEE system performance.

4.5.3 System Trades

The mass of the power cable against the mass of the shielding required to protect the electronics is traded in this study. A longer cable will reduce the shielding required but increase the mass of the cable to overcome losses. Conversely, a short cable will reduce cable mass but increase shielding requirements. Figure 4.32 shows the loss vs wire gauge for a 100 m cable. The minimum wire gauge for umbilical system at any length in a vacuum is 20 gauge. At 100 m this presents minimal losses. Therefore, the cable can extend to 100 m without incurring a mass penalty to account for cable losses. Figure 4.32 shows the cable loss versus mass trade at 100 m.

4.5.4 Analytical Methods

Monte Carlo analysis is used to estimate the mass of the wiring harness, not including the sled umbilical. Assumptions and results are shown in Table 4.39 and Figure 4.33.

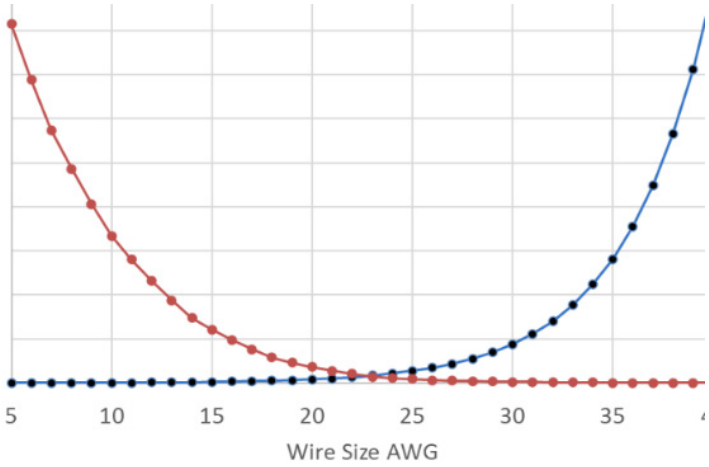

Figure 4.32.—Cable Loss vs Mass Trade at 100 m.

TABLE 4.39.—MONTE CARLO ANALYSIS ASSUMPTIONS AND RESULTS

Unit	Peak Continuous Power (W)	Voltage (V)	Wire size
Spool Deployment Motor	10	28	26 AWG
Heaters	10	28	26 AWG
Radiator Deployment Motors	50	28	20 AWG
Screw Jack Motors	50	28	20 AWG
Coolant Pumps	50	28	20 AWG
Flow Diverter Valves	5	28	26 AWG
Servo Valves	5	28	26 AWG

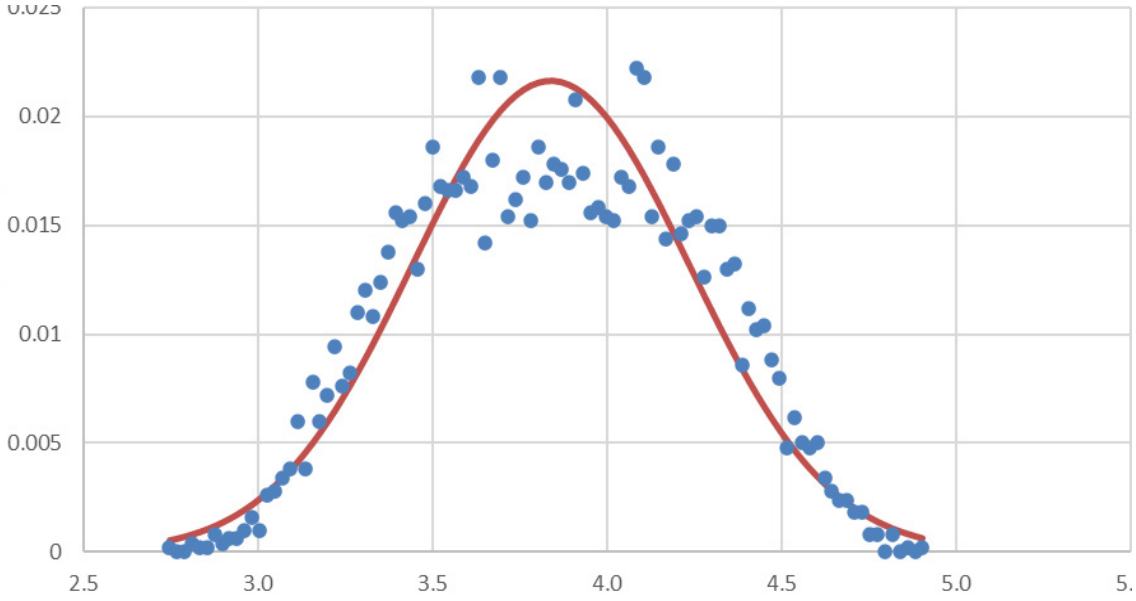

Figure 4.33.—Wiring Harness Mass PDF.

4.5.5 Risk Inputs

The radiation environment around the reactor may cause SEEs on the electronics as well as long-term damage from ionizing doses of radiation. Due to the dual fault tolerance requirement of the system, there is a low risk of single event upset interrupting critical operations. However, C&DH failure due to radiation will result in loss of control of the reactor and may be catastrophic.

4.5.6 System Design

The C&DH system consists of an Al enclosure with a 3U Compact Peripheral Computer Interface form factor backplane. The size, weight, and power (SWAP) of the DC to DC converters is included within the SWAP of the enclosure. The computer hardware contained in the avionics box is:

- AiTech Single Board Computer (SBC)
- Analog Interface Card (AMOAB)
- Standard Interface Card (SMOAB)
- Mass memory card
- Sensor conditioning card
- Actuator driver cards.

4.5.7 Master Equipment List

MEL's for both cases are equivalent for the C&DH subsystem. The MEL for these cases is shown in Table 4.40.

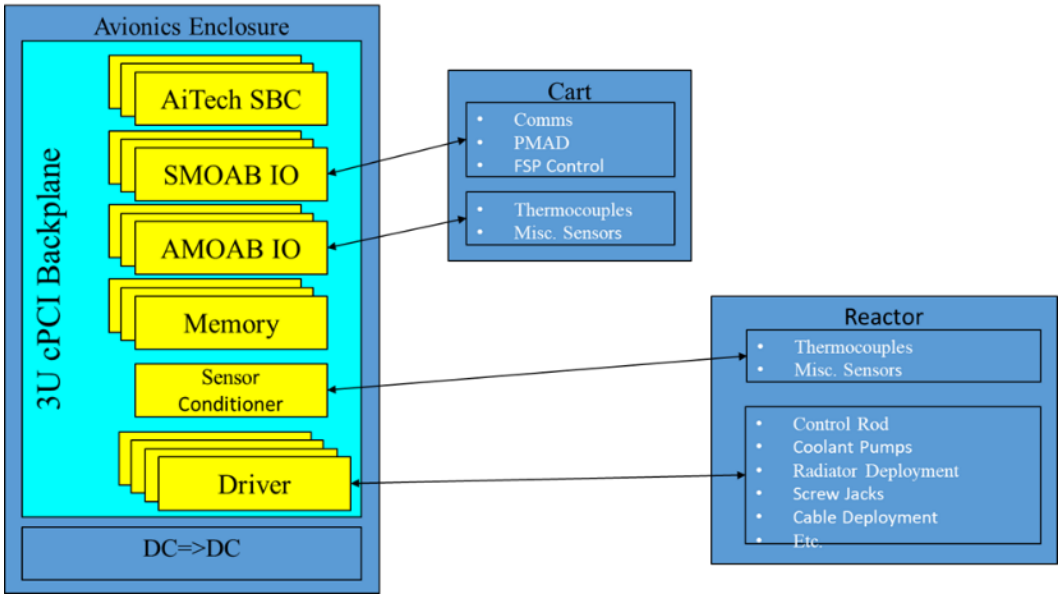

Figure 4.34.—C&DH System Block Diagram.

TABLE 4.40.—COMMAND AND DATA HANDLING: CONTROL SYSTEM

Description 40kW_Case 2_FSPS Deployability CD-2021-187	QTY	Unit Mass	Basic Mass	Growth	Growth	Total Mass
Command & Data Handling			**46.4**	**30%**	**13.9**	**60.3**
C&DH Hardware			**17.4**	**30%**	**5.2**	**22.6**
AiTech SP0 SBC	3	0.4	1.2	30%	0.4	1.6
AMOAB	3	0.4	1.2	30%	0.4	1.6
SMOAB	3	0.4	1.2	30%	0.4	1.6
Moog Motor Controller	4	0.4	1.6	30%	0.5	2.1
Mass Memory Module	3	2.0	6.0	30%	1.8	7.8
cPCI CDH Enclosure w/ PS	1	5.8	5.8	30%	1.7	7.5
Sensor Conditioning Card	1	0.4	0.4	30%	0.1	0.5
Instrumentation & Wiring			**29.0**	**30%**	**8.7**	**37.7**
Harness	1	4.0	4.0	30%	1.2	5.2
Deployment Cable	1	25.0	25.0	30%	7.5	32.5

5.0 Conclusions

The 40 kWe conceptual design shows just one design solution for such a power system, focusing on nearer-term technologies. The ~10 t-design is far above the goal of 6 t and cannot be landed with the chosen mobility system. Using the current rover chassis to deploy the 40 kWe system requires that it be deployed as three separate elements due to volume and mass constraints of the rover. These three separate elements add complexity, mass, and an additional trip to/from the lander. A new, dedicated rover could be developed, but at added cost.

By laying down the reactor and placing the control electronics 50 m away, directional shielding can be optimized to provide the 5 rem/year for the crew and eliminate added shielding for the control electronics. In the current configuration, adding distance between the reactor and the crew or moving the reactor over the horizon will not reduce shield mass.

Two other options are addressed at least cursorily: modifying the design for lunar equatorial use and keeping the reactor on the lander. Modifying the design for equatorial use is estimated to require 62 percent more radiator area and different radiator configurations for all elements. Keeping the reactor on the lander seems to have a similar design solution to the current point design; assuming the lander can be placed more than 1 km from the crew, the current reactor pallet could be kept on the lander – only the control system and cable and spool system would need to be unloaded and deployed. Further work is needed to assess radiation and any interactions with the lander.

Appendix A.—Acronyms And Abbreviations

ΔV	Delta-V, Change in Velocity
AIAA	American Institute for Aeronautics and Astronautics
AMOAB	Analog Interface Card
C&DH	Command and Data Handling
CBE	Current Best Estimate
CER	Cost Estimating Relationships
CONOPS	Concept of Operations
COTS	Commercial Off-The-Shelf
DDT&E	Design, Development, Test, and Evaluation
DDCU	DC to DC Converter Units
DG	Design Goals
ECLSS	Environmental Control and Life Support System
EPC	Electronic Power Conditioners
EPS	Electrical Power System
FET	Field Effect Transistor
FSP	Fission Surface Power
FSPS	Fission Surface Power System
GRC	Glenn Research Center
HALEU	High-Assay Low-Enriched Uranium
HW	Hardware
ISRU	In-situ Resource Utilization
ISS	International Space Station
JSC	Johnson Space Center
MEL	Master Equipment List
MGA	Mass Growth Allowance
MLI	Multi-Layer Insulation
MMOD	micrometeoroid and orbital debris
MMPDS	Metallic Materials Properties Development and Standardization
MWe	Megawatts electric
PDU	Power Distribution Unit
PEL	Powered Equipment List
PMAD	Power Management and Distribution
PPE	Power and Propulsion Element
PSR	Previously Shadowed Region
RF	Radio Frequency
S/C	Spacecraft
SBC	Single Board Computer
SDST	Small Deep Space Transponder
SEE	Single Event Effects
SMOAB	Standard Interface Card
SWAP	Size, Weight, and Power
TBR	to be resolved
TID	Total Ionizing Dose
TRL	technology readiness level
TWTA	Traveling Wave Tube Amplifiers
VAC	Volts of Alternating Current
Vdc	volts of direct current
YH	Yttrium Hydride

Appendix B.—Study Participants

40 kW Fission Surface Power System (FSPS) Deployability Design Session			
Subsystem	Name	Affiliation	Contact email
Design Customer POC/PI	Todd Tofil	GRC	Todd.a.tofil@nasa.gov
Design Customer POC/PI	William Taylor	GRC	William.j.taylor@nasa.gov
Compass Team			
Compass Team Lead	Steve Oleson	GRC	Steven.r.oleson@nasa.gov
System Integration, MEL, and Final Report Documentation	Betsy Turnbull	GRC	Elizabeth.r.turnbull@nasa.gov
Technical Editing	Lee Jackson	HX5, LLC	Lee.a.jackson@nasa.gov
Thermal	Tony Colozza	HX5, LLC	Anthony.j.colozza@nasa.gov
Reactor Design	Dasari Rao	LANL	dvrao@lanl.gov
Power Systems	Paul Schmitz Brandon Klefman Lucia Tian Chris Barth Scott Wilson	GRC GRC GRC GRC GRC	Paul.c.schmitz@nasa.gov Brandon.t.klefman@nasa.gov lucia.tian@nasa.gov Christopher.b.barth@nasa.gov scott.d.wilson@nasa.gov
Mobility and Spool	Jim Fittje	SAIC	James.e.fittje@nasa.gov
Structures	John Gyekenyesi	HX5, LLC	John.z.gyekenyesi@nasa.gov
C&DH	Nick Lantz	GRC	Nicholas.c.lantz@nasa.gov
Communications	Bushara Dosa	GRC	Bushara.dosa@nasa.gov
Configuration	Tom Packard	HX5, LLC	Thomas.w.packard@nasa.gov
Cost	Natalie Weckesser Cassandra Chang Marissa Conway Jon Drexler	GRC GRC GRC GRC	Natalie.j.weckesser@nasa.gov Cassandra.l.chang@nasa.gov marissa.conway@nasa.gov Jonathan.a.drexler@nasa.gov

References

1. Drake, B., Editor, “Human Exploration of Mars: Design Reference Architecture 5.0,” NASA/SP-2009-566, B. Drake, Ed., NASA, 2009.
2. Poston, D.; Mason, L.; and Houts, M., “Radiation Shielding Architecture Studies for NASA’s Lunar Fission Surface Power System,” in Nuclear and Emerging Technologies for Space (NETS), Atlanta, 2009.
3. Fission Surface Power Team, “Fission Surface Power System Initial Concept Definition,” Cleveland: NASA, 2010.
4. Mason, L.; Poston, D.; and Qualls, L., “System Concepts for Affordable Fission Surface Power,” Cleveland: NASA, 2008.
5. “Fission Surface Power (FSP) Project Statement of Work (SOW) No. 18960 Revision ID: 0,” sam.gov, 2021. [Online]. Available: https://sam.gov/api/prod/opps/v3/opportunities/resources/files/721695753b8e4ad1acd6c0d67eab2dfb/download?&status=archived&token=. [Accessed 13 July 2022].
6. NASA, “Human Class Cargo Lunar Lander (HCCLL) System to Cargo Interface Requirements Documents (IRD)- HLS-IRD-010,” Houston: NASA, 2021.
7. NASA, “NASA Facts: Space Exploration Vehicle Concept: FS-2011-08-045-JSC”, Houston: NASA, 2011.
8. Gernhardt, M. et al., Unpublished analysis and conceptual design in support of Human Exploration and Operations Mission Directorate, Systems Engineering and Integration, NASA, 2020.
9. American Institute of Aeronautics and Astronautics (AIAA), “Standard: Mass Properties Control for Space Systems (ANSI/AIAA S-120A-2015 (2019)),” AIAA, Reston, VA, 2019.
10. K. J. Metcalf, “Power Management and Distribution (PMAD) Model Development Final Report,” NASA, Washington D.C., 2011.
11. Barth, C. and Pike, D., “Lunar Power Transmission for Fission Surface Power,” in Nuclear and Emerging Technologies for Space (NETS-2022), Cleveland, OH, 2022.
12. Bozak, Karin; De Jesus-Arce, Yaritza; Soeder, James; Gardner, Brent; Csank, Jeff; and Boomer, Kristen, “Advanced Modular Power Systems (AMPS) Project 101,” Cleveland, OH USA: NASA Technical Reports Server (NTRS), 2020.
13. Lee, Kwan Hee, Product Specification/Rechargeable Lithium Ion Battery/Model:INR18650 MJ1, Seoul, South Korea: LG Chem, 2016.
14. Lefholz, Tyler and Bienvenu, Lindsey, LG Chem MJ1 Cell Space Qualification, El Segundo, CA USA: 38th Annual Space Power Workshop, 2021.
15. Williams, J.P.; et al, “Seasonal Polar Temperatures on the Moon,” JGR Planets, vol. 124, no. 10, pp. 2505-2521, 2019.
16. Federal Aviation Administration, Metallic Materials Properties Development and Standardization (MMPDS) Handbook-16, Columbus, OH: Battelle Memorial Institute, 2021.
17. Mankins, J. C., “Technology Readiness Levels,” NASA, Washington, 1995.
18. Heinemann, Jr., W., “Design Mass Properties II: Mass Estimating and Forecasting for Aerospace Vehicles Based on Historical Data,” NASA Johnson Space Center, Houston, TX, 1994.